AN INVESTIGATION OF THE UTILIZATION OF SMART METER DATA TO ADAPT OVERCURRENT PROTECTION FOR RADIAL DISTRIBUTION SYSTEMS WITH A HIGH PENETRATION OF DISTRIBUTED GENERATION

A Thesis

by

RICHARD HENRY DOUGLIN

Submitted to the Office of Graduate Studies of
Texas A&M University
in partial fulfillment of the requirements for the degree of

MASTER OF SCIENCE

May 2012

Major Subject: Electrical Engineering

AN INVESTIGATION OF THE UTILIZATION OF SMART METER DATA TO ADAPT OVERCURRENT PROTECTION FOR RADIAL DISTRIBUTION SYSTEMS WITH A HIGH PENETRATION OF DISTRIBUTED GENERATION

A Thesis

by

RICHARD HENRY DOUGLIN

Submitted to the Office of Graduate Studies of
Texas A&M University
in partial fulfillment of the requirements for the degree of

MASTER OF SCIENCE

Approved by:

Chair of Committee,	Karen Butler-Purry
Committee Members,	Deepa Kundur
	Le Xie
	Salih Yurttas
Head of Department,	Costas Georghiades

May 2012

Major Subject: Electrical Engineering

ABSTRACT

An Investigation of the Utilization of Smart Meter Data to Adapt Overcurrent Protection for Radial Distribution Systems with a High Penetration of Distributed Generation.

(May 2012)

Richard Henry Douglin, B.S., Prairie View A&M University

Chair of Advisory Committee: Dr. Karen Butler-Purry

The future of electric power distribution systems (DSs) is one that incorporates extensive amounts of advanced metering, distribution automation, and distributed generation technologies. Most DSs were designed to be radial systems and the major philosophies of their protection, namely, selectivity and sensitivity, were easily achieved. Settings for overcurrent protective devices (OCPDs) were static and based on the maximum load downstream of its location, with little concern of major configuration changes. However, the integration of distribution generators (DGs) in radial distributions systems (RDSs) causes bidirectional power flows and varying short circuit currents to be sensed by protective devices, thereby affecting these established protection principles.

Several researchers have investigated methods to preserve the selectivity of overcurrent protection coordination in RDSs with DGs, but at the expense of protective device sensitivity due to an inherent change in system configuration. This thesis presents an investigation to adapt the pickup settings of the substation relay, based on configuration changes in a DS with DGs, using smart meter data from the prior year. An

existing protection scheme causes the faulted areas of DSs with DGs to revert to a radial configuration, thereby allowing conventional OCPDs to isolate faults. Based on the location of the fault, the created radial segments are known and vary in length. The proposed methodology involves using demand information available via smart metering, to determine the seasonal maximum diversified demands in each of the radial segments that are formed. These seasonal maximum diversified demands are used to yield several pickup settings for the substation overcurrent relay of the DS.

The existing protection approach enables the selectivity of radial overcurrent protection coordination to be maintained. The sensitivity of the substation relay is improved by adapting its pickup settings based on seasonal demand and system configuration changes. The results of the studies are reported through simulation in EMTP™ /PSCAD® using a multi-feeder test system that includes DGs and smart meters located at the secondary distribution load level. The results show that using seasonal settings for the substation relay based on configuration changes in a DS with DGs can improve the sensitivity of the substation relay.

DEDICATION

To my family and friends

ACKNOWLEDGEMENTS

I would like to thank my committee chair, Dr. Karen Butler-Purry, and my committee members, Dr. Deepa Kundur, Dr. Le Xie, and Dr. Salih Yurttas, for their guidance and support throughout the course of this research.

Thanks also go to my friends and colleagues and the department faculty and staff for making my time at Texas A&M University a great experience.

Finally, thanks to my mother, father and brother, aunts and uncles, for their encouragement and to my dearest for her patience and love.

TABLE OF CONTENTS

Page

LIST OF FIGURES

Page

Page

LIST OF TABLES

Page

Page

1 INTRODUCTION

1.1 Background and Motivation

Electric power has become the foundation of our livelihood and has greatly improved our daily efficiency. It is involved in almost every aspect of our lives and its beginnings can be traced back to the early 1880s [1]. The purpose of the electric power grid is to deliver electric energy to its customers with high quality and in the required quantity. The electric power grid consists of three major parts: the customers who require electric energy to power their electrical devices, the sources of electric energy, and the delivery system by which electric energy is moved from the source to the customer. In the U.S., nuclear, natural gas, and coal encompass the principal sources for the production of electric energy and are usually located far away from the customer [2]. A network of overhead power lines, underground cables, and submarine cables are used to transport electric power from these remotely located generating stations to the customers.

The electric power transport system can be classified into two major parts: transmission and distribution, both of which are distinguished by their voltage level. The voltages from the generating stations, normally 13kV-24kV, are increased to high quantities (115kV-765 kV) using step-up transformers, and are transported over long distances to distribution substations via the transmission and subtransmission systems of

---

This thesis follows the style of *IEEE Transactions on Power Systems*.

the transmission network. Transformers at the distribution substations then step down the voltage levels of the electric energy (4 kV – 34.5 kV). The electric energy is transported via the primary distribution system to distribution transformers, which are located close to a number of customers. These distribution transformers further reduce the voltage level to common utilization voltages (120/240 V, 120/208 V, 277/480 V), and the power is routed directly to the customer entrances by the secondary distribution system. Depending on the maximum power requirements, customers, who can be classified as residential, commercial and industrial, can be connected to the transmission, subtransmission, primary distribution or secondary distribution systems.

Despite the fact that the electric power grid is considered to be 99.97% reliable [3], people have become cognizant that the electric distribution and transmission systems are subject to periodic failure due to an aging and deteriorating infrastructure. Coupled with the fact that customer peak demand for electric power has exceeded the construction of new transmission lines by almost 25% every year since 1982, the electric power grid is quickly reaching its limitations [3]. This is further complicated by the unavailability of real-time data, causing the forecasting of customer demand to be based on the historical trend of energy sales, past grid topologies and estimated statistical factors, which creates optimistic and error-bound load forecasts. An automated power grid, "A Smart Grid", that encompasses abilities such as self-healing, high reliability, energy management, and real-time pricing, will increase the reliability and security of the electric power grid through the incorporation of new technologies such as smart metering, distributed automation, communication, distributed generation, and distributed

storage [4]. The first step toward achieving an autonomous grid was realized by the mass roll out of smart meters to customers of all classes – residential, commercial and industrial [5]. Smart (Advanced) meter technology provides customers with the opportunity to have greater control of their power usage, and gives the utilities a more detailed insight into consumer power consumption. Another aspect of achieving a smarter grid is the connection of distributed energy resources (DER) and distributed generators (DGs) close to customer loads as a means of increasing the reliability of the distribution system (DS). Grid interconnection of DG and DER also presents an economical and an environmentally friendly option to provide a higher quality of power for customers.

The connection of DGs to radial distribution systems can be detrimental to latter's existing overcurrent protection scheme. Most power distribution systems are designed and operated as radial circuits [6], i.e. power flows exclusively away from the substation and out to customers along a single path, which, if interrupted, results in the complete loss of power to customers. Radial design is by far the most widely used form of distribution system topology of all distribution construction in North America. Its predominance is due to two overwhelming advantages: 1) it is much less costly than the other two alternatives (loop and network), and 2) it is much simpler in planning, design, and operation [7]. A radial feeder provides power to the customers via a substation transformer and a main feeder. The main feeder is a three-phase trunk, which branches out into several routes, also known as laterals, and can be 3-phase, 2-phase or 1-phase. The components that make up a feeder, include but are not limited to line segments,

loads, in-line transformers, shunt capacitor banks, switches, voltage regulators, and overcurrent protection devices (OCPDs).

The protection of a radial distribution system is designed such that a single power source feeds a network of downstream feeders. Proper overcurrent protection should have a high degree of sensitivity and selectivity such that, it allows for temporary (80% of the faults in a distribution system are temporary) to be cleared and permanent faults to be quickly isolated from the system in a manner that minimizes the number of customers impacted. Overcurrent protection practices in distribution systems involve the selective coordinated operation of many devices, such as circuit breakers, relays, reclosers, sectionalizing switches, and fuses. These devices are coordinated such that the device nearest to the fault will isolate the fault. The connection of DGs to radial distribution systems makes the system multi-sourced and thus compromises the existing protection schemes. The problems that may arise with the installation of DGs in distribution systems are false tripping in feeders and generation units, protection blinding, increases and decreases in short-circuit levels, undesirable network islanding, and asynchronous reclosing [6]. Numerous strategies have been proposed to mitigate and in some cases eliminate the impact of DGs on protection coordination in radial distribution systems (RDS).

1.2 Research Objective and Organization

The objective for this research is to develop a methodology to utilize prior year smart meter measurements to determine seasonal overcurrent pickup settings for

substation relays in an existing protection scheme for DS with DG. The protection scheme addresses the issues of loss of overcurrent protective device selectivity and unintentional islanding, as a consequence of a high penetration of DG in RDSs. The methodology to use smart meter measurements aims to provide a higher degree of sensitivity for the substation relays in the existing protection scheme by providing pickup settings based on seasonal maximum diversified demand and known system configuration changes. A multi-feeder test system was implemented in EMTP™ /PSCAD® software and used to test the proposed methodology. Studies are performed with substation relay having a seasonal pickup setting and the results are compared to the substation relay with a pickup setting based on maximum load.

This thesis consists of six sections. In section 2, an overview of overcurrent protection (OCP) coordination in RDSs is presented. In addition, the impact of DG on RDSs is presented, and an assessment of protection schemes developed by other researchers along with their strengths and weaknesses are briefly discussed. In section 3, an overview of the existing protection scheme is presented and one of its shortcomings is analyzed. In section 4, an approach to adapt the settings of the substation relays of the protection scheme, applied to a developed multi-feeder test system, using smart meter data is presented. Simulation studies and results from applying the adaptive settings to the protection scheme for the simulated test system are described in section 5. Finally, conclusions and future work are given in section 6.

2 OVERCURRENT PROTECTION OF RADIAL DISTRIBUTION SYSTEMS WITH DISTRIBUTED GENERATION

2.1 Introduction

Many problems may arise with the installation of DGs in a RDS including false tripping in feeders and generation units, protection blinding, increasing and decreasing of short-circuit levels, undesirable network islanding and asynchronous reclosing [6]. With the penetration of DGs on distribution systems set to drastically increase in the future, disconnecting the DGs at every occurrence of a fault may be impractical and even uneconomical in some cases. The presence of DGs not only change the short-circuit levels of the distribution system, but also causes bi-directional power flow, which invalidates the radial concept [8, 9, 10, 11]. Fuses and reclosers are the overcurrent protective devices that are predominantly used to protect radial distribution feeders, but due to their non-directionality, their performance is compromised when DGs are added to the circuit. Over the past decade, several researchers have dedicated significant efforts in developing methods to mitigate the impact of distributed generation on the OCP schemes in radial distribution feeders. Some of these methods include the use of distance protection, pilot protection, neural networks, software agents, system reconfiguration and adaptive overcurrent protection schemes [12]. This section focuses on primary and secondary radial distribution systems and their progression to a smart distribution system. Conventional OCP devices found in radial distribution systems and the adverse effects that DGs have on them will also be discussed.

2.2 Background

2.2.1 Distribution Systems

The principal operation of a distribution system is to deliver power to electrical consumers at their place of consumption in ready-to-use form. There are essentially three different ways power distribution systems are laid out, each of which has variations in its own design - radial, looped or network. In radial distribution systems, power flows exclusively away from the substation and out to the customer along a single path, which, if interrupted, results in the complete loss of power to the customer. In looped systems, there are two paths between power sources and each customer, whereas in network systems, there are multiple paths between all points in the network.

Fig. 2-1 shows an example of two radial primary distribution feeders. Power is routed from the substation throughout its service area via three-phase feeders - either overhead distribution lines mounted on wooden poles, or buried or ducted underground cable sets [6, 7]. Main primary feeders deliver electricity from distribution substations to distribution transformers where voltages range from 4.16 kV to 34.5 kV, with the most common being the 15-kV class (e.g., 12.47 kV, 13.8 kV). Branching out from the main feeder is one or more laterals which can be single-phase, two-phase or three-phase. For improved reliability, radial circuits are often provided with normally open tie points to other radial feeders [13] and this is represented in the figure by a normally open switch at the end of the two radial feeders.

The feeder's main protective devices are normally relayed circuit breakers, which can either be separate units (relay and circuit-breaker) or metal-enclosed switchgear. For

smaller substations, however, many utilities prefer to use reclosers instead of breakers. Lateral protective devices can either be fuses or overcurrent-relayed circuit breakers, depending on the practices of the utility.

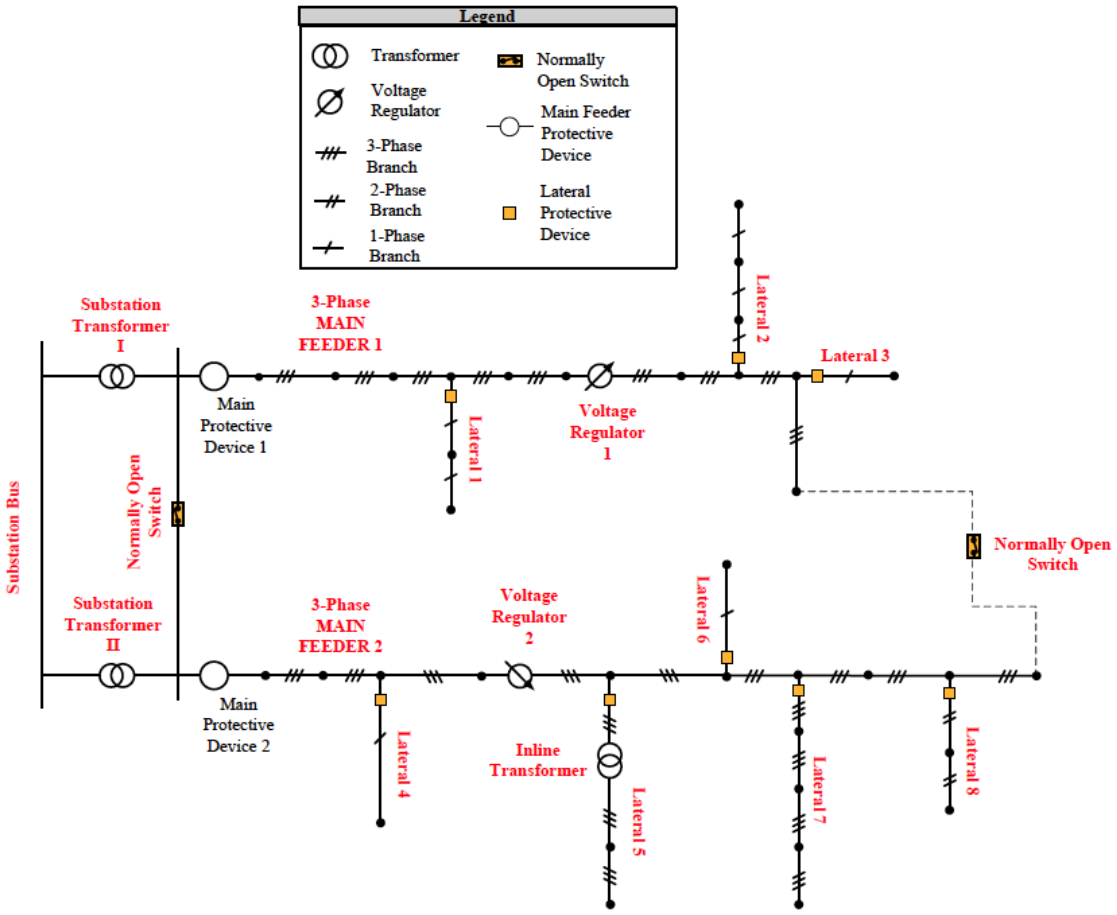

Fig. 2-1. Sample layout of two radial primary distribution feeders.

Distribution transformers, which are either pad-mounted or pole-mounted, convert primary distribution voltages to utilization voltages, and their typical sizes range from 5 kVA to 2500 kVA. There are two types of distribution transformers, namely a

single-service distribution transformer that provides power to a single customer, and a common secondary bus distribution transformer, that provides power to several customers. Industrial and commercial loads are normally served from single-service distribution transformers whereas a common secondary bus distribution transformer serves residential loads. Secondary distribution feeders deliver electricity from distribution transformers to customer service entrances, and voltages are typically 120/240V single phase, 120/208V three phase, or 277/480V three phase.

2.2.2 End-Users of Power

Table 2-1 shows the typical end-uses of electric power, and it can be seen that different types of consumers purchase electricity for different reasons. They also have different requirements for the amount and quality of the power they buy. Different rates are assessed to different types and sizes of electric consumers and so electric utilities monitor their sale of electricity by consumer classes. Utilities charge a lower rate for usage of electricity in the home when compared to commercial or industrial applications [14].

Table 2-1 End Uses of Electric Power in Various Load Classes [15]

RESIDENTIAL	COMMERCIAL	INDUSTRIAL
Incandescent Lighting	Fluorescent Lighting	Lighting
Water Heating	Water Heating	Water Heating
Space Heating	Space Heating	Space Heating
Air Conditioning	Air Conditioning	Air Conditioning
Computer	Computer	Computer
Air Circulation	Air Circulation	Air Circulation
Cooking	Cooking	Filtration
Water Well	Elevators	Fluid Pumps
Clothes Dryers	Inventory Systems	Finishing Dryers

Consumers' need for electric power, and the significance they place upon its distribution to them, has two interrelated but separate dimensions, namely quantity – the amount of power needed – and quality – the dependability of supply. The relative importance of these two features varies from one consumer to another depending on their individual needs. Each consumer, nevertheless, finds value in both the amount of power he or she obtains and its availability as a constant, steady source that will be there whenever needed [15]. However, meeting the ever-increasing consumers' reliability and power quality needs is causing a terrific strain on the existing power system infrastructure. The perceived modification for the improvement of the North American electric grid is termed the "smart grid". The smart grid incorporates distributed intelligence at all levels of the electric grid to improve reliability, security, and efficiency, which in essence amounts to a greater quality of supply to the consumer.

2.2.3 The Smart Grid

The smart grid is essentially added 'intelligence' to the current electric power grid. A smart grid is expected to integrate new technologies such as advanced metering, distribution automation, and distributed generation and distributed energy resources [4]. Fig. 2-2 shows the details of a conceptual smart grid [16]. The figure illustrates that there will be multiple sources of power generation such as wind turbines, solar panels, small generators and battery storage on the load side of the electric power system. These power sources will be at various places within the network and will be high in number. Sensors and advanced communication links will also be a part of the smart grid, enabling power system operators to be aware of the state of the power grid in real-time. Power system operators will be able to efficiently monitor voltages, currents, power factor and overall demand, and remotely control field devices such as circuit breakers and switches, with the sensing and communication equipment that a smart grid will possess. The advanced metering infrastructure will incorporate devices such as smart appliances and smart meters that will allow customers to have greater control of their power usage. Customers will be able to control appliances within their household or their business in response to pricing signals from the utility, thereby providing the customer with greater autonomy of his/her power usage.

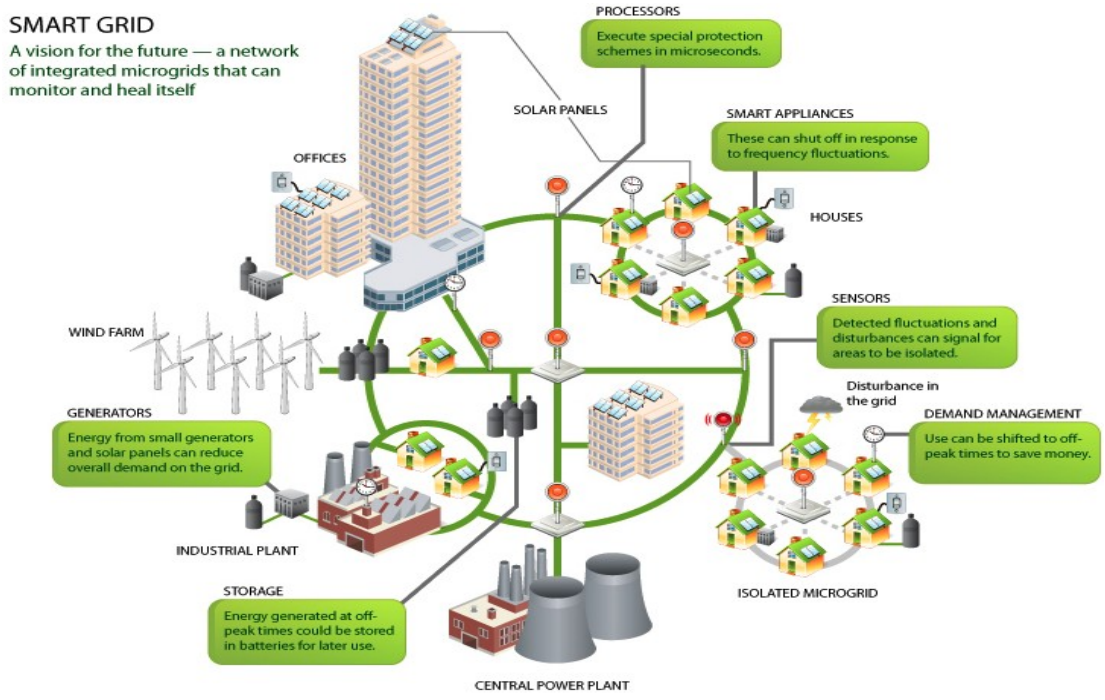

Fig. 2-2. A conceptual smart grid system [16].

The philosophies of the smart grid when applied to distribution systems may differ from those of transmission systems. The high voltage transmission system is reliable and controllable but suffers from cascading failures. The transmission system is already considered to be advanced and 'smart' when compared to the distribution system. The transmission system is highly interconnected, highly automated and active, is constantly monitored by the use of supervisory control and data acquisition (SCADA) and Phasor measurement units (PMUs), but also requires a means of integrating efficient, cleaner and more environment-friendly generating sources. While the electric power system progresses to a smart grid, the changes made to the transmission system are expected to be more from an evolutionary perspective when compared to the

distribution system, where the transition is considered to be a revolutionary change [17]. As was previously discussed, the majority of electric distribution systems in North America were designed to be radial and passive, whereas 'smart' distribution systems are expected to be networked and active. A smart distribution system is envisioned to be more interconnected and reconfigurable, contain multiple generation sources, allow for more customer participation and provide the utility with real-time information. The recognized technologies that would see distribution systems become smart include distributed generation and distributed storage, demand response, smart meters and the advanced metering infrastructure, distribution automation, low-cost communication systems, and closed-loop systems using advanced protection [4, 17].

A. Advanced Metering Infrastructure (AMI) – Smart Meters

Electronic meters have been in use for over fifteen years, providing the utility an effective means of delivering accurate billing data to only a portion of its customer base. The customer base of the electronic meter was reserved for primarily commercial and industrial customers due to their agreement for more complex rates and coarse billing requirements. Other customers, mainly from the residential sector, used electromechanical meters. These consumers were billed from a meter reading taken once a month or less frequently in some cases. This more traditional meter reading produced a divide between the consumer and their energy consumption. Smart meters are electronic meters with two-way communication between the utility and the consumer. Smart meters are expected to replace the unidirectional electronic and the more common electromechanical meters, and will be installed at all customer

(residential, commercial, industrial) locations. Smart meters have the ability to monitor customer energy usage, maximum demand and average demand over a specified time period. The smart meter can also monitor voltage and current, record waveforms, and provide the consumer with near real-time electricity rates. Utilities are able to collect usage data from each smart meter along with operational parameters such as outage, tampering, and power quality information.

From a utility perspective, the data that smart meters are able to provide will yield a more detailed insight into the quantity and time of use of electric energy. This information can provide a basis for better planning and operations management, which can lead to higher reliability, and better quality of service for consumers. Previously, detailed information such as customer average demand and maximum demand over a specified period was estimated by the utility using inaccurate energy consumption data and service factors. Now that this information is readily available to the utility via smart meter measurements, accurate peak demand forecasts are possible because energy consumption data and service factors are accurate. Table 2-2 summarizes the benefits that smart meters are expected to bring to both the utility and the customer.

Table 2-2 Benefits of Smart Meters to the Utility and the Customer

Utility	Consumer
Ability to collect a variety of data on consumer power usage to provide more fine grained services	Access to timely information that will allow consumers to make timely decision concerning their energy usage.
Reduction in the manpower hours needed to read consumer energy usage data.	Participate in demand side management programs such as rate plans and expanded product option.
Combat power theft.	Ability to use in-home monitors.
Ability to disconnect/reconnect customers depending on their fulfillment of an obligation.	Accurate energy billing compared to the sometimes estimated or manual meter reads.
Service interruption can be detected more quickly without have to rely on customer calls.	Improved service and reliability.

A typical AMI infrastructure and the way in which data collected at the smart meters can be made available to the utility operator is shown in Fig. 2-3 [18]. Smart meters communicate using either wired or wireless medium. Data gathered by the meters are relayed to a collector or hub and then are transmitted to the utility. To supplement the potential of the loss of data during transmission, the data may be passed through a repeater. Depending on the landscape of the service area, each smart meter can transmit its data directly to the collector or the data may hop from one smart meter to the other until it makes its way to the collector.

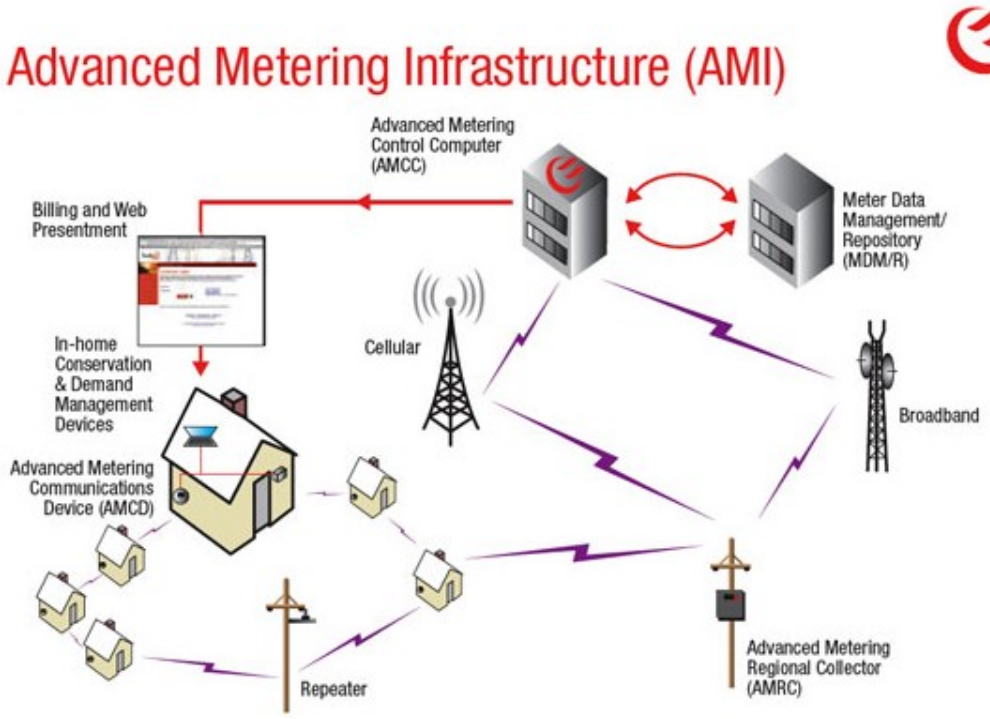

Fig. 2-3. Advanced metering infrastructure system [18].

B. Distribution Automation (DA)

Distribution automation is a communication-based ideology in which basic switches, capacitors, reclosers and relays, and other devices, can be all monitored, controlled and operated remotely by the utility. Distributed automation devices serve as an 'intelligent node' in the distribution system; they interrupt fault current, monitor currents, voltages, power factor and overall demand, communicate with one another and reconfigure the system to restore power to customers by using more than one path for power delivery [4]. When faults occur, an automated distribution system has the ability to identify outage locations and causes, and to restore power swiftly, thus minimizing the frequency and duration of unplanned power outages. Currently, distribution systems are

mostly radial in design, but with the transition to a smarter grid, distributions systems are envisioned to be a system of interconnected feeders.

C. Distributed Generation

Distributed Generation can be any small-scale electrical power generation technology and can be either interconnected to the primary distribution system or directly to the customer's facilities, or both [19]. Fig. 2-4 shows the different types of energy sources that are utilized in DG systems [11]. Distributed generators are classified as one of two types of generators, namely, the traditional combustion engine generators or the non-traditional generators. Non-traditional generators are further classified as renewables, which consist of the wind power, solar power and small hydro, storage devices such as battery storage and flywheels, and electromechanical devices such as fuel cells. The DG interfacing technology in distribution systems are inverter-interfaced generators, induction-based generators or synchronous-based generators.

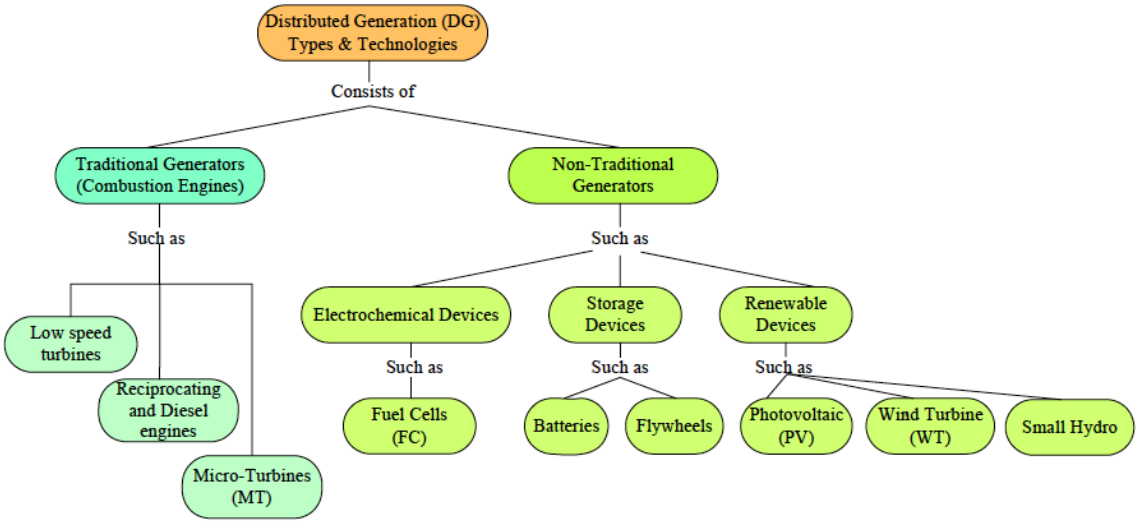

Fig. 2-4. Energy sources utilized as distributed generation [11].

The connection of DGs to the distribution system has many benefits. They (DGs) provide the customer with a more reliable and higher quality source of power, and reduce the need for building new transmission and distribution lines. Distributed generators can be easily assembled as modules close to the customer as opposed to the remote locations of bulk power generating stations. They (DGs) can be installed in small quantities to act as spinning reserve during peak demand periods and allow for a more diversified use of fuels, thus reducing the current dependence on fossil fuels. Furthermore, DGs can also improve system voltage profile and power quality, and reduce distribution network losses. The integration of additional sources of power to distribution systems enables the last-mentioned to resemble transmission systems, and therefore a need exists to consider design issues such as bidirectional power flow and increased fault current duty. System reconfiguration through distribution automation can

allow for the ability of distribution systems to operate as islands, where DGs are the main source of power, as opposed to the utility.

The traditional protection scheme of a radial distribution system entails the use of time-current coordinated protective devices, such that the device closest to the fault will operate to clear the fault. In smart distribution systems, where customers have greater control over their demand, system configuration is adaptable to prevailing conditions, and there are multiple sources of variable power, system protection must be dynamic, flexible, and operate faster than before. In the following section, the devices that are used to detect unusual conditions and interrupt the power flow whenever a failure, fault, or other unwanted condition occurs in a radial distribution system will be discussed.

2.2.4 Overcurrent Protection for Radial Distribution Systems

In radial feeders, due to the uni-directionality of power flow, overcurrent protection is the simplest and most economical solution. Feeder protection strategy aims at optimizing the service continuity to allow for the maximum number of users to be connected following a disturbance on the network. This means applying a combination of overcurrent relays, automatic reclosers, and fuses to clear temporary and isolate permanent faults.

A. Fuses

Fig. 2-5 shows the time-current characteristic curve of a fuse. A fuse is an overcurrent protective device, which possesses an element that is directly heated by the passage of current and is destroyed when the current exceeds a predetermined value [20]. A fuse has two characteristics, Minimum Meting (MM) and Total Clearing (TC)

as shown in the figure. The MM characteristic identifies the time at which the fuse becomes partially damaged for a given value of fault current whereas the TC characteristic signifies the time when the fuse becomes totally damaged for a given value of fault current. The current through the fuse in amperes is plotted along the x-axis and the duration in seconds of the fault current through the fuse that would initiate the fuse operation on the MM or TC curve is plotted on the y-axis.

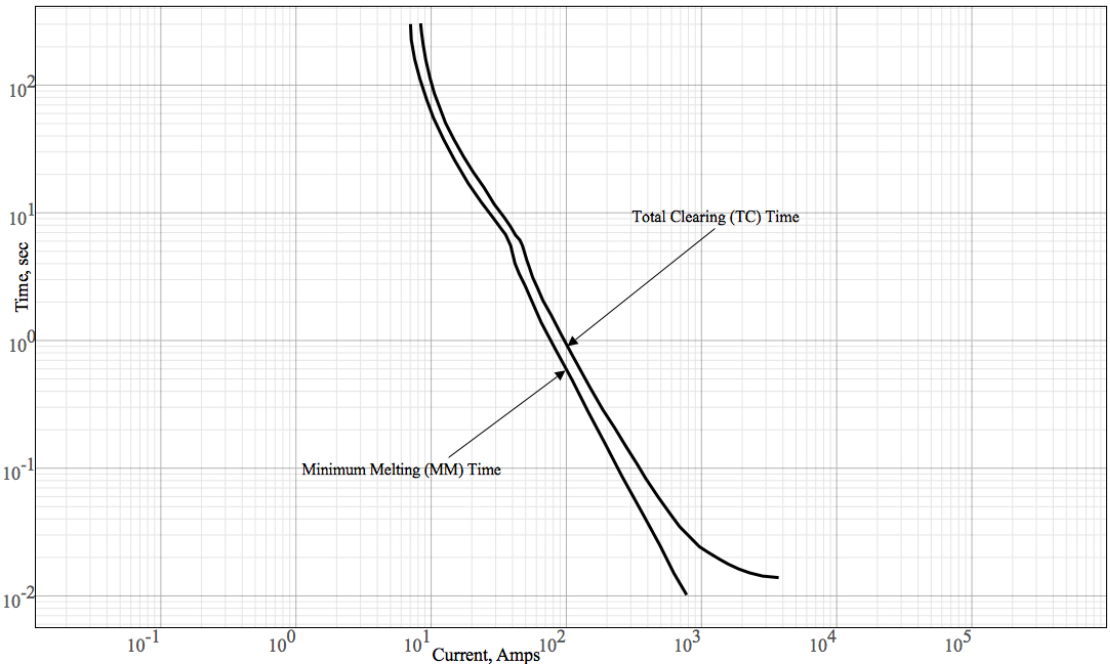

Fig. 2-5. Time current characteristic curve of a fuse.

B. Reclosers

In distribution systems, 80%-95% of faults are temporary in nature, and last at the most for a few cycles or seconds [21]. The recloser is a self-controlled and self-

contained device, which has the ability to interrupt the distribution circuit after a predetermined period and then automatically reclose to re-energize the line. If the fault persists upon reclosure, the recloser can be programmed to de-energize and re-energize the circuit at variable intervals in order to clear the fault. Typically, reclosers are designed to have up to three open-close operations, after which, a final open operation ensues to lock out the sequence. Fig. 2-6 shows a recloser programmed to operate in the A-B-B mode. This mode denotes one fast operation followed by two delayed operations and a lockout operation.

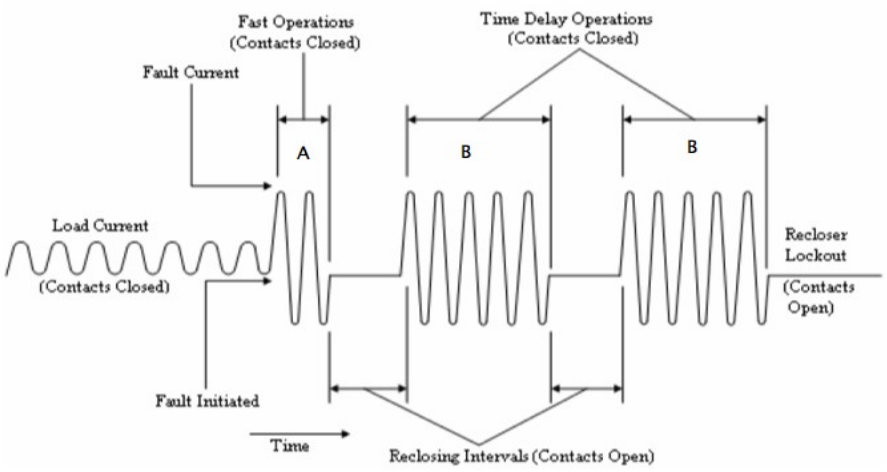

Fig. 2-6. Open-close operations of a recloser programmed to operate in A-B-B mode [21].

C. Overcurrent Relays

Overcurrent relaying is the simplest and cheapest form of protective relaying, and is generally used for phase- and ground-fault protection for distribution circuits by electric utilities. There are two types of overcurrent relays, instantaneous and time-delay

overcurrent (TDOC) relays. As the names suggests, instantaneous overcurrent relays operate immediately when the current reaches a predetermined value. The second type, TDOC, is further divided into definite-time and inverse-time overcurrent relays. Definite-time overcurrent relays operate in a set time, which can be adjusted in fixed steps for values above the preset current. Contrarily, inverse-time overcurrent relays operate in a time that is inversely proportional to the fault current.

There are two settings that must be applied to all TDOC relays: the pickup setting and the time dial setting (TDS). The pickup setting is selected so that the relay will operate for all currents greater than the pickup current in the line section for which it is to provide protection. The minimum operating criteria is to typically fix the pickup setting to 1.5 times the maximum load current and at least two times lower than the minimum fault current. The time dial setting is an independent parameter, whose purpose is to enable relays to coordinate with each other. Inverse-time overcurrent relays are generally classified in accordance with their characteristic curve that indicates the speed of operation; based on this they are commonly defined as being moderately inverse, very inverse, or extremely inverse [21]. Fig. 2-7 shows the family of curves of a moderately inverse, inverse-time overcurrent relay. There are normally 11 TDSs available for each characteristic curve, which are multiples of the characteristic curve equation. The y-axis is time in milliseconds or seconds depending on the relay type; the x-axis is in multiples of pickup to normalize the curve for all fault current values.

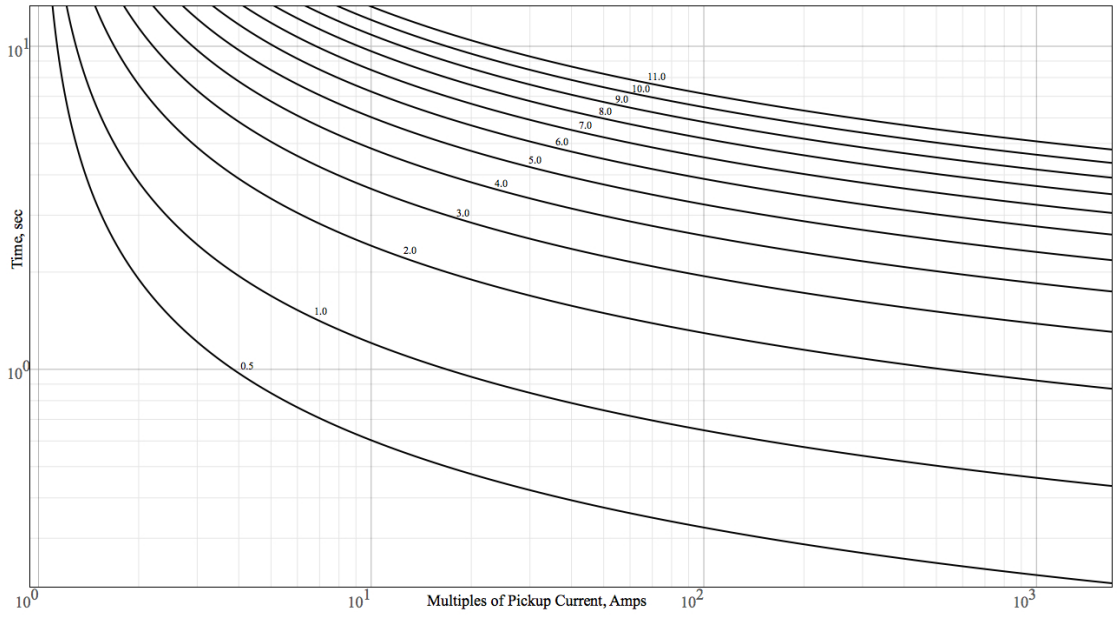

Fig. 2-7. Family of moderately inverse time current characteristic curves for overcurrent relay.

D. Overcurrent Protection Coordination in Radial Distribution Systems

The protection scheme of a radial distribution system is designed under the assumption of a single source feeding a network of downstream feeders. Proper overcurrent protection allows the primary protection to clear a temporary fault or isolate a permanent fault before the backup protection operates. If there is a loss of supply caused by permanent faults, the smallest part of the system should be isolated in a manner that minimizes the number of customers impacted. OCPDs are coordinated based on various time current characteristic curves, relay pickup settings, and fuse melting/damage curves, so that the device nearest to the fault will operate to clear the fault.

Fig. 2-8 shows how fuse-fuse coordination is traditionally performed in a radial distribution system. The schematic in (b) shows a one-line diagram of a radial feeder where the *Main Fuse* protects the main feeder, and lateral one and lateral two are protected by *Fuse 1* and *Fuse 2*, respectively. The time current characteristic curves (TCC) shown in (a), depict the overcurrent coordination of the *Main Fuse* and *Fuse 2*. For a fault on lateral 2, *Fuse 2* provides the primary protection. If *Fuse 2* fails to clear the fault, the *Main Fuse* would operate as the backup protective device. For faults on the main feeder, neither *Fuse 1* nor *Fuse 2* will detect the fault, thus the *Main Fuse* will be the primary protection required to clear the fault. The fundamental condition for fuse-fuse coordination is that the total clearing time for a primary fuse should not exceed 75% of the minimum melting time of the backup fuse, for the same current level [21]. This means that $t_1 \leq 0.75t_2$, which ensures that the primary fuse interrupts and clears the fault before the backup fuse is affected.

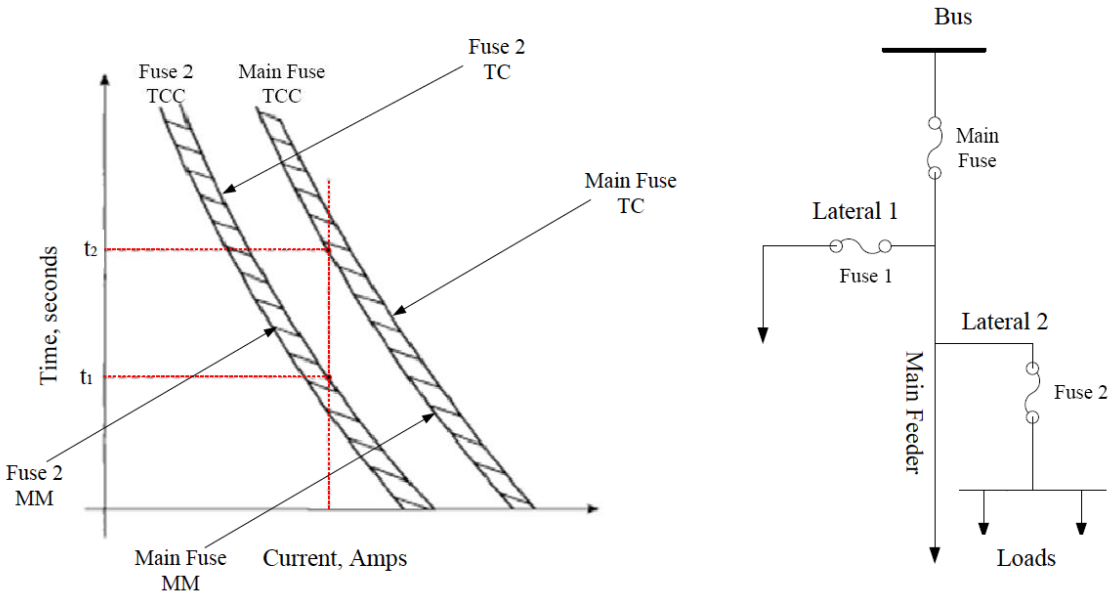

(a) Main Fuse – Fuse 2 TCC curves

(b) Sample radial feeder protected by fuses

Fig. 2-8. Fuse-fuse coordination of a sample radial distribution feeder.

The criterion for recloser-fuse coordination, shown in Fig. 2-9, is that *Fuse 2* should only operate in times of permanent fault on the lateral it protects. The time current characteristic curves (TCC) shown in (a), depict the overcurrent coordination of the *Recloser* and *Fuse 2*. The minimum melting (MM) time of the fuse is greater than the fast curve of the recloser and the total clearing (TC) time of the fuse is smaller than the slow curve of the recloser. For a fault on lateral 2 of the radial feeder shown in (b), the recloser opens the circuit with a fast operation, in time t_{rec}*fast*, giving the fault a chance to clear. Opening the circuit makes consequently de-energizes the feeder, as there is no longer a source of power. If the fault was temporary, upon the reclosure of the recloser, the fault should have been cleared, and the system would return to normal operating conditions. If the fault on lateral 2 was permanent, *Fuse 2* would have begun

to melt at time t_{Fuse2},MM and isolate the faulted lateral at time t_{Fuse2},TC. If *Fuse 2* fails to operate, the recloser will provide backup protection to the fuse through its slow mode operation, subsequently locking out the circuit at time, $t_{rec},slow$.

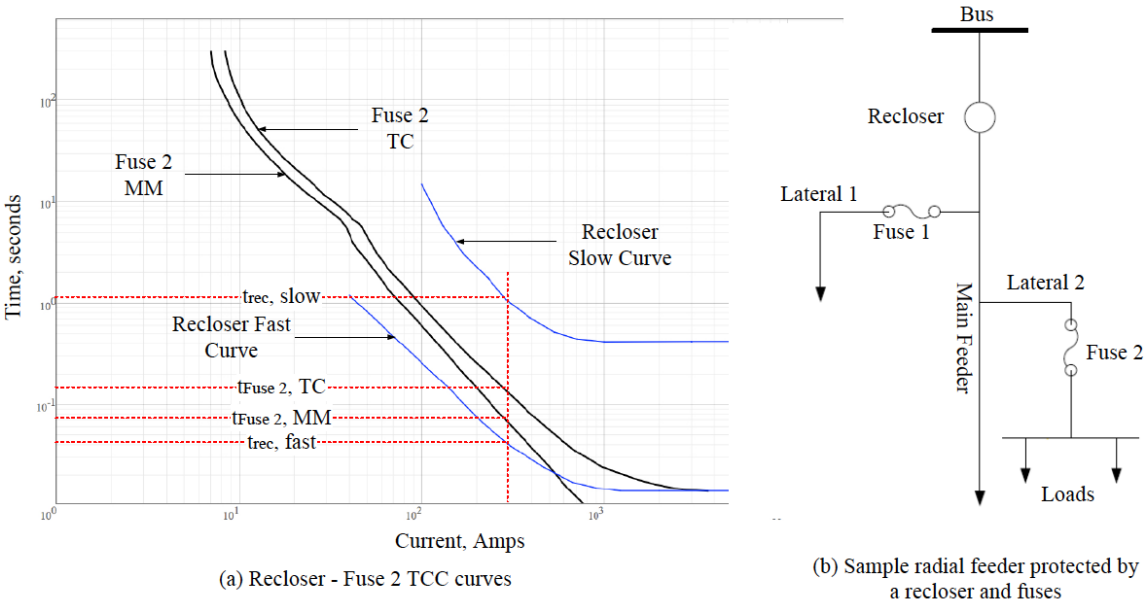

(a) Recloser - Fuse 2 TCC curves

(b) Sample radial feeder protected by a recloser and fuses

Fig. 2-9. Fuse-recloser coordination of a sample radial distribution feeder.

Fig. 2-10 shows an example of a philosophy for relay-relay coordination in radial distribution systems using inverse-time overcurrent relays. The time current coordination curves for the both relays are shown in (a). Both relays have a moderately inverse characteristic. The TDS for *Relay 2* and the *Main Relay* is 0.5 and 1.0 respectively. In (b), the *Main Relay* protects the main feeder while *Relay 1* and *Relay 2* protect lateral 1 and lateral 2 respectively. For a fault that occurs on lateral two, *Main Relay* must operate before *Relay 2*. For the fault to be properly cleared, the coordinating

margin for the *Main Relay* must include the time it takes for *Relay 2* to operate, and the associated circuit breaker operating time. This coordinating margin is referred to as the coordination time interval (CTI). Assuming for the fault shown, both *Relay 2* and the *Main Relay* see the same fault current, due to their TDS differences, *Relay 2* will operate before the *Main Relay*.

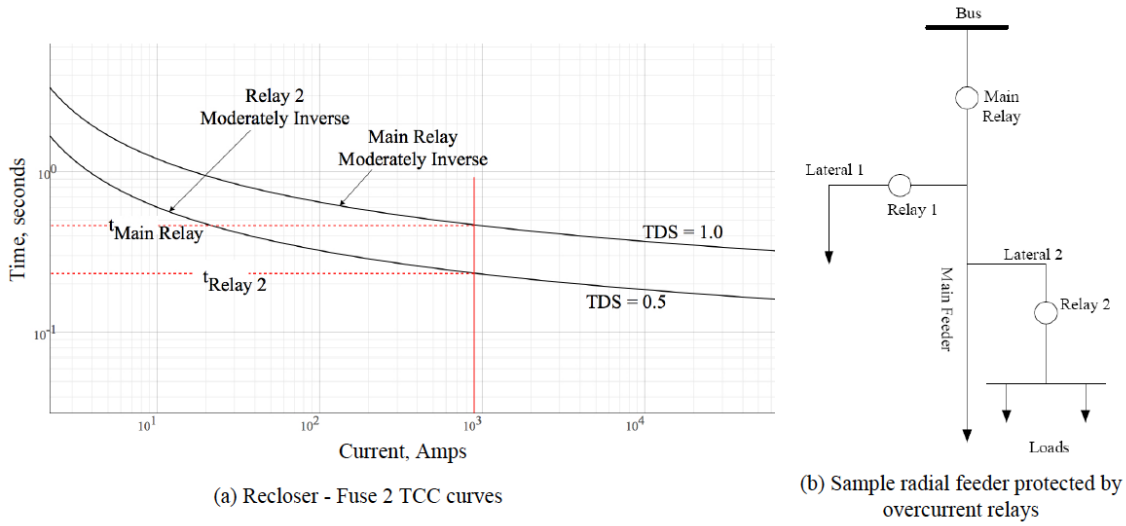

(a) Recloser - Fuse 2 TCC curves

(b) Sample radial feeder protected by overcurrent relays

Fig. 2-10. Relay-relay coordination of a sample radial distribution system.

The protection schemes adopted by utilities for radial distribution systems are simple and cost-effective due to the single direction of power flow. The connection of DGs to radial distribution systems, however, makes the system multi-sourced and thus compromises the existing protection schemes.

2.2.5 Impact of Distributed Generation on Radial Distribution System Protection

The protective devices that were explored in the previous section (Section 2.2.4) are designed and operated based on the location of the fault, the distance of the fault from the main source of power – substation, and the uni-directional flow of power. The interconnection of DGs to RDSs will redistribute the short circuit current in a radial distribution system and cause bi-directional power flow, thus it is expected that overcurrent protection schemes in distribution systems based on radial design will not be effective with DG integration [8, 9, 11, 12]. According to [6], the connection of DGs to RDS creates two primary safety concerns: desensitization of the RDS protection schemes and the creation of unintentional islands. Additionally, from a reliability perspective, DG may cause misoperation or miscoordination of OCPDs in RDS [6].

Overcurrent protective devices in RDS can be desensitized by the additional short circuit contribution provided by DG. This contribution leads to slower clearing of faults thereby creating a greater safety hazard for a person nearby the faulted area and a higher risk of potential damage to sensitive equipment [6]. When DGs are added to a RDS, all protective devices downstream of its connection point will experience an increase in short circuit current for downstream faults. Radial protection design, based on fuse-fuse coordination, recloser-fuse coordination, and relay-relay coordination, may fail due to the increased short circuit current and bidirectional power flow [8] introduced by DGs. In fact, OCPDs may need to be recalibrated – overcurrent relays and microprocessor-based reclosers, or replaced – recloser, fuses [6] with the introduction of DGs to RDS. Distributed generation also introduces asynchronous reclosing issues in

RDS that are designed under a recloser-fuse protection coordination scheme. The recloser de-energizes the radial distribution system for faults by automatically opening to allow the chance for the fault to clear. With DG in the system, a portion of the distribution system will remain energized (unintentional island) during faulted conditions and upon the reclosure of the recloser; two live systems will be connected. This may result in a loss of synchronism between the substation powered distribution system, and the DG sourced unintentional island, leading to potentially damaging transients [6]. DG installation may also generate bidirectional power flow in distribution systems, which may cause protective devices to operate incorrectly and thus lead to unnecessary interruptions. For radial feeders that are fed from the same source, the issue of bidirectional power flow can lead to dire consequences.

The overcurrent protection schemes for RDSs are straightforward as they are based on a single source providing power down a single path to its customers. Fuses, reclosers, and overcurrent relays are the principal devices that are used to protect RDSs and their operation and coordination with other devices were described in Section 2.2.4. When DGs are added to RDSs, the increased fault current and bidirectional power may cause the protection schemes for RDSs to operate incorrectly.

2.3 Review of Existing Adaptive and Non-Adaptive Protection Schemes that Address Protection Issues of RDSs with DGs

Distributions systems have traditionally been designed to operate radially and this simple configuration has enabled straightforward overcurrent protection strategies.

Factors such as changes in utility structures, exorbitant expenses associated with building new transmission lines, advancement of renewable generation technologies, and a need for higher quality of power for customers, have all fueled the motivation for a higher penetration of distributed generation on distribution systems. With the introduction of DGs in RDSs, however, the radial structure no longer exists and thus overcurrent protection of RDSs is impacted. In fact, radial coordination of overcurrent protective devices such as reclosers, fuses, and overcurrent relays may not appropriately protect the DS with DG due to the penetration level, the connection point, and the type of DG technology (Synchronous, Asynchronous, Inverter-based) [8, 9, 10, 11, 22]. There have been many methods developed to mitigate the effect of distributed generation on the conventional overcurrent protection scheme of radial distribution systems.

Adaptive protection may be a possible approach in protecting RDS with DGs because of bi-directional power flow and varying short circuit currents that exist with multiple generation sources on the system. Adaptive-based protection techniques require the settings of protective devices to be changed on-line in a timely manner, so that the appropriate protective response is initiated when there is a change in system conditions [23]. Changes in system conditions may include variations in load, topological changes and the loss of a generator or a distribution line. Table 2-3 shows the methods that were investigated for the work reported in this thesis. The methods in the table are classified into two groups: adaptive- and nonadaptive-based protection techniques.

The first two methods in the table are non-adaptive-based methods that utilized fault current limiters to significantly reduce or negate the contribution of DGs for a fault in the distribution system. During normal operation, however, the output of DGs was unimpeded. It was not necessary to change the original protective devices on the system, because during a fault the substation was the major source of fault current, while the DG's output was limited to acceptable levels [24], [25]. In [24] the fault current limiter was characterized by solid-state components, which is known to introduce harmonics into the system and reduce power quality, especially in instances of high DG penetration [24]. A passive fault current limiter was utilized in [25] and the goal was to determine the optimal impedances necessary to achieve coordination. Two types of impedance based fault current limiters were surveyed, namely resistive and inductive, to determine their limitation on fault current. A drawback to this method is that due to the varying output of DG power, it is difficult to obtain optimal impedances during both normal operation and fault conditions.

The third method [26], presented a nonadaptive technique that enabled all conventional overcurrent protective devices (over-current relays, fuses and re-closers) to keep their functions and their coordination when DGs were added to radially-operated looped (meshed) distribution systems. In this method, the normally open switches in the radially operated looped systems were closed when DGs were added. The distribution system was then divided into several protection coordination areas in which distance relays coordinated by a permissive overreach transfer trip (POTT) scheme were used to break up the loop [26] when a fault occurred. The DGs on the faulted section of the distribution system were disconnected, and those on the unfaulted section remained connected. With the loop broken and the appropriate DGs disconnected, the faulted section reverted to a radial topology with the substation being the only source of short circuit current. A combination of conventional OCPDs was then used to isolate the fault. In this method the selectivity of OCP was maintained. However, depending on the location of the fault, different lengths of radial sections were created when the loop was broken by the modified POTT scheme. The static settings of the overcurrent protective devices (fuses, reclosers, overcurrent relays), in the created radial section, could result in a reduction in the sensitivity of the OCPD.

Table 2-3 Adaptive and Non-adaptive Protection Coordination Techniques for RDS

#	Ref	Title of Paper	Problem(s) Addressed	Protection Technique	Protective Devices Used	Adaptive	DG
1	[24]	Application of a fault current limiter to minimize distributed generation impact on coordinated relay protection	Miscoordination of protective devices	Utilized a solid-state fault current limiter to reduce or negate the contribution of the DG during faulted conditions	Fault Current Limiter, Overcurrent Relays	No	Y
2	[25]	Reducing the impact of DG in distribution networks protection using fault current limiters	Miscoordination of protective devices	Used a passive fault current limiter and determines the optimal impedances necessary to main protective device coordination	Fault Current Limiter, Overcurrent Relays	No	Y
3	[26]	Protection Scheme for Meshed Distribution Systems with High Penetration of Distributed Generation	Miscoordination of protective devices	Radial feeders fed from the same substation were operated as a closed loop system by closing a normally open switch between both feeders. When DG was added to the circuit, two breakers were added, such that the DG could supply power to both feeders. When a fault occurred, distance relays coordinated by a modified POTT scheme would break up the loop and all DG on the faulted feeder was disconnected. The faulted section would then be radial and the fault was cleared by conventional radial overcurrent techniques	Distance Relays, Reclosers, Fuses	No	Y
4	[27]	Microprocessor-based reclosing to coordinate fuse and recloser in a system with high penetration of distributed generation	Recloser-fuse mis-coordination	Developed a user-defined recloser curve to achieve coordination between the recloser and fuse when DG was added to the feeder. This was achieved by replacing the recloser by a microprocessor-based one and its fast curve was adjusted by a factor of I_R/I_F, so that coordination between the fuses and the recloser was maintained when DG was added to the circuit.	Microprocessor Recloser, Fuses	No	Y
5	[28]	A strategy for protection coordination in radial distribution networks with distributed generators				No	

Table 2-3 Continued

#	Ref	Title of Paper	Problem(s) Addressed	Protection Technique	Protective Devices Used	Adaptive	DG
6	[29]	An approach to mitigate the impact of distributed generation on the Overcurrent Protection scheme for radial feeders	Recloser-fuse mis-coordination	A fuse on a lateral with DG was replaced with a multifunction recloser and a relay was added at the DG point of connection	Microprocessor based recloser, fuses & relays	No	Y
7	[30]	Study on Adaptive Protection System of Power Supply and Distribution Line	Frequent load and topological changes	Determined the operating status of the distribution system, loading and fault conditions, and computed the real time settings of the protective devices.	Adaptive Overcurrent Relay	Yes	N
8	[31, 34]	Application of a proposed overcurrent relay in radial distribution networks	Reduced relay sensitivity, Long tripping times	The pickup current of the main substation overcurrent relay was modified as function of the load current, and adjusted its operating time as a function of the operating response of the back-up device.	Adaptive Overcurrent Relay	Yes	N
9	[35]	Designing a new protection system for distribution networks including DG	Miscoordination of protective devices	The distribution system was divided into zones such that each zone was capable of islanded operation. A Computer-based relay located at the substation compared measured currents, and offline results, and determined which zone was to be isolated due to fault	Directional Overcurrent Relays	Yes	Y
10	[36]	Development of adaptive protection scheme for distribution systems with high penetration of distributed generation	Miscoordination of protective devices	The distribution system was broken into zones and the main relay sensed and identified the type of fault. The faulted zone was isolated by tripping the appropriate breakers and DG in that zone	Directional Overcurrent Relays	Yes	Y
11	[37]	A simple adaptive over-current protection of distribution systems with distributed generation	Change in short-circuit currents in grid connected and islanded mode	Updated the trip characteristics of directional overcurrent relays when a portion the distribution system condition changes from grid connected or islanded mode.	Adaptive Directional Overcurrent Relay	Yes	Y

Table 2-3 Continued

#	Ref	Title of Paper	Problem(s) Addressed	Protection Technique	Protective Devices Used	Adaptive	DG
12	[38]	Adaptive over current protection for distribution feeders with distributed generators	Under reaching and blinding of protection	Updated the OC relay minimum pickup current based on amount of power injected by the DGs in the system	Adaptive Overcurrent Relay	Yes	Y
13	[39]	A New Protection Scheme for Distribution System with Distributed Generations	Bidirectional power flow Nuisance tripping of protective devices	According to the connection point of DGs, the distribution system was divided into different zones, with directional pilot protection configured at the upstream side of DG and the overcurrent protection with a directional component is retained for the remaining portion of the feeder. Definite-time or inverse-time overcurrent protection was separately adopted based on different locations of DGs	Directional Pilot Protection, Overcurrent Relays	Yes	Y
14	[40]	An adaptive distance protection scheme for distribution system with distributed generation	Sensitivity of protective devices	Based on the connection point of DGs, radial feeders were divided into different zones, with adaptive distance protection configured at the upstream side of DG. The scheme was based on the fact that inverter interfaced DG produces only positive sequence current irrespective of the type of fault.	Adaptive Distance Relays	Yes	Y

Distributed generators provide an additional source and direction of current, and fuses, which are the most used overcurrent protective device on distribution systems, will become a liability. This is because the protection settings of fuses are static and nondirectional. Nevertheless, the forth and fifth methods in the table illustrated approaches to eliminate the fuse-recloser mis-coordination that may exist with the inclusion of DGs to a RDS [27, 28]. These non-adaptive techniques did not require the replacement of any fuses, but included the replacement of the substation recloser with a microprocessor-based recloser. These methods resulted in the DG being disconnected after the first operation of the recloser, to eliminate the possibility of asynchronous reclosing. However, with a high penetration of DG on the distribution system, it will become very onerous to disconnect the DG for every fault. These schemes also involved recalculating a new recloser curve every time a new DG was added to the distribution system. An approach that revised the existing OCP scheme of a radial feeder to address the presence of DGs was presented by Funmilayo [29]. The fuses on the laterals with DGs were removed and multi-function recloser/relays (MFRs) were added to address three specific OCP issues; fuse fatigue, nuisance fuse blowing, and fuse misoperation. The recloser-fuse coordination worked best for nuisance fuse blowing but not for fuse fatigue as there were occasions where a fuse began melting before the recloser fast operation was initialized [29].

Several adaptive protection schemes are discussed in the remaining entries of the table. The possibility of adapting the settings of relays in distribution networks based on the topology or the loading of the system was investigated in [30, 31, 32, 33, 34]. These

approaches did not take into consideration instances when DGs are connected to the distribution system. The ninth and tenth entries of the table are adaptive protection schemes for DSs with DGs, where the distribution systems are divided into predefined zones that contain a balance of generation and load [35], [36]. These zones can be operational with or without grid support and are separated by breakers, which are controlled by a computer-based relay located at the substation. For temporary and permanent faults, the computer-based relay send signals to the appropriate breakers so that the faulted zones are isolated to clear the faults or remain de-energized until the fault are repaired. The unfaulted zones either operate in islanded mode, grid connected mode, or are de-energized due to the absence of a generating source. The existing OCPD in the distribution system are no longer used since inter-zonal breakers perform fault-clearing functions for temporary faults and isolation functions for permanent faults. It is left up to the utility company to dispatch personnel to find the fault. In islanded mode, the nonexistence of the stiff grid can cause voltage and frequency problems. Due to the high variability of load and renewable generation sources, there can be an imbalance in generation and load even if predefined zones have been established. Also, relying on one central relay to trigger the control of all zonal breakers can cause much harm in the event of losing such a relay due to a cyber-attack or malfunctioning of the component.

The third entry in the table [26], provided an efficient means of maintaining the selectivity of the OCPDs in radially operated looped distribution systems. However, depending on the location of the fault, different lengths of radial sections were created when the loop was broken by the modified POTT scheme. The pickup settings of the

substation relay were based on the maximum load downstream of its location and the different lengths of the created radial sections could result in its desensitization. The sensitivity of the substation relay may be improved by computing pickup settings based on historical measured load data and possible variations in the radial configuration of the distribution system. The work reported in this thesis investigates the use of smart meters to obtain the per interval demand data from the previous year of the customers on a distribution system. The data that is obtained is then used to determine seasonal maximum diversified demands of the radial configurations that are created by the protection scheme presented in [26]. The seasonal maximum diversified demands are then used to determine the corresponding overcurrent pickup settings for the aforementioned radial configurations.

2.4 Summary

This section presented an overview of radial distribution systems and their conventional protection schemes, which are based on the principle of a single source feeding a set of downstream feeders. As distribution systems continue to age, and become more strained due to increasing load and the reluctance to build new transmission lines, distributed generation will offer an avenue for relief. Strategic placement of distributed generators on distribution systems provides a way to reduce the stress on the distribution system as it can supplement the load expectation while improving power quality and service reliability from the customer standpoint. Overcurrent protection of radial distribution systems is greatly affected by distributed

generation, and it was discussed that radial overcurrent protection schemes would not hold in most cases. It is anticipated that there may need to be a total revamp of the radial distribution topology and its protection schemes, to progress toward a more transmission-style network where multiple sources of power is common. The ideas of several researchers to mitigate DG effects on the protection of RDS have been presented, along with their shortcomings. The next section presents an overview of the protection scheme in [26] and discusses the way in which smart meters can be used to improve the sensitivity of the substation relays in a distribution system with DG.

3 RATIONALE FOR THE USAGE OF SMART METER DATA TO ADAPT THE PICKUP SETTINGS OF SUBSTATION RELAYS IN A NON-ADAPTIVE PROTECTION SCHEME FOR RDS WITH DGS

3.1 Introduction

It was discussed in Section 2.2.5 that distributed generation, in addition to potentially causing unintentional islands to be formed in DSs, might also cause the desensitization and misoperation or miscoordination (loss of selectivity) of OCPDs in RDSs due to increased short circuit current and bidirectional power flow. To circumvent the array of complications that DGs present, the IEEE 1547 Standard [6] suggests that all DGs connected to the distribution system, that violate certain thresholds for faulted conditions, should be disconnected. This, however, may prove to be problematic when there is a high penetration of DGs on the DS, if most/all DGs are disconnected, even for temporary faults.

Some protection schemes that have been developed to mitigate the impact of DGs on DSs were discussed in Section 2.3 and tabulated in Table 2-3. The methods [32], [38], that focused on the modification of overcurrent relay settings will lead to several changes of settings when there is a large variation in DG output, or there are frequent system configuration changes. Transmission system-based protective devices such as distance relays and directional overcurrent relays are expected to minimize the numerous readjustments of OCPD settings for DSs with DGs. Directional overcurrent relays will mitigate the problems of misoperation of protective devices on adjacent

feeders while distance protection will reduce the overcurrent relay issues due to varying short-circuit currents. The protection schemes in [27] and [28], that addressed the impact of DGs on distribution systems with reclosers, run the risk of connecting two live systems together, which causes synchronization problems. Disconnecting all DGs on the distribution system after the first operation of the recloser solves this issue, but will make the system very unreliable, since all DGs will be disconnected every time a temporary fault occurs. Zonal protection schemes [35], [36], allow most DGs to be kept online during faulted conditions by dividing the distribution system into several intentional islands or zones. These zones are expected to have a reasonable balance of load and distributed generation, but such an expectation is highly unlikely when load and DG output vary greatly throughout the day.

This section discusses the overview of an existing non-adaptive protection scheme for DSs with DG, and proposes an approach that uses smart meter load measurements to adapt OCP settings of the substation relay, as a means of improving its sensitivity.

3.1.1 Overview of an Existing Protection Scheme for Radially Operated Meshed Distribution Systems with a High Penetration of DG [26]

Viawan presents a non-adaptive protection scheme that is able to preserve conventional radial overcurrent protection schemes, keep most DGs connected during faults, and prevent any part of the distribution system from being intentionally or unintentionally islanded [26]. This non-adaptive protection scheme is for radially operated meshed distribution systems with a high penetration of distributed generation.

It should be noted that meshed systems operating as radial feeders (open loop operation) are protected with conventional OCPDs, such as overcurrent relays, fuses, and reclosers, with appropriate time delays [41]. The functions and coordination of these protection devices were discussed in Section 2.2.4. Fig. 2-1 showed an example of an open loop operation of two radial feeders. The protection scheme requires the existing normally open switches between radial feeders in radially operated meshed systems, to be closed, so that a closed loop system is formed when DG is added. In Fig. 3-1, which shows the protection scheme applied to Fig. 2-1., the normally open switch at the end of the two radial feeders is closed, thereby forming a closed loop system. When a fault occurs, the DGs connected to the faulted feeder are disconnected, while the DGs connected to the unfaulted feeder are maintained. To allow for DGs to be connected to both feeders during normal operation, breakers are added, with the number and location of breakers dependent on the connection points of the DGs.

For DGs connected to the main feeder, two breakers are added to the main feeder on each side of the DG connection point. For DGs connected to the end of a lateral, three breakers are added; two breakers are added on the main feeder on each side of the lateral tap off point, and one breaker is added to the connection point of the DG to the lateral. If there is a fuse on the lateral to which a DG is connected, the fuse is removed to prevent misoperation or long interruption for the DG. In Fig. 3-1, when DG1 is connected to the main feeder, breakers, BRK1 and BRK2 are added on each side of the DG's connection point on the main feeder. When DG2 is connected to the end of lateral 5, three breakers are added to the system: BRK3 and BRK4 are added to the main feeder

on each side of the lateral tap-off point, while BRK5 is added to the end of the lateral at the connection point of the DG. The relays of the added breakers are coordinated to form protection coordination areas. The figure shows the four protection coordination areas that are formed, which are demarcated by Area I through Area IV.

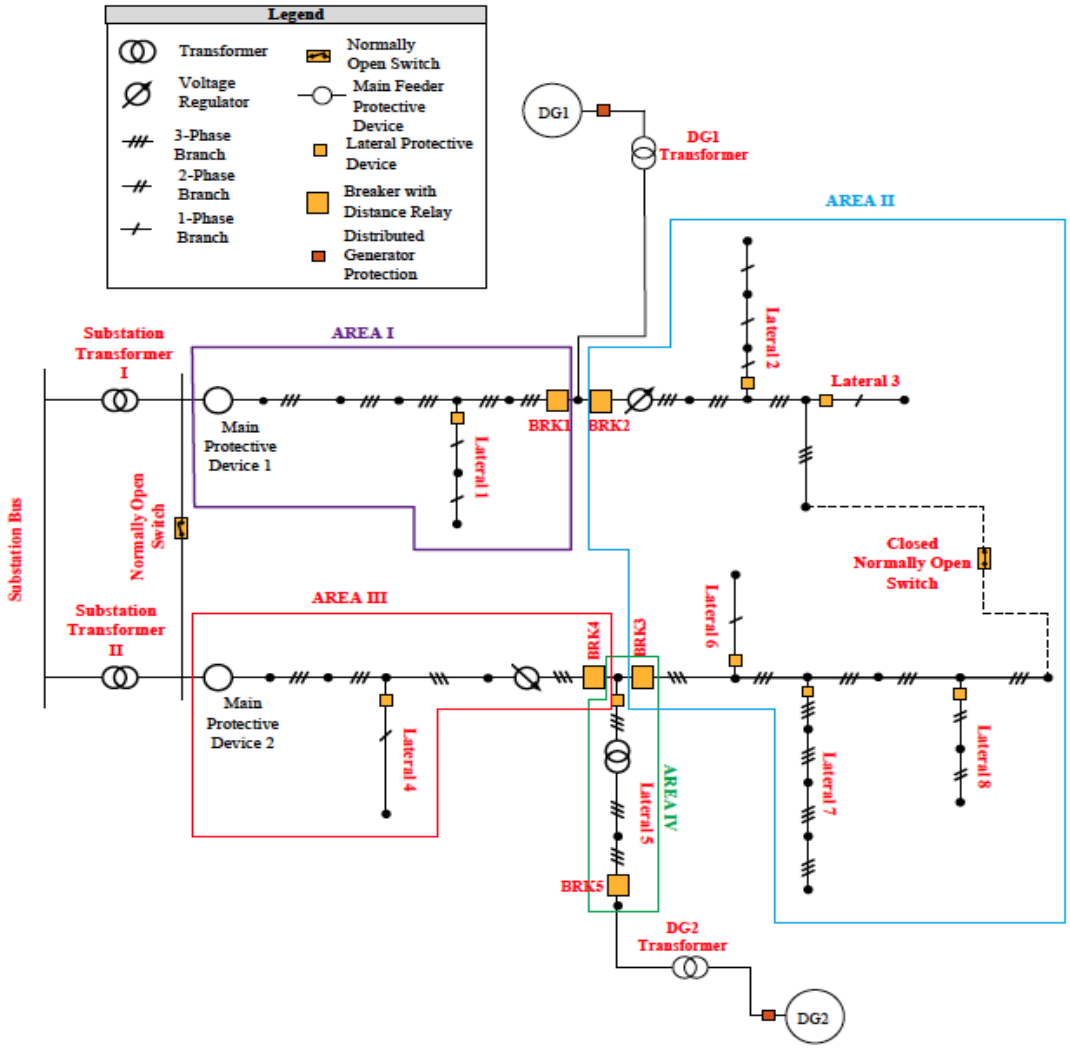

Fig. 3-1. Application of protection scheme [26]to two sample radial feeders.

The protection scheme [26] performs three tasks: 1) Breaking up the loop, 2) Clearing the fault, and 3) Manual reclosing to return to Meshed Operation.

3.1.2 Breaking Up the Loop

Distance relays are added to the breakers at the boundaries of the protection coordination areas. The distance relays distinguish between faults occurring in the protection coordination areas by measuring the impedance of the line segment in the area. The threshold with which distance relays are set is known as a mho circle - a circle whose circumference passes through the origin and whose diameter signifies the length of the line segment that is to be protected. Distance relays function by comparing the fault current against the voltage at the relay location to determine the impedance down the protected line to the fault. During normal operating conditions, the relay sees the impedance of the load downstream of the relay. When there is a fault on the line, the impedance seen by the distance relay will be in the zone of operation, demarcated by the circumference of the mho circle. The distance relays are coordinated with each other by a pilot distance modified POTT scheme. This is backed up by a non-pilot distance protection scheme, since the modified POTT scheme may fail due to the breakdown of a communication channel or excessive noise. In the modified POTT scheme, which is an overreaching pilot distance protection scheme, the thresholds for distance relays at the boundaries of the protection coordination area are set as a multiple of the fixed impedance of the line segment in the protection coordination area. For a fault in any of the protection coordination areas, both distance relays at the boundaries of a protection coordination area must detect the fault so that one or more breakers open and all of the

DGs connected to the faulted section are disconnected while the DGs on the unfaulted section remain connected.

The modified POTT scheme depends on the zone 2 overreaching phase and ground elements of the distance relays to detect a fault in the protection area. The reach of the zone 2 phase and ground elements for each distance relay is set to cover all the protected line plus 20%-50% of the next line segment. In the conventional POTT scheme, when a fault in the protected area is detected by the zone 2 elements of each distance relay, both breakers open thereby de-energizing and isolating the protected line. In the modified POTT scheme, depending on the connection point of the DG, one or more breakers open and some DGs are disconnected, such that the resulting faulted section is made radial.

For a DG connected to the main feeder, two coordination areas are formed, both of which are on the main feeder. Fig. 3-2 shows a distribution line segment AB on the main feeder that is to be 100% protected by the modified POTT scheme. Zone 2 overreaching distance elements control breakers BRKA and BRKB. There may be DG connected upstream of bus A, in the direction of the substation and also DG connected downstream of bus B.

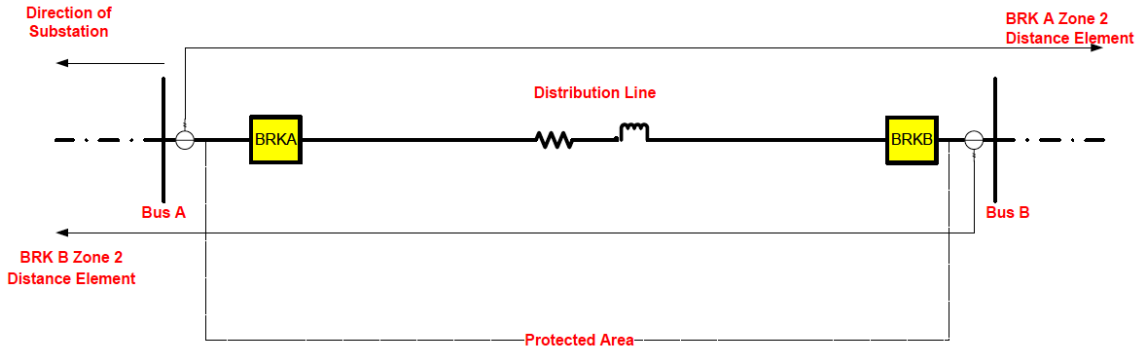

Fig. 3-2. One-line diagram illustrating modified POTT scheme on main feeder.

For a fault on the protected line segment AB, the overreaching zone 2 elements of the distance relays at bus A and B, both detect the fault. The breaker, BRKB, opens at high speed (80-90ms); and all connected DGs downstream of bus B remain connected, while all connected DGs upstream of bus A are disconnected. With BRKB open and all DGs upstream of bus A disconnected, the substation is the only source of short circuit current for the fault on line segment AB.

For a DG connected at the end of a lateral, three coordination areas are formed, two of which are on the main feeder, and one on the lateral. The modified POTT scheme for the coordination areas on the main feeder operate in the same way as when the DG is connected to the main feeder. The modified POTT scheme for the coordination area on the lateral, however, is slightly different. Fig. 3-3 shows a lateral line segment that is to be 100% protected by the modified POTT scheme. The DG is connected to the end of the lateral at the bus downstream of BRKB. The distance relay at BRKA has both a forward and a reverse distance element and the coordination area is formed between its distance relay and the distance relay at BRKB.

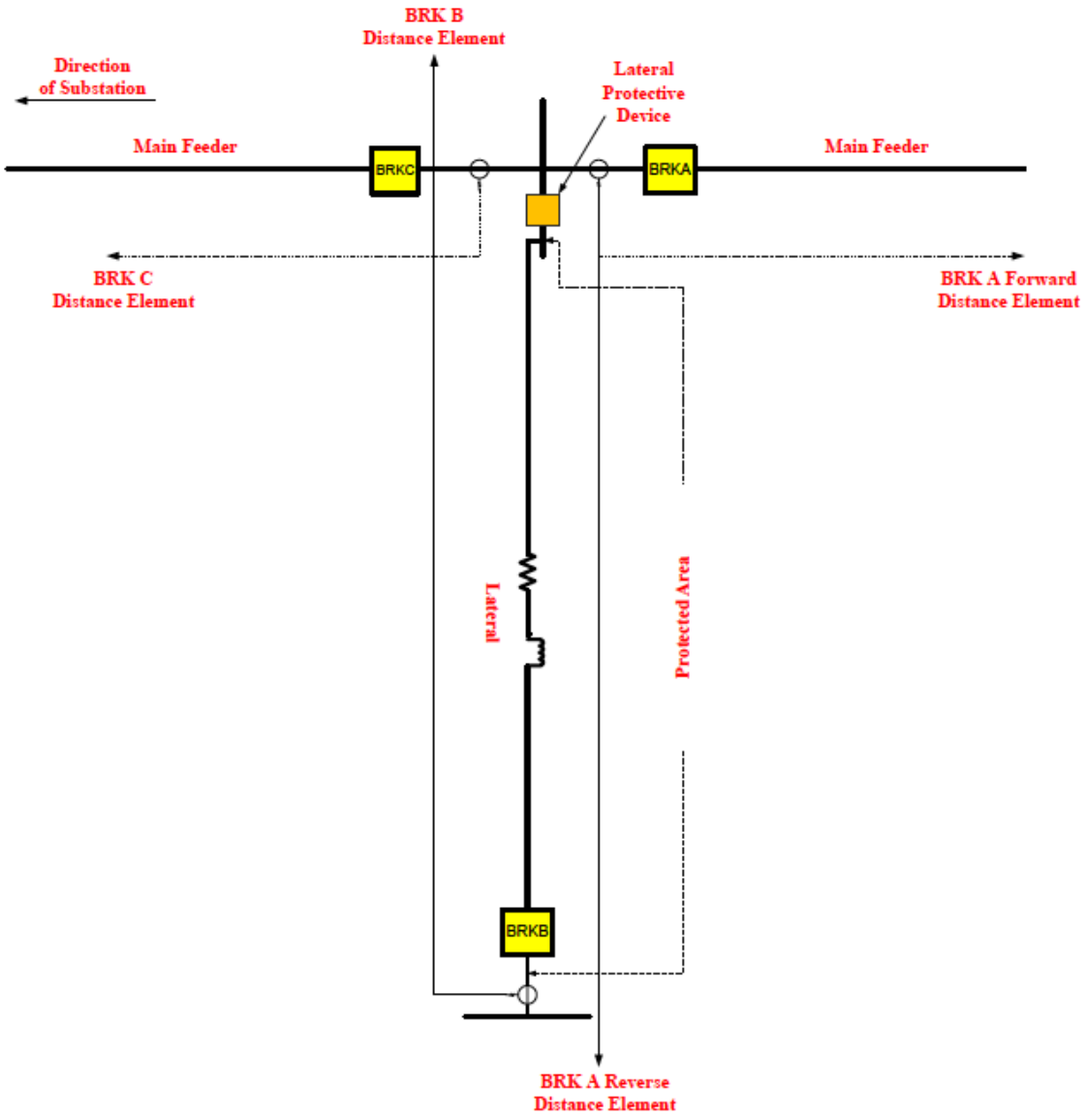

Fig. 3-3. One-line diagram illustrating modified POTT scheme on a lateral.

When a fault occurs in the protected area, the overreaching zone 2 elements of the distance relays at BRKA and BRKB detect the fault. Both breakers, BRKA and BRKB, open at high speed; all connected DGs downstream of BRKB and upstream of BRKC are disconnected; and all connected DGs downstream of BRKA, remain

connected. The portion of the feeder from the substation to the terminals of BRKB is now a faulted radial section of the distribution system.

The modified POTT scheme for Area I through Area IV in Fig. 3-1 can be explained as follows:

Area I: In this coordination area, *Main Protective Device 1* and BRK1 are coordinated with each other via the modified POTT scheme. This suggests that a distance function is added to *Main Protective Device 1*. When there is a fault in this area on the main feeder (or lateral), BRK1 opens, allowing DG1 to continue to supply the unfaulted section of the system. The faulted section is now radial and extends from the substation transformer I to the terminals of BRK1.

Area II: In this area, BRK2 and BRK3 are coordinated with each other via the modified POTT scheme and BRK3 will open when a fault is detected. DG1 will be disconnected using its own generator protection, making the faulted section radial. This radial segment extends from substation transformer 1 to the terminals of BRK3 on feeder 2. DG2 remains connected to the unfaulted section of the system.

Area III: For faults in Area III, a similar approach is taken as for Area I; *Main Protective Device 2* and BRK4 are coordinated with each other via the modified POTT scheme and BRK4 will open during fault. The radial faulted section extends from the substation transformer II to the terminals of BRK4.

Area IV: In this area – a lateral, BRK3 and BRK5 are coordinated with each other via the modified POTT scheme. This implies that BRK3 has the ability to detect faults in the reverse direction. When a fault occurs on the lateral, both BRK3 and BRK5 open,

and DG2 is disconnected from the system. The faulted section, which is radial, extends from *Substation Transformer II* to the terminals of BRK5.

3.1.3 Clearing the Fault

The second task of the protection scheme is to clear temporary faults or isolate permanent faults when the modified POTT scheme returns the faulted section to a radial topology. Overcurrent protective devices such as reclosers, fuses and overcurrent relays are used to clear or isolate the fault when the modified POTT scheme has operated to break up the loop. The radial segments that are formed after the loop is broken up by the modified POTT scheme were discussed in Section 3.1.2. Referring to Fig. 3-1, Table 3-1 shows the radial segments that are formed, the main source of fault current, and the primary overcurrent protective device for faults on the main feeder in the respective protection coordination area. Coordination between OCPDs in RDS was discussed in Section 2.2.4.

Table 3-1 Primary Overcurrent Protective Devices for Faults on the Main Feeder for Second Task of Protection Scheme

Radial Segment	**From**	**To**	**Source**	**Primary Protective Device**
I	Substation 1	BRK1	Substation Transformer 1	Main Protective Device 1
II	Substation 1	BRK3	Substation Transformer 1	Main Protective Device 1
III	Substation 2	BRK4	Substation Transformer 2	Main Protective Device 2
IV	Substation 2	BRK5	Substation Transformer 2	Main Protective Device 2

3.1.4 Reclosing to Return to Meshed Operation

The third task of the protection scheme is to return the distribution system into meshed operation by manually reclosing the breakers that were opened by the modified POTT scheme. This reclosing needs a synchronism-check and should only be performed after ensuring that the fault has been isolated.

3.2 Improving the Sensitivity of the Substation Overcurrent Relay of the Protection Scheme

The reach of the substation overcurrent relay in RDSs is set to protect the full length of the feeder. The pickup settings of the substation relay are computed based on the maximum load of the entire feeder and the minimum fault current of the feeder. The pickup settings of the substation relay is normally set to 1.5 times the normal load current at maximum loading, obtained from load flow studies, and at least 2 times less than the minimum fault current, obtained from short circuit studies [41]. The substation relay should operate as the primary protective device for faults on the main feeder and the backup protective device for faults on laterals. The time the substation relay takes to operate as the primary protection for faults on the main feeder and as backup protection for faults on a lateral depends on the amount of fault current contributed by the substation. Furthermore, the fault current contribution from the substation depends on the type of fault and the electrical distance of the fault from the substation.

In [26], the length of the radial section formed by the modified POTT scheme, can be shorter or longer than the original length of the feeder. For example, Fig. 3-4

illustrates one of the resulting configurations of the distribution system after a fault has occurred on the main feeder of area II and the loop has been broken up by the modified POTT scheme. The distributed generator, DG1, on the main feeder has been disconnected and BRK3 is opened. The faulted section has a radial topology where the fault is fully sourced by *Substation Transformer I*, while the unfaulted segment has two sources of power, namely *Substation Transformer II* and DG2. *Main Protective Device 1* was designed to protect up to the end of *FEEDER 1*. The figure illustrates that the new radial configuration is longer than the original length of the radial feeder 1, that *Main Protective Device 1* was designed to protect. From the terminals of BRK3 to the end of *FEEDER 2,* is now a part of the faulted radial feeder. The fault current contribution from the substation is reduced due to the length and impedance of additional section of feeder from *FEEDER 2*. The substation relay under-reaches due to original settings of *Main Protective Device 1*, and may not be able to provide the necessary protection for the fault shown.

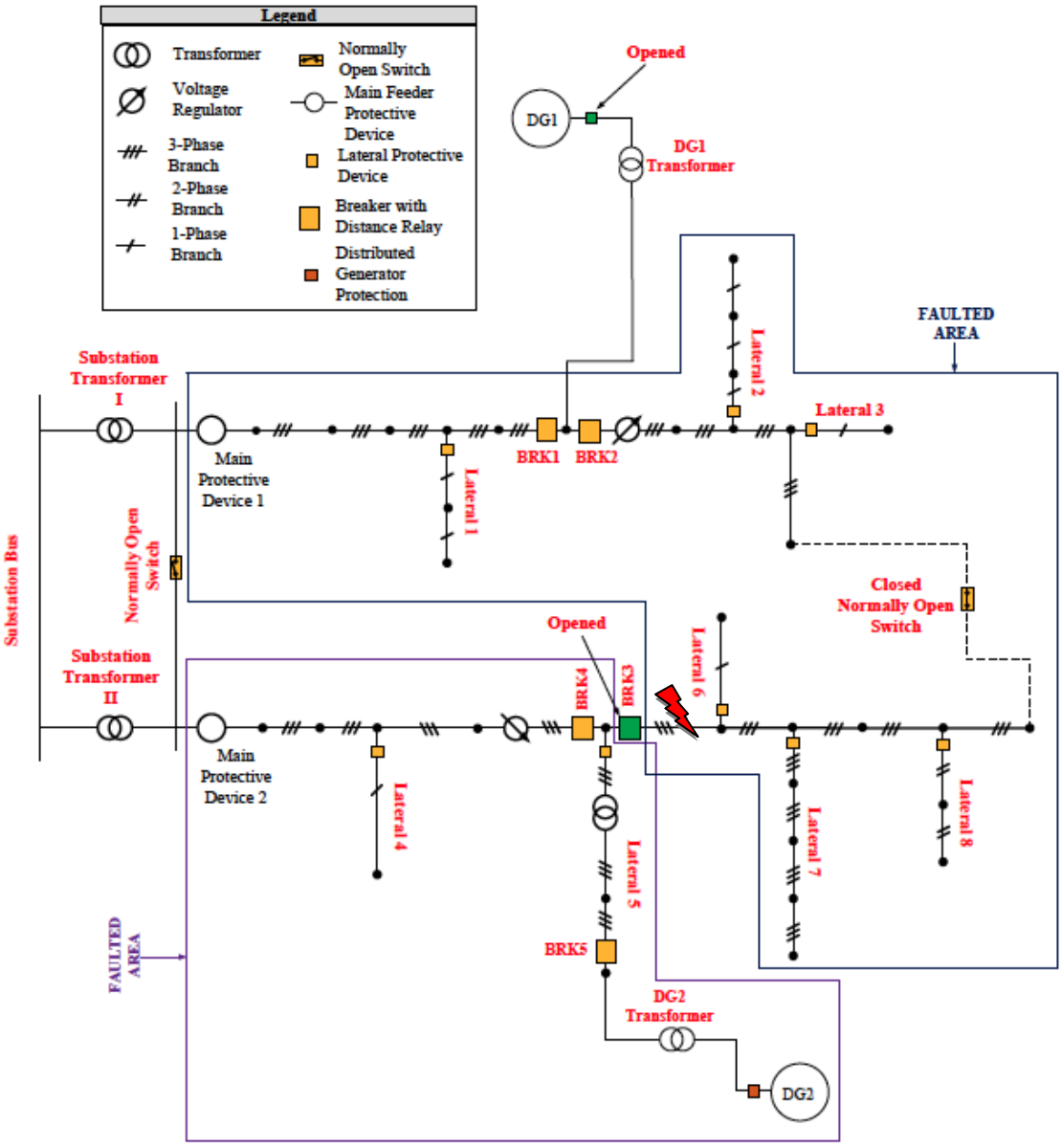

Fig. 3-4. A sample radial and non-radial topology when the closed loop system is broken up by the modified POTT scheme due to a fault.

Knowledge of the radial segments created by the modified POTT scheme and the loading within these segments can be used to provide the substation relay with settings for each radial segment. Loads in distribution systems change over time and based on

the customer's class (residential, commercial, industrial), only a limited amount of information about customer energy usage is available to the utility. Seldom do customers operate at maximum loading [30]. Additionally, the configuration changes in RDSs are taken into consideration for the settings of the system protective devices. In Section 2.2.3, it was discussed that smart meters can provide power demand information per customer over a specified time interval. Analysis of customer power demand data from smart meters can provide more precise load patterns and consumption data, which can be used to produce more comprehensive and accurate peak demand forecasts in distribution systems. These accurate peak demands can be used to provide settings for the substation relay for the faulted radial segments that are created by the modified POTT scheme of the protection method. According to [42], there are distinct peak demands for distribution systems based on the seasons of the year. Therefore, for each radial segment, smart meter data can be used to determine the peak demands of each season. The work reported in this thesis aims to improve the sensitivity of the substation relay by computing pickup settings for each season (Fall, Summer, Winter, Spring) for each possible radial segment, by using the smart meter load data from the previous year.

4 AN APPROACH FOR ADAPTING THE PICKUP SETTINGS OF SUBSTATION RELAYS IN A NON-ADAPTIVE PROTECTION SCHEME FOR RDS WITH DGS

4.1 Introduction

In this section, the solution methodology to increase the sensitivity of the substation relays when the protection scheme that discussed in Section 3.1.1, is applied to two radial feeders operated as a closed looped, is presented. A step-by-step method is presented, which utilizes smart meter load information to determine the pickup settings for the substation relays for each radial segment created by the protection scheme, for each season of the year. These seasonal pickup settings for each radial segment created by the modified POTT scheme of the protection scheme will be used to increase the sensitivity of the substation overcurrent relays.

4.2 Approach for Computation of Seasonal Pickup Settings for the Substation Overcurrent Relay

Customers on distribution systems can be classified as residential, commercial or industrial. In a smart distribution system, it is expected that these distribution customers will have smart meters installed at their household or facility. To determine the seasonal settings for the substation relay using smart meter data, the seasonal load of the prior year downstream of the substation relay is determined. This is done by using the measurements made available by the smart meters at all utility customer locations on the

secondary distribution system. Individual customer daily demand information measured by the smart meters is aggregated in order to compute the daily diversified demand per distribution transformer. The number of distribution transformers in the distribution system is known by the utility. The steps below outline the methodology for using smart meter data to obtain the seasonal settings for the substation overcurrent relay.

Step 1: Obtain the per interval demand per customer for each day of the prior year on the distribution system from smart meter measurements. Most manufactured smart meters are capable of providing this information. For customers connected to phase, x, of the distribution system, the demand for a customer, k, for a day, d, is obtained by storing each per interval demand per customer in a (1xm) vector as shown in (1). For three-phase customers, each per interval demand is computed on a per phase basis, and stored using (1).

$$ {}_{x}\mathbf{P}_{k}^{d}(\Delta t) = \left[{}_{x}P_{k}^{d}(\Delta t_1),\ {}_{x}P_{k}^{d}(\Delta t_2),\ldots,\ {}_{x}P_{k}^{d}(\Delta t_m) \right]_{1\times m} \quad \text{(kW)} \qquad (1) $$

where ${}_{x}\mathbf{P}_{k}^{d}(\Delta t)$ is a vector of m per interval demands for customer, k, connected to phase, x, for day, d; ${}_{x}P_{k}^{d}(\Delta t_m)$ is the demand of customer, k, connected to phase, x, of the distribution system, at the m^{th} demand interval, for day, d;. To obtain the daily per interval demand for customer, k, connected to phase, x, for a year, each row vector, ${}_{x}\mathbf{P}_{k}^{d}(\Delta t)$, is stored as a row in a matrix as shown in (2).

$$ {}_{x}\mathbf{P}_{k}(\Delta t) = \begin{bmatrix} {}_{x}\mathbf{P}_{k}^{1}(\Delta t) \\ {}_{x}\mathbf{P}_{k}^{2}(\Delta t) \\ \vdots \\ {}_{x}\mathbf{P}_{k}^{365}(\Delta t) \end{bmatrix}_{d\times m} \quad (kW) \tag{2} $$

where ${}_{x}\mathbf{P}_{k}(\Delta t)$ is a (365xm) matrix, and element $\left[{}_{x}P_{k}(\Delta t)\right]_{d,m}$ refers to customer, k's, m^{th} per interval demand for a specified day, d, of the year, on phase, x, of the distribution system.

Step 2: Compute each per interval diversified demand for each distribution transformer, g, connected to phase, x, of the distribution system, for each day, d, of the prior year. The per interval diversified demand for a day, of a single-phase distribution transformer that serves a group of customers is the sum of the individual customer demands on the same phase, over each demand interval, during the same day. This can be obtained using (3).

$$ {}_{x}\mathbf{T}_{g}^{d}(\Delta t) = \left[\sum_{k=1}^{n} {}_{x}\mathbf{P}_{k}^{d}(\Delta t) \right]_{1\times m} \quad (kW) \tag{3} $$

where ${}_{x}\mathbf{T}_{g}^{d}(\Delta t)$ is a (1xm) vector of the per interval diversified demands for distribution transformer, g, connected to phase, x, of the distribution system, for day, d; ${}_{x}\mathbf{P}_{k}^{d}(\Delta t)$ is a (1xm) row vector of m per interval demands for customer, k, connected to phase, x, for day, d; n is the number of customers served by the distribution transformer. The per interval diversified demand of distribution transformer, g, on phase, x, for each day, d, of the year, is determined using (4).

$$ {}_{x}\mathbf{T}_{g}(\Delta t) = \begin{bmatrix} {}_{x}\mathbf{T}_{k}^{1}(\Delta t) \\ {}_{x}\mathbf{T}_{k}^{2}(\Delta t) \\ \vdots \\ {}_{x}\mathbf{T}_{k}^{365}(\Delta t) \end{bmatrix}_{d\times m} \quad (\text{kW}) \tag{4} $$

where ${}_{x}\mathbf{T}_{g}(\Delta t)$ is (365xm) matrix; element $\left[{}_{x}T_{g}(\Delta t) \right]_{d,m}$ refers to the m^{th} per interval diversified demand for distribution transformer, g, on phase, x, for a specified day, d, of the year; n is the number of customers served by the distribution transformer.

Step 3: Determine the maximum per interval diversified demand for each day of the year, for each phase, in each radial segment. Each per interval diversified demand for a day, d, for a phase, x, in a radial segment, p, can be calculated by summing each per interval diversified demand for each distribution transformer, g, connected to the same phase, during the same day within the same radial segment using (5).

$$ {}_{x}\mathbf{RSP}_{p}^{d}(\Delta t) = \left[\sum_{g=1}^{t} {}_{x}\mathbf{T}_{g}^{d}(\Delta t) \right]_{1\times m} \quad (\text{kW}) \tag{5} $$

where ${}_{x}\mathbf{RSP}_{p}^{d}(\Delta t)$ is a (1xm) row vector of the per interval diversified demands for phase, x, of radial segment, p, for day, d; ${}_{x}\mathbf{T}_{g}^{d}(\Delta t)$ is a (1xm) row vector of the per interval diversified demands for day, d, of distribution transformer, g, connected to phase, x; t is the number of distribution transformers in radial segment, p, on phase, x. The maximum per interval diversified demand for day, d, on phase, x, in radial segment, p, is calculated using (6).

$$ {}_{x}D_{p}^{d} = \max\left[{}_{x}\mathbf{RSP}_{p}^{d}(\Delta t)\right]_{1\times m} \text{ (kW)} \tag{6} $$

where ${}_{x}D_{p}^{d}$ is the maximum per interval diversified demand for day, d, on phase, x, in radial segment, p; ${}_{x}\mathbf{RSP}_{p}^{d}(\Delta t)$ is a (1xm) row vector of the per interval diversified demands for phase, x, in radial segment, p, for day, d. The per interval diversified demand of phase, x, in radial segment, p, for each day of the year, is obtained using (7).

$$ {}_{x}\mathbf{RSP}_{p}(\Delta t) = \begin{bmatrix} {}_{x}\mathbf{RSP}_{p}^{1}(\Delta t) \\ {}_{x}\mathbf{RSP}_{p}^{2}(\Delta t) \\ \vdots \\ {}_{x}\mathbf{RSP}_{p}^{365}(\Delta t) \end{bmatrix}_{d\times m} \text{ (kW)} \tag{7} $$

where ${}_{x}\mathbf{RSP}_{p}(\Delta t)$ is (365xm) matrix; element $\left[{}_{x}RSP_{p}(\Delta t)\right]_{d,m}$ refers to radial segment, p's, per interval diversified demand for day, d, of the year. The maximum diversified per interval demand for each day of the year is shown in (8).

$$ {}_{x}\mathbf{D}_{p} = \begin{bmatrix} {}_{x}D_{p}^{1} \\ {}_{x}D_{p}^{2} \\ \vdots \\ {}_{x}D_{p}^{365} \end{bmatrix}_{d\times 1} \text{ (kW)} \tag{8} $$

where ${}_{x}\mathbf{D}_{p}$ is a (365x1) column vector of maximum per interval diversified demands for each day, d, of the year for phase, x, of radial segment, p; ${}_{x}D_{p}^{d}$ is the maximum diversified per interval demand for day, d, on phase, x, in radial segment, p.

Step 4: Determine the seasonal maximum diversified demand for each phase, in each radial segment. Apportion the column vector, ${}_{x}\mathbf{D}_{p}$, into the maximum diversified

demands for phase, x, in radial segment, p, for each season, ${}_{x}\mathbf{D}_{p}^{season}$ [(9)-(12)]. The seasons of the year are winter, spring, summer and autumn (or fall). Table 4-1 shows the number of days, the beginning and ending months, and the range of days, assuming a 365-day year, of the seasons of the year.

Table 4-1 The Number of Days and the Months that Make Up the Seasons of the Year

Season	Number of Days	Beginning Month	Ending Month	Day Range
Winter	90	December	January	335-365, 1-59
Spring	92	February	May	60-151
Summer	92	June	August	152-243
Fall	91	September	November	244-334

$$ {}_{x}\mathbf{D}_{p}^{Winter} = \left[{}_{x}D_{p}^{1}, {}_{x}D_{p}^{2},\ldots, {}_{x}D_{p}^{59}, {}_{x}D_{p}^{335},\ldots, {}_{x}D_{p}^{365} \right]^{T} \quad (kW) \tag{9} $$

$$ {}_{x}\mathbf{D}_{p}^{Spring} = \left[{}_{x}D_{p}^{60}, {}_{x}D_{p}^{61},\ldots, {}_{x}D_{p}^{151} \right]^{T} \quad (kW) \tag{10} $$

$$ {}_{x}\mathbf{D}_{p}^{Summer} = \left[{}_{x}D_{p}^{152}, {}_{x}D_{p}^{153},\ldots, {}_{x}D_{p}^{243} \right]^{T} \quad (kW) \tag{11} $$

$$ {}_{x}\mathbf{D}_{p}^{Fall} = \left[{}_{x}D_{p}^{244}, {}_{x}D_{p}^{245},\ldots, {}_{x}D_{p}^{334} \right]^{T} \quad (kW) \tag{12} $$

where ${}_{x}\mathbf{D}_{p}^{Winter}$, ${}_{x}\mathbf{D}_{p}^{Spring}$, ${}_{x}\mathbf{D}_{p}^{Summer}$, and ${}_{x}\mathbf{D}_{p}^{Fall}$ represents a vector of the maximum per interval diversified demands for each day of each season (Winter, Spring, Summer and Spring) of the year, for phase, x, in radial segment, p. Select and store the greatest maximum diversified demand value for each season, for each phase, in each radial segment. The greatest seasonal maximum diversified demand value for phase, x, in radial segment, p, is found using (13)-(16).

$$ {}_{x}\mathrm{SMDD}_{p}^{\mathrm{Winter}} = \max\left[{}_{x}\mathbf{D}_{p}^{\mathrm{Winter}} \right] \quad (\mathrm{kW}) \tag{13} $$

$$ {}_{x}\mathrm{SMDD}_{p}^{\mathrm{Spring}} = \max\left[{}_{x}\mathbf{D}_{p}^{\mathrm{Spring}} \right] \quad (\mathrm{kW}) \tag{14} $$

$$ {}_{x}\mathrm{SMDD}_{p}^{\mathrm{Summer}} = \max\left[{}_{x}\mathbf{D}_{p}^{\mathrm{Summer}} \right] \quad (\mathrm{kW}) \tag{15} $$

$$ {}_{x}\mathrm{SMDD}_{p}^{\mathrm{Fall}} = \max\left[{}_{x}\mathbf{D}_{p}^{\mathrm{Fall}} \right] \quad (\mathrm{kW}) \tag{16} $$

where ${}_{x}\mathrm{SMDD}_{p}^{s}$ is the maximum 15-minute diversified demand for season, s, for phase, x, of radial segment, p.

Step 5: For each radial segment, determine the overcurrent substation relay's pickup settings based on the seasonal maximum diversified demand in step 4. The phase current corresponding to the seasonal maximum diversified demand power per phase in each radial segment is obtained by taking the ratio of each of the seasonal maximum diversified demand per phase in each radial segment to the primary line-to-ground voltage of the distribution system. This is shown in (17)-(20).

$$ \left| {}_{x}\mathrm{I}_{p}^{\mathrm{Winter}} \right| = \frac{{}_{x}\mathrm{SMDD}_{p}^{\mathrm{Winter}}}{|\mathrm{V_{ln}}|} \quad (\mathrm{A}) \tag{17} $$

$$ \left| {}_{x}\mathrm{I}_{p}^{\mathrm{Spring}} \right| = \frac{{}_{x}\mathrm{SMDD}_{p}^{\mathrm{Spring}}}{|\mathrm{V_{ln}}|} \quad (\mathrm{A}) \tag{18} $$

$$ \left| {}_{x}\mathrm{I}_{p}^{\mathrm{Summer}} \right| = \frac{{}_{x}\mathrm{SMDD}_{p}^{\mathrm{Summer}}}{|\mathrm{V_{ln}}|} \quad (\mathrm{A}) \tag{19} $$

$$ \left| {}_{x}\mathrm{I}_{p}^{\mathrm{Fall}} \right| = \frac{{}_{x}\mathrm{SMDD}_{p}^{\mathrm{Fall}}}{|\mathrm{V_{ln}}|} \quad (\mathrm{A}) \tag{20} $$

where ${}_{x}I_{p}^{s}$ is the phase current for phase, x, of radial segment, p, and season, s; V_{ln} is the line-to-ground voltage of the distribution system. In each radial segment and in each season, the largest current of each of the phases is used to calculate the pickup values for the substation relays. The pickup values of the substation relays are calculated by multiplying 1.5 times the largest phase current in each radial segment for each season.

The assumptions made in this solution methodology are:

a. Each customers' energy usage and per interval demand has been carefully monitored and understood over the prior year.
b. Seasonal weather is assumed to affect each customer's daily demand such that the cumulative disparity in each customer's energy usage will provide variations in the loading of the distribution system per season.
c. A communication medium exists between each distance relay and the substation relay, such that when the modified POTT scheme operates, a signal is sent to the substation relay such that the appropriate pickup setting is selected (based on the radial segment formed and the season of the year)

The proposed methodology is illustrated using the system shown in Fig. 4-1. The figure shows radial segment 1 obtained from Fig. 3-1. Radial segment I is formed when there is a fault in protection coordination area I and BRK1 opens by the modified POTT scheme. The group of houses in the square represents a group of five residential customers (P_1, P_2, P_3, P_4, P_5) with smart meters served from the same distribution

transformer, T1. The lateral, a single-phase (A-phase) lateral, to which T1 is connected, also serves another distribution transformer T2, which has two residential customers with smart meters.

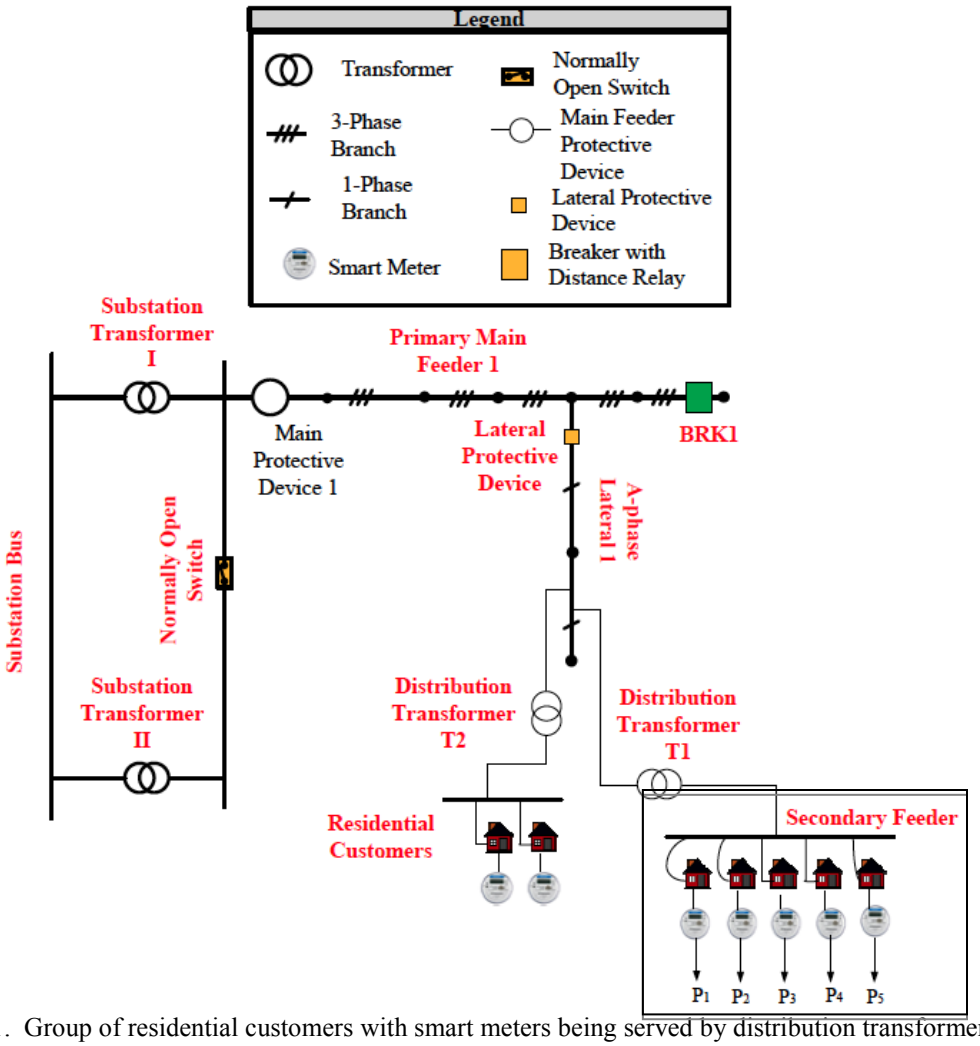

Fig. 4-1. Group of residential customers with smart meters being served by distribution transformers on Radial Segment 1 of Fig. 3-1

Step 1: In distribution systems, the smart meters at the customer locations compute the individual customer demands from their instantaneous power based on a specified

demand interval. A 15-minute demand interval is chosen for the smart meters shown in Fig. 4-1 for illustration purposes. A sample of P_1's 15-minute demand curve for a day is shown in Fig. 4-2, which can be obtained by the smart meter. Each bar in the graph represents, ${}_{x}P_k^d(\Delta t_m)$ of (1), where ${}_{A}P_1^1(\Delta t_m)$ is customer P_1's 15-minute demand at the m^{th} demand interval, for day 1 on phase, A, of the distribution system. All of Customer P_1's 15-minute demands are stored in ${}_{A}\mathbf{P}_1^1 = \left[{}_{A}P_1^1(\Delta t_1), {}_{A}P_1^1(\Delta t_2), \ldots {}_{A}P_1^1(\Delta t_{96}) \right]$, which represents a vector of Customer P_1's 15-minute demand for day 1, on phase x. The amount of 15-minute demands in a day is 96, which corresponds to the number of bars in of the graph in Fig. 4-2.

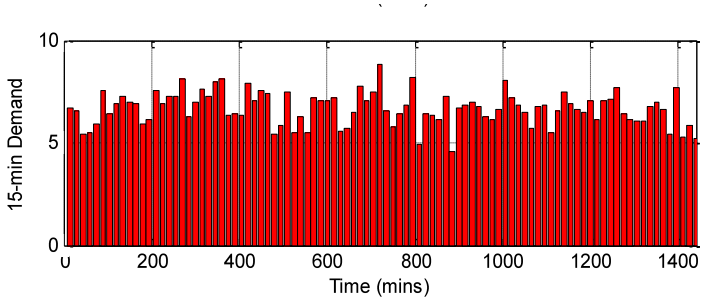

Fig. 4-2. Sample of Customer 1, P_1, on distribution transformer T1, discretely sampled instantaneous demand and 15-minute demand for day 1.

The demand curves for customers P_2 to P_5 for a day are shown in Fig. 4-3, Fig. 4-4, Fig. 4-5, and Fig. 4-6, respectively.

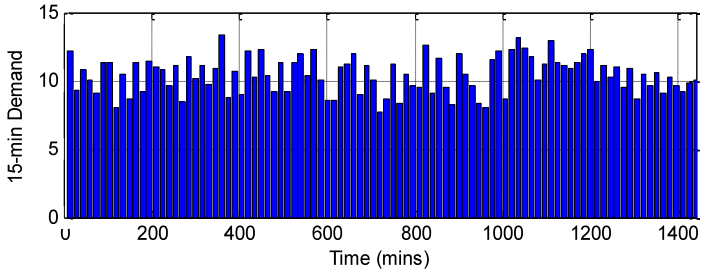

Fig. 4-3. Sample of Customer 2, P_2, on distribution transformer T1, discretely sampled instantaneous demand and 15-minute demand for day 1.

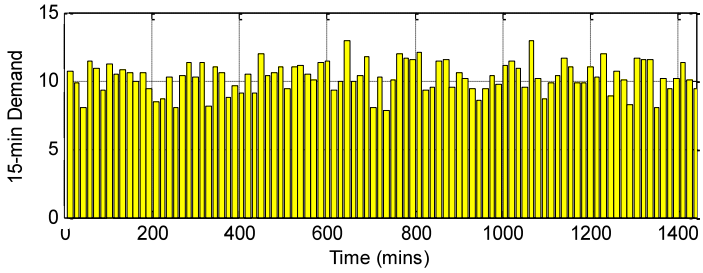

Fig. 4-4. Sample of Customer 3, P_3, on distribution transformer T1, discretely sampled instantaneous demand and 15-minute demand for day 1.

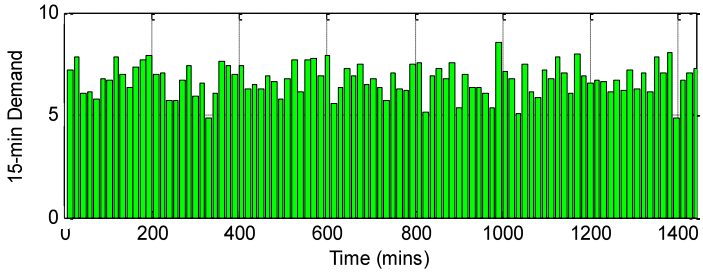

Fig. 4-5. Sample of Customer 4, P_4, on distribution transformer T1, discretely sampled instantaneous demand and 15-minute demand for day 1.

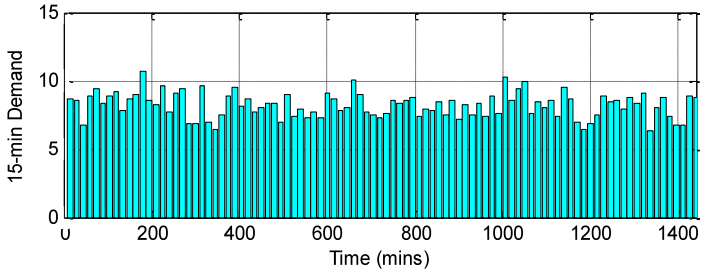

Fig. 4-6. Sample of Customer 5, P_5, on distribution transformer T1, discretely sampled instantaneous demand and 15-minute demand for day 1.

The 15-minute demand curves for the same day for the two customers that are fed from distribution transformer T2 are shown in Fig. 4-7 and Fig. 4-8.

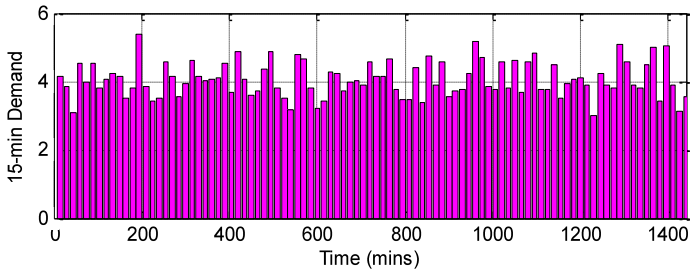

Fig. 4-7. Sample of Customer 1 on distribution transformer T2 discretely sampled instantaneous demand and 15-minute demand for day 1.

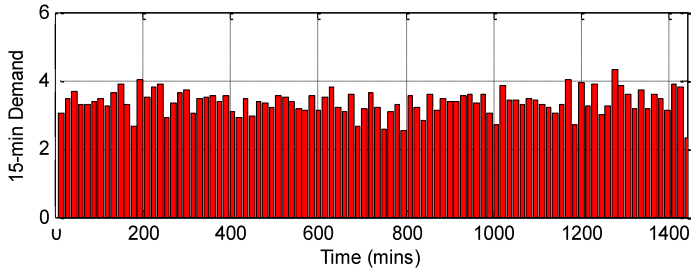

Fig. 4-8. Sample of Customer 2 on distribution transformer T2 discretely sampled instantaneous demand and 15-minute demand for day 1.

Step 2: The day 1 15-minute diversified demand of distribution transformer, T1, found by using (3), is the sum of the 96 15-minute demands of each customer served by T1 on phase, A, of the distribution system.

$$ {}_{\mathbf{A}}\mathbf{T}_1^1 = \sum_{k=1}^{5} {}_{\mathrm{A}}\mathbf{P}_k^1 = {}_{\mathrm{A}}\mathbf{P}_1^1 + {}_{\mathrm{A}}\mathbf{P}_2^1 + {}_{\mathrm{A}}\mathbf{P}_3^1 + {}_{\mathrm{A}}\mathbf{P}_4^1 + {}_{\mathrm{A}}\mathbf{P}_5^1 $$

Fig. 4-9 shows a sample of the day 1 15-minute diversified demand for all the customers that are served by transformer, T1. The x-axis is the time in minutes for a day, and the y-axis is the transformer's diversified demand for a 15-minute demand interval.

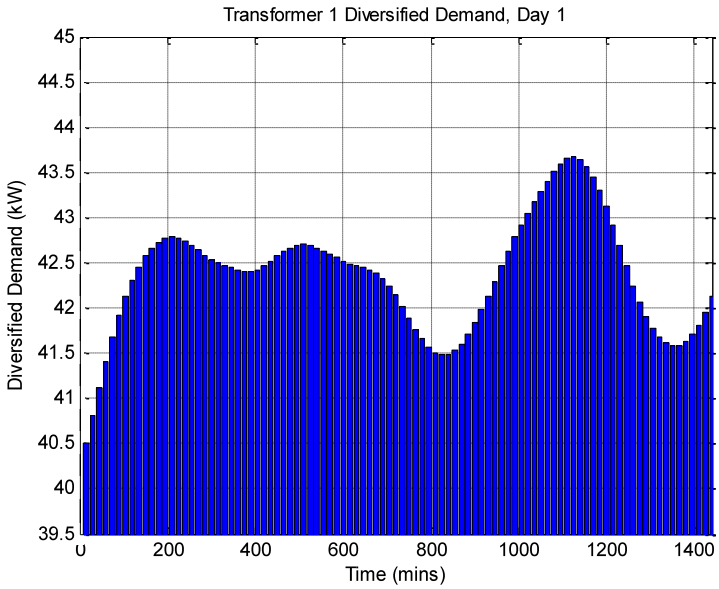

Fig. 4-9. Sample of the diversified 15-minute demand for distribution transformer, T1, for day 1.

The 15-minute diversified demand of day 1 for distribution transformer, T2, is also found using (3), and is illustrated in Fig. 4-10.

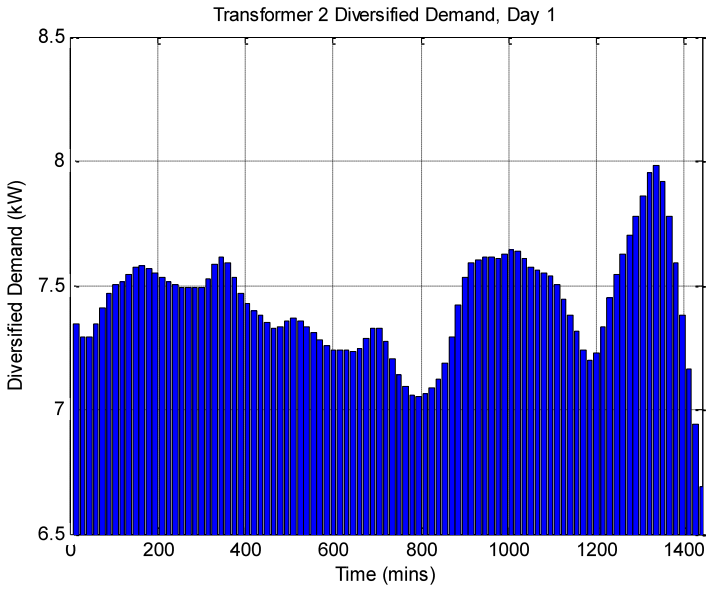

Fig. 4-10. Sample of the diversified 15-minute demand for distribution transformer, T2, for day 1.

Step 3: Radial segment I is created when there is a fault detected in Area I of Fig. 3-1. BRK1 opens after the distance relay at BRK1 and main protective device 1 detect a fault in protection coordination area I. The radial segment is sourced by substation transformer I. The primary distribution level view of radial segment 1 is shown in Fig. 4-11.

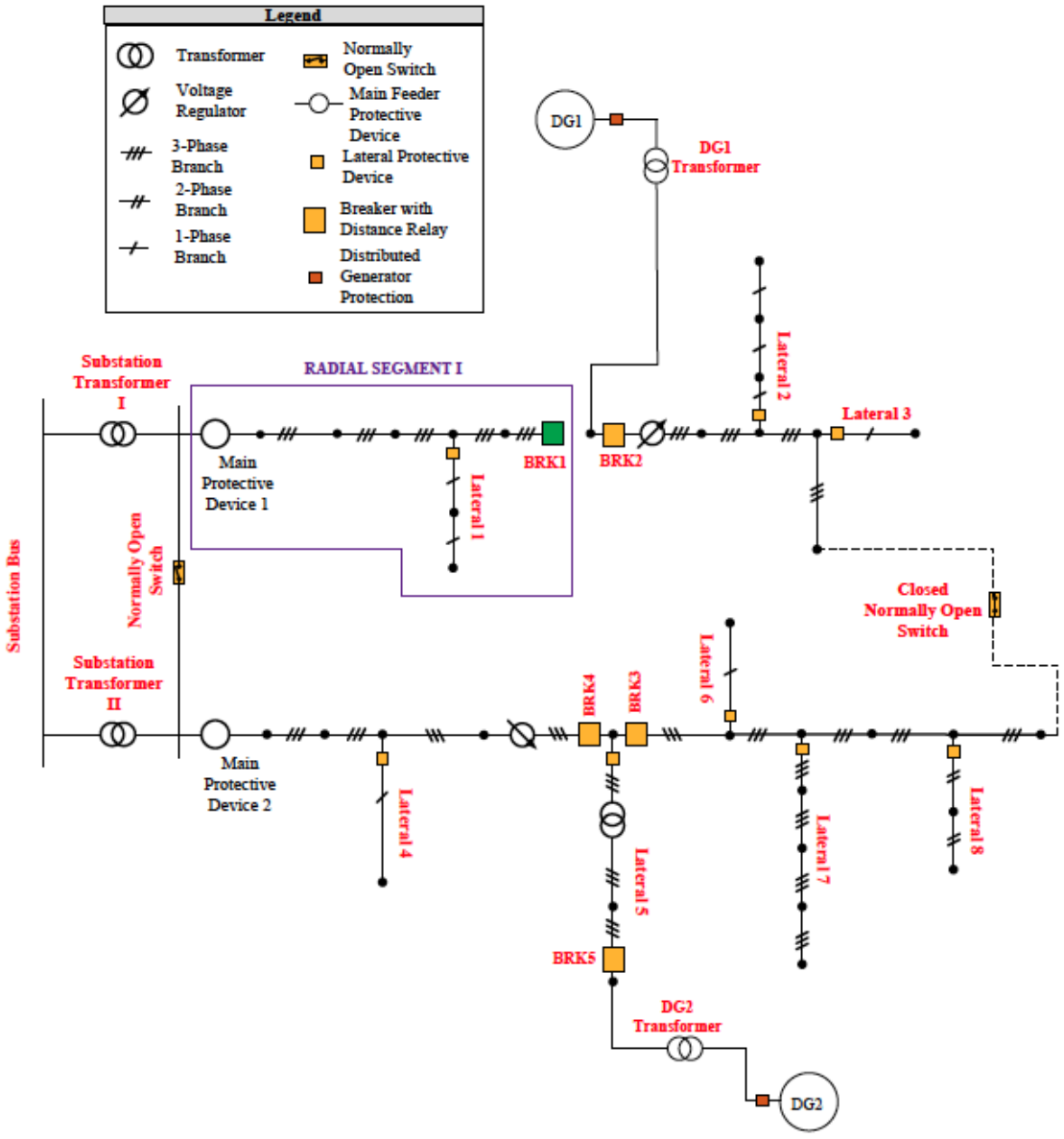

Fig. 4-11. Sample of radial segment I for fault in Area I.

Fig. 4-1 showed the secondary distribution level of radial segment I, and the number of distribution transformers in this radial segment is 2. Both of these distribution transformers are connected to phase A of the primary distribution circuit in

radial segment I. With the number of distribution transformers known, the day 1 15-minute diversified demands for phase A of radial segment I can be calculated using (5).

$$ {}_{A}\mathbf{RSP}_{1}^{1}(\Delta t) = \sum_{g=1}^{2} {}_{A}\mathbf{T}_{g}^{d}(\Delta t) = {}_{A}\mathbf{T}_{1}^{1}(\Delta t) + {}_{A}\mathbf{T}_{2}^{1}(\Delta t) $$

The maximum 15-minute diversified demand for day 1 for phase A of radial segment I is the greatest value of the 96 15-minute diversified demands for day 1 for phase A of radial segment 1. This is determined using (6).

$$ {}_{A}D_{1}^{1} = \max\left[{}_{A}\mathbf{RSP}_{1}^{1}(\Delta t) \right] $$

A sample of the 15-minute diversified demand for day 1 and the corresponding maximum diversified demand for the same day of radial segment I is shown in Fig. 4-12.

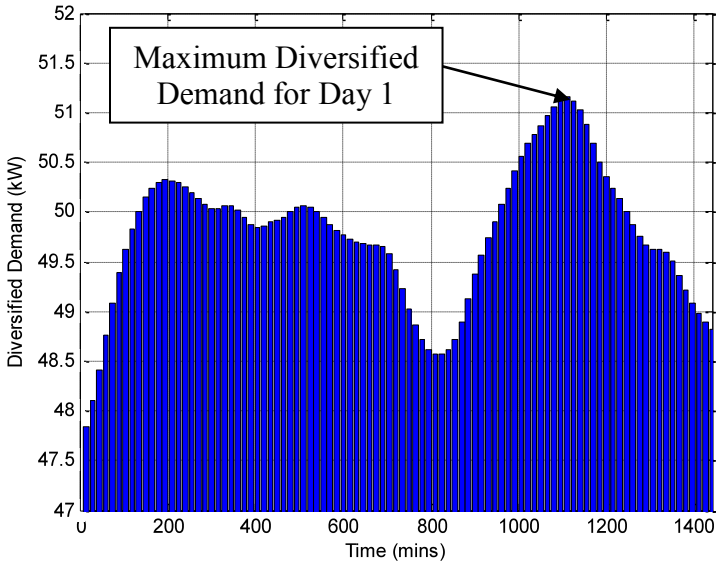

Fig. 4-12. Sample of 15-minute diversified demand and maximum diversified demand for a day of radial segment I.

Step 4: Steps 1-3 is done for every day of the year. When this is done, the daily maximum 15-minute diversified demands for a year for each phase of each radial segment would be known. The year is then divided into four seasons and the greatest maximum diversified 15-minute demand value from each season for each phase of each radial segment is chosen. Table 4-2 shows the maximum diversified demands that would be obtained for each phase of each radial segment for all four seasons. In each radial segment, the largest values per phase are chosen for each season and these values represent the radial segment's seasonal maximum diversified demand.

Table 4-2 Seasonal Maximum Diversified Demand per Radial Segment of the Sample Distribution System

Radial Segment	Winter (kW)			Spring (kW)			Summer (kW)			Fall (kW)		
	Phase A	Phase B	Phase C	Phase A	Phase B	Phase C	Phase A	Phase B	Phase C	Phase A	Phase B	Phase C
I												
II												
III												
IV												

Step 5: The number of possible pick-up settings that each substation overcurrent relay would contain depends on the number of radial segments that each substation transformer sources (Refer to Table 3-1). The current corresponding to the seasonal maximum diversified demands for each radial segment is found by dividing the latter by the line-to-ground voltage of the primary distribution system voltage. There are 8 settings available for each substation overcurrent relay because each substation transformer sources two radial segments. The pickup settings for substation relay I are:

$$1.5 \times \begin{bmatrix} I_1^{Fall} & I_2^{Fall} \\ I_1^{Winter} & I_2^{Winter} \\ I_1^{Spring} & I_2^{Spring} \\ I_1^{Summer} & I_2^{Summer} \end{bmatrix}$$

and the pickup settings for substation relay II are:

$$1.5 \times \begin{bmatrix} I_3^{Fall} & I_4^{Fall} \\ I_3^{Winter} & I_4^{Winter} \\ I_3^{Spring} & I_4^{Spring} \\ I_3^{Summer} & I_4^{Summer} \end{bmatrix}$$

where I_p^s represents the seasonal maximum current downstream of the substation during season, s, and radial segment, p.

A communication medium is required such that when a distance relay operates for a fault in its protected area, a signal is simultaneously sent to the respective substation overcurrent relay. The substation relay is then able to choose the appropriate pickup setting based on the radial segment formed and the current season of the year. The information that the substation relays contain is shown in Fig. 4-13.

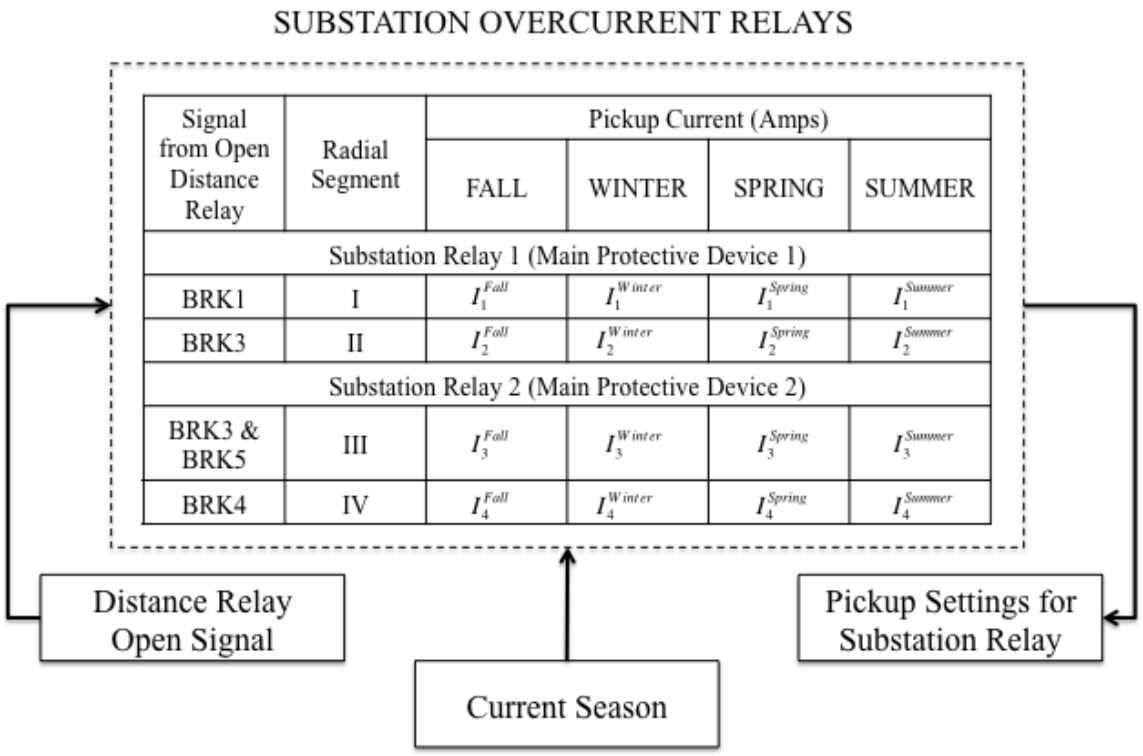

Fig. 4-13. The overview of the substation adaptive overcurrent relay with several pickup settings.

4.3 Summary

The protection scheme presented by Viawan [26] utilized distance relays coordinated by a modified POTT scheme to form protection areas on radial feeders, which are operated as closed loop systems with a high penetration of DG. When there is a fault in any of the protected areas, a breaker(s) is/are opened and some DGs are disconnected to make the faulted area radial, with only the substation being the source of fault current. Depending on the faulted area, several radial configurations are possible, thereby conceivably causing the substation overcurrent relay to underreach, overreach, or provide longer primary or backup trip times. An adaptive approach based on the

knowledge of the radial segments formed by the modified POTT scheme of the protection scheme and seasonal maximum diversified demand was discussed. With the fact that there is great disparity in customer power consumption during the season's of the year, utilizing smart meter data to determine the maximum diversified demand for each season and for each radial segment, allows for seasonal pickup settings for the substation overcurrent relay to be produced. When there is a fault in any of the protected areas as outlined by the protection scheme, the distance relay that operates to open its associated breaker, will send a signal to the appropriate substation relay. Furthermore, depending on the season, the substation relay will automatically choose a corresponding pickup setting and operate as primary or backup protection with increased sensitivity.

5 SIMULATIONS AND RESULTS

5.1 Introduction

The selected system for testing the proposed methodology was the IEEE 34 node radial test feeder [43]. The IEEE 34 node test feeder was revised into a multi-feeder system, which preserved the structure of the original test feeder. Synchronous-based DG, distance protection and overcurrent relays were added to the multi-feeder test system, in order to implement the non-adaptive protection scheme [26]. A secondary distribution design that included estimating the secondary load rating, transformer sizing, and the classification of customers, was developed to allow for the implementation and allocation of the smart meters. The multi-feeder test system was implemented in EMTP™/PSCAD® software and used to test the proposed methodology.

5.2 Simulation of a Multi-Feeder Test System

5.2.1 The IEEE 34 Node Radial Test Feeder

The IEEE 34 Node Radial Test Feeder [43] shown in Fig. 5-1 is a radial primary distribution feeder of a nominal voltage of 24.9 kV, which is fed from a substation transformer rated at 2.5 MVA, 69/24.9 kV. The feeder is very long with a total of eight laterals, of which, six are single phase and two are 3-phase, and is lightly loaded with a total load of 1.769 MW and 1.051 MVAr. The loading is unbalanced, with various spot loads – loads connected at a node, and distributed loads – loads connected between two

nodes. Furthermore, the loads are modeled as constant current, constant impedance and constant power loads. There are two in-line voltage regulators that are used to maintain a good voltage profile, because there is appreciable voltage drop due to the long length of some line segments. There is also an in-line transformer that is used to reduce the voltage from 24.9 kV to 4.16 kV. The types of cables that were used in the IEEE 34 Node Test Feeder are shown in Table 5-1 [43]. The table shows the phasing of the different types of cables used in the test feeder. The spacing ID signifies the spacing distance between the phase conductors and neutral conductors when the lines are mounted on a pole.

Table 5-1 Overhead Line Configurations for IEEE 34 Node Test Feeder [43]

Configuration	Phasing	Phase (ACSR)	Neutral (ACSR)	Spacing ID
300	BACN	1/0	1/0	500
301	BACN	#2	#2	500
302	AN	#4	#4	510
303	BN	#4	#4	510
304	BN	#2	#2	510

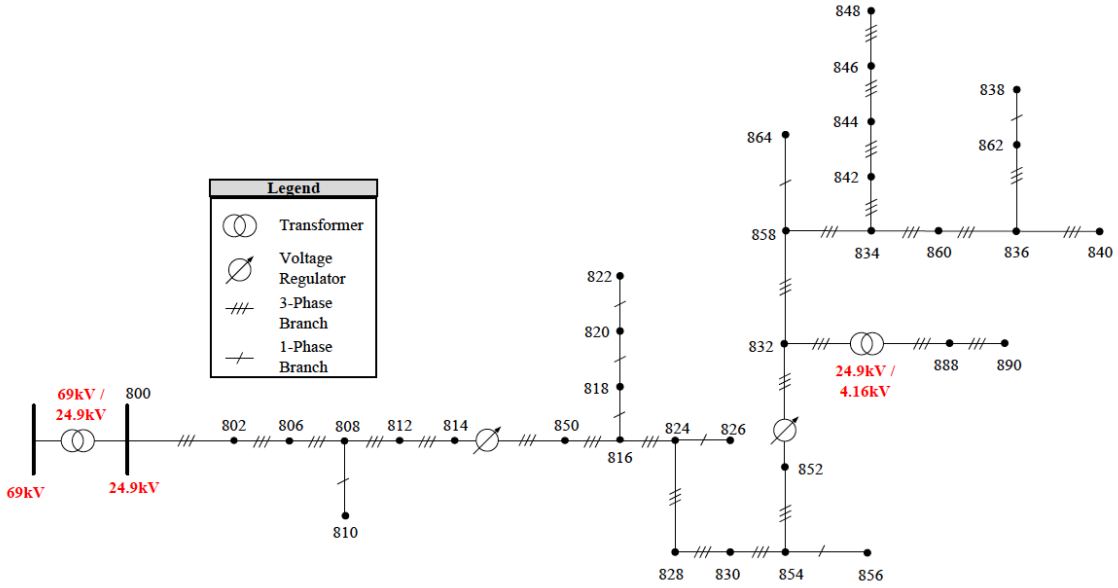

Fig. 5-1. IEEE 34 node test feeder (adopted from [43]).

5.2.2 The Multi-Feeder Test System

The IEEE 34 node test feeder was revised into a multi-feeder test system, shown in Fig. 5-2, which preserved the structure of the original test feeder. A dual bus substation configuration was adopted for the purpose of this work. This design provided a redundancy via the normally open switch located at node 800, which allowed both feeders to remain energized if a substation transformer failed or was taken out of service for maintenance purposes.

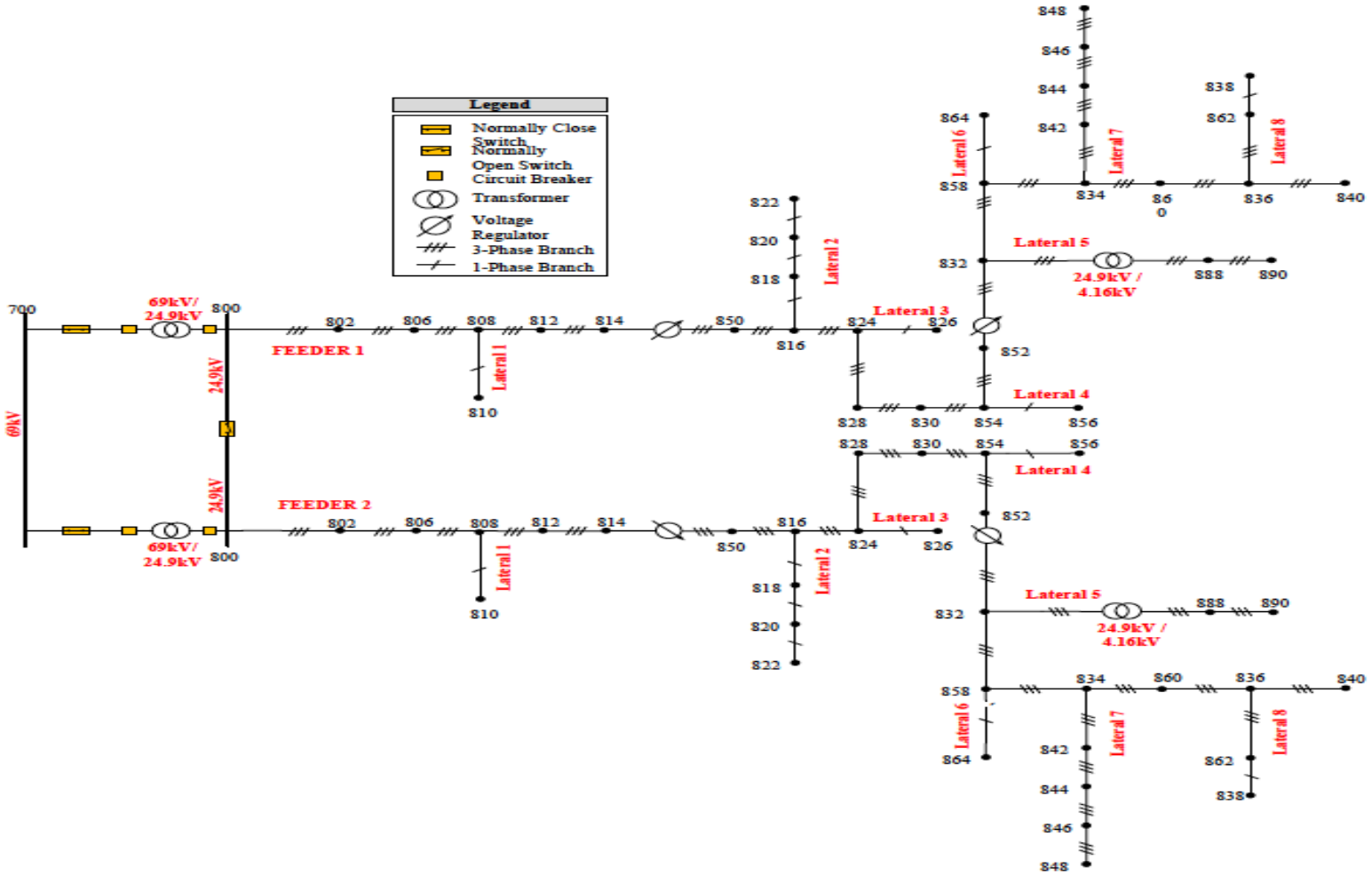

Fig. 5-2. Multi-feeder test system.

The spot loads of the IEEE 34 node radial test feeder as reported in [44] were used on each feeder of the multi-feeder test system. The values of the spot loads are shown in Table 5-2. The distributed load ratings at the primary level of the feeder were an aggregate of an estimated secondary level loading developed for the multi-feeder test system. The derivation of the secondary distribution level loads for the multi-feeder test system is discussed in Section 5.2.3. Table 5-3 shows the aggregated values of the secondary distributed loads as represented on the primary distribution level.

Table 5-2 kW and kVAR Ratings of Spot Loads at Primary Distribution Level of Feeder 1 and Feeder 2 of Multi-feeder Test System

Node	Phase A		Phase B		Phase C	
	P (kW)	Q (kVAR)	P (kW)	Q (kVAR)	P (kW)	Q (kVAR)
860	24.57	18.43	24.57	18.43	24.57	18.43
840	10.93	8.2	10.93	8.2	10.93	10.93
844	164.69	123.52	164.69	123.52	164.69	123.52
848	24	18	24	18	24	18
890	33.33	25	33.33	25	33.33	25
Total	257.52	193.15	257.52	193.15	257.52	193.15

Table 5-3 kW and kVAR Ratings of Distributed Loads at Primary Distribution Level of Feeder 1 and Feeder 2 of Multi-feeder Test System

Node A	Node B	Phase A		Phase B		Phase C	
		P (kW)	Q (kVAR)	P (kW)	Q (kVAR)	P (kW)	Q (kVAR)
802	806	0	0	131	63	84	41
808	810	0	0	32	15	0	0
818	820	76	37	0	0	0	0
820	822	623	302	0	0	0	0
816	824	0	0	0.42	0.2	0	0
824	826	0	0	153	74	0	0

Table 5-3 Continued

Node A	Node B	Phase A		Phase B		Phase C	
		P (kW)	Q (kVAR)	P (kW)	Q (kVAR)	P (kW)	Q (kVAR)
824	828	0	0	0	0	5	3
828	830	10	5	0	0	0	0
854	856	0	0	5	2	0	0
832	858	15	7	1.47	0.71	9	4
858	864	0.87	0.42	0	0	0	0
858	834	9	4	30	14	32	16
834	860	39	19	52	25	597	289
860	836	78	38	28	14	132	64
836	840	35	17	71	34	0	0
862	838	82	40	0	0	0	0
842	844	17	8	0	0	0	0
844	846	0	0	100	48	80	39
846	848	0	0	39	19	0	0

The substation transformers and the cables on the multi-feeder were changed to match the new loading of the system. Due to the choice of the substation configuration, if a substation transformer was rendered inoperable due to fault conditions or maintenance, the other substation transformer was sized to be able to supply the cumulative load of both feeders. The original substation transformer on the IEEE 34 Node Radial Test Feeder was 2.5 MVA and was expected to supply a total load of 1.769 MW. The total load on the multifeeder system is 7.5 MW; therefore, a 10 MVA transformer was selected for each substation transformer.

The types of cables that were used in the multifeeder test system are shown in Table 5-4. The third column signifies the size of the cable and the amount of aluminum and steel conductors in the cable. For example configuration 300 has an American Wire Gauge (AWG) cable size of 556.5 and the cable is made up of 26 aluminum conductors that requires a core of 7 steel conductors.

Table 5-4 Overhead Line Configurations for Multi-Feeder Test System

Configuration	Phasing	Phase ACSR	Neutral ACSR	Spacing ID
300	B A C N	556,500 26/7	4/0 6/1	500
302	A N	1/0	1/0	500
303	B N	1/0	1/0	510

Table 5-5 shows the overhead line configurations for each line segment for both feeders of the multi-feeder test system. The impedance matrices for each line configuration can be found in Appendix I.

Table 5-5 Overhead Line Configurations for the Line Segments on the Multi-Feeder Test System

Node A	Node B	Line Configuration
800	802	300
802	806	300
806	808	300
808	810	303
808	812	300
812	814	300
814	850	300
816	818	302
816	824	300
818	820	302
820	822	302
824	826	303
824	828	300
828	830	300
830	854	300
832	858	300
832	888	XFMR-1
834	860	300
834	842	300
836	840	300
836	862	300
842	844	300
844	846	300
846	848	300
850	816	300
852	832	300
854	856	303

Table 5-5 Continued

Node A	Node B	Line Configuration
854	852	300
858	864	302
858	834	300
860	836	300
862	838	302
888	890	300

The voltage regulator model included the following controls: set voltage, initial tap setting, bandwidth, out-of-band detector, control time delay, tap position calculator, timer reset and line compensation. Table 5-6 provides the voltage regulator compensator settings.

Table 5-6 Voltage Regulator Compensator Settings

Regulator Data			
Regulator ID:	1		
Line Segment:	814 - 850		
Location:	814		
Phases:	A - B -C		
Connection:	3-Ph,LG		
Monitoring Phase:	A-B-C		
Bandwidth:	2.0 volts		
PT Ratio:	120		
Primary CT Rating:	100		
Compensator Settings:	Phase-A	Phase-B	Phase-C
R - Setting:	2.7	2.7	2.7
X - Setting:	1.6	1.6	1.6
Voltage Level:	122	122	122
Regulator ID:	2		
Line Segment:	852 - 832		
Location:	852		
Phases:	A - B -C		
Connection:	3-Ph,LG		
Monitoring Phase:	A-B-C		

Table 5-6 Continued

Regulator Data			
Bandwidth:	2.0 volts		
PT Ratio:	120		
Primary CT Rating:	100		
Compensator Settings:	Phase-A	Phase-B	Phase-C
R - Setting:	2.5	2.5	2.5
X - Setting:	1.5	1.5	1.5
Voltage Level:	124	124	124

Prior to the addition of overcurrent relays to the multi-feeder system, the nominal load current corresponding to the maximum loading for the various laterals was determined by executing a transient simulation in PSCAD. Table 5-7 shows the load current through each phase at the substation and the beginning of each lateral in the multi-feeder system.

Table 5-7 Load Current in Each Phase at Substation and the Beginning of Each Lateral on Multi-Feeder Test System without DG

Measurement Location	Feeder 1 (Amps)			Feeder 2 (Amps)		
	Phase A	Phase B	Phase C	Phase A	Phase B	Phase C
Substation	99.258	79.872	112.496	98.821	79.543	112.656
Lateral 1	0	2.432	0	0	2.436	0
Lateral 2	55.316	0	0	55.201	0	0
Lateral 3	0	11.824	0	0	11.832	0
Lateral 4	0	0.376	0	0	0.376	0
Lateral 5	11.457	11.823	11.97	11.455	11.822	11.975
Lateral 6	0.058	0	0	0.058	0	0
Lateral 7	16.846	23.255	19.837	16.836	23.259	19.834
Lateral 8	0	6.119	0	0	6.118	0

With the information above, the pickup setting for each relay was determined using (21).

$$I_{pickup} = 1.5 \times I_{maximum\ load} \tag{21}$$

where I_{pickup} is the pickup setting for the overcurrent relay; $I_{maximum\ load}$ is the greatest of the maximum load currents through each phase of the overcurrent relay. Each substation overcurrent relay was the primary protective device for its corresponding main feeder and served as back-up protection for the lateral overcurrent relays on the corresponding feeder. All overcurrent relays were assigned an IEEE Standard Inverse-Time moderately inverse characteristic curve [45]. The equation of the curve is shown in (22) [46].

$$t(I) = \left(\frac{0.0515}{M^{0.0200}-1} + 0.1140\right) \tag{22}$$

where t(I) is the relay operating time as a function of the fault current, and M is the multiples of pickup current. Referring to Fig. 5-2, the lateral relays were the primary protection for faults on their respective laterals and were assigned a TDS of 0.5. The substation relays were the backup protection for faults on the laterals and the primary protection for faults on the main feeder were assigned a TDS of 1.0. The reach of each substation relay was set to detect faults on the main feeder from node 800 to node 840 on both feeders, respectively. Table 5-8 shows the relay pickup settings that were obtained using (21) based on maximum loads, for the inverse-time overcurrent relays on the multi-feeder test system. The table shows the maximum load current, the pickup current, and the TDS for all overcurrent relays. The TDS for all lateral relays was 0.5, whereas the TDS for substation relays was set to 1.0.

Table 5-8 Inverse-time Overcurrent Relay Settings for Feeder 1 and Feeder 2

Feeder 1 & Feeder 2 Relays	Maximum Load (Amps)	Pickup Current (Amps)	TDS
Substation	112.49	168.74	1.0
Lateral 1	2.436	3.648	0.5
Lateral 2	55.316	82.974	0.5
Lateral 3	11.832	17.736	0.5
Lateral 4	0.376	0.564	0.5
Lateral 5	11.95	17.955	0.5
Lateral 6	0.058	0.087	0.5
Lateral 7	23.255	34.8825	0.5
Lateral 8	6.119	9.1785	0.5

Maximum load values in Table 5-2 and Table 5-3 were connected for a transient simulation study in PSCAD to determine the load flow results. The simulation was run and after 4s, the steady state voltages at the primary nodes were recorded. The per-unit (p.u.) node voltages for the case when there were no DGs connected to the multi-feeder test system are shown in Table 5-9. It can be seen that the voltages are within +/-5% of the nominal value.

Table 5-9 Revised IEEE 34 Multi-feeder Node Voltage without DG

	Feeder 1			Feeder 2		
Node	Phase A V (p.u.)	Phase B V (p.u.)	Phase C V (p.u.)	Phase A V (p.u.)	Phase B V (p.u.)	Phase C V (p.u.)
800	1.0500	1.0520	1.0410	1.0500	1.0530	1.0440
802	1.0460	1.0520	1.0400	1.0480	1.0530	1.0380
806	1.0350	1.0530	1.0060	1.0520	1.0520	1.0360
808	1.0350	1.0530	1.0060	1.0340	1.0520	1.0060
810	0.0000	1.0530	0.0000	0.0000	1.0520	0.0000
812	1.0380	1.0290	1.0270	1.0160	1.040	0.9765
814	0.9982	1.0510	0.9535	1.0030	1.040	0.9503
850	1.0330	1.0340	1.0380	1.0340	1.0350	1.0350
816	1.0320	1.0370	1.0350	1.0310	1.0360	1.0370
818	1.0300	0.0000	0.0000	1.0320	0.0000	0.0000

Table 5-9 Continued

Node	Feeder 1			Feeder 2		
	Phase A V (p.u.)	**Phase B V (p.u.)**	**Phase C V (p.u.)**	**Phase A V (p.u.)**	**Phase B V (p.u.)**	**Phase C V (p.u.)**
820	0.9757	0.0000	0.0000	0.9841	0.0000	0.0000
822	0.9677	0.0000	0.0000	0.9761	0.0000	0.0000
824	1.0380	1.0290	1.0270	1.0360	1.0280	1.0290
826	0.0000	1.0310	0.0000	0.0000	1.0270	0.0000
828	1.0330	1.0330	1.0330	1.0320	1.0290	1.0320
830	1.0380	1.0260	1.0100	1.0370	1.0250	1.0130
854	1.0390	1.0220	1.0100	1.0370	1.0210	1.0160
856	0.0000	1.0260	0.0000	0.0000	1.0200	0.0000
852	1.0140	0.9853	0.9669	1.0400	1.0140	0.9853
832	1.0440	1.0410	1.0530	1.0460	1.0390	1.0530
888	0.9650	0.9953	0.9789	0.9829	1.0400	1.0020
890	0.9650	0.9953	0.9789	0.9577	1.0180	0.9713
858	1.0350	1.0390	1.0500	1.0490	1.0350	1.0510
864	1.0450	0.0000	0.0000	1.0470	0.0000	0.0000
834	1.0460	1.0360	1.0500	1.0450	1.0350	1.0510
842	1.0460	1.0390	1.0470	1.0440	1.0370	1.0480
844	1.0490	1.0380	1.0450	1.0480	1.0360	1.0460
846	1.0510	1.0350	1.0460	1.0500	1.0330	1.0470
848	1.0490	1.0340	1.0490	1.0450	1.0350	1.0510
860	1.0460	1.0360	1.0490	1.0440	1.0370	1.0480
836	1.0460	1.0380	1.0460	1.0490	1.0330	1.0460
862	1.0490	1.0370	1.0440	1.0470	1.0320	1.0490
838	0.0000	1.0380	0.0000	0.0000	1.0310	0.0000
840	1.0340	1.0350	1.0450	1.0440	1.0370	1.0470

The protection scheme presented in [26] was implemented on the multi-feeder test system as discussed in Section 3.1.1 and the result is shown in Fig. 5-3. Five (5) DGs were connected to the multi-feeder system, two (2) of which were connected to Feeder 1 at nodes 814 and 848, and three were connected to Feeder 2 at nodes 828, 890, and 836. Each DG was modeled as a synchronous generator with a rating of 2 MVA. The DG model parameters are as shown in Table 5-10.

Table 5-10 Synchronous-Based Distributed Generator Parameters

Armature Time Constant [Ta]	0.0042 pu
Potier Reactance [Xp]	0.18 pu
D: Unsaturated Reactance [Xd]	1.25 pu
D: Unsaturated Transient Reactance [Xd']	0.24 pu
D: Unsaturated Transient Time (Open) [Tdo']	4.11 s
D: Unsaturated Sub-Transient. Reactance [Xd'']	0.19 pu
D: Unsaturated Sub-Transient Time (open) [Tdo'']	0.023 pu
Q: Unsaturated Reactance [Xq]	0.62 pu
Q: Unsaturated Transient Reactance [Xq']	0.228 pu
Q: Unsaturated Transient Time (Open) [Tqo']	0.85 s
Q: Unsaturated Sub-Transient. Reactance [Xq'']	0.26 pu
Q: Unsaturated Sub-Transient Time (open) [Tqo'']	0.061 s
Air Gap Factor	1

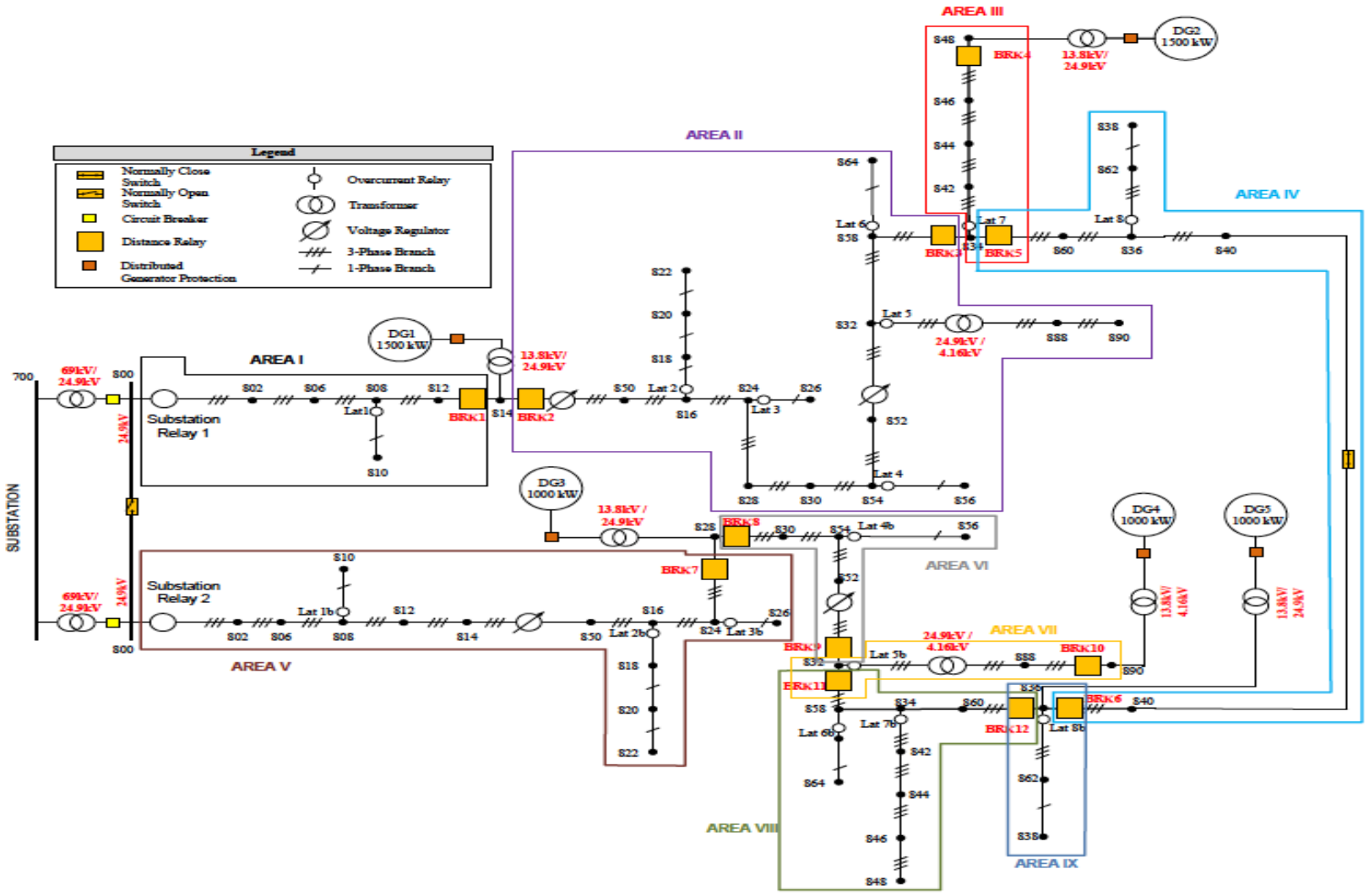

Fig. 5-3. Protection coordination areas on multi-feeder test system for the application of the protection scheme.

Table 5-11 shows the DG locations on the multi-feeder test system, their apparent power ratings (S Rated), their real power output (P Output), and their rated line-to-line voltage (V_{LL}) and line current (I_L).

Table 5-11 Synchronous DG Ratings on Multi-Feeder Test System

DG Number	Feeder	Node	S Rated (kVA)	P Output (kW)	V_{LL} (kV)	I_L (kA)
1	1	814	2000	1500	13.8	0.0837
2	1	848	2000	1500	13.8	0.0837
3	2	828(II)	2000	1000	13.8	0.0837
4	2	890(II)	2000	1000	13.8	0.0837
5	2	836(II)	2000	1000	13.8	0.0837

When DGs were introduced on the multifeeder test system, the measurement of the real power at the overcurrent relay locations were monitored and are shown in Table 5-12 below. For DGs on a three-phase lateral, e.g. Lateral 7 on Feeder 1, it was observed that the DG output power was large enough to serve the load on the lateral and other loads on the main feeder as well. This shows the bidirectional power flow effect that DG has in radial systems.

Table 5-12 Real Power Measurements at Relay Locations before and after DG Connection

Relay Location	Feeder 1		Feeder 2	
	P (kW)		P (kW)	
	Before DG	After DG	Before DG	After DG
Substation	4164.39	1370	4163.69	1604.36
Lateral 1	36.98	35.17	36.96	35.94
Lateral 2	796.26	795.30	795.10	797.72
Lateral 3	171.86	168.25	171.94	167.38
Lateral 4	5.41	5.14	5.41	5.40
Lateral 5	468.85	465.02	468.98	-462.60
Lateral 6	0.93	0.93	0.93	0.93
Lateral 7	865.08	-477	864.17	854.20
Lateral 8	88.26	88.29	87.98	88.11

When DGs were added to the multi-feeder test system, a closed switch was added at the end of the feeders, so that both feeders were connected via node 840 on each feeder. Distance relays and breakers were also added. Fig. 5-3 shows the locations of the DGs on the multi-feeder system, and the associated distance relays and breakers that were added. From the figure it can be seen that when a DG was added to the main feeder, two (2) breakers were added, and when a DG was added to the end of a lateral, three (3) breakers were added. Table 5-13 shows the nodes at which the DGs were connected and the associated breakers that were added with their connection.

Table 5-13 Connection Point of DG, Rating of DG and Associated Breakers

DG	Feeder	DG Connection Point		Added Distance Relay Controlled Breakers
		Node	Lateral/Main Feeder	
1	1	814	Main	BRK1, BRK2
2	1	848	Lateral	BRK3, BRK4, BRK5
3	2	828(II)	Main	BRK7, BRK8
4	2	890(II)	Lateral	BRK9, BRK10, BRK11
5	2	836(II)	Main	BRK6, BRK12

Distance protection coordination areas for the multi-feeder test system were designated as shown in Fig. 5-3. The distance function was added to *Substation Relay 1* and *Substation Relay 2*, and they formed coordination areas with the distance relays at BRK1 and BRK7, respectively. Table 5-14 further describes the figure, giving the lengths of each area to be protected, the distance relay controlled breakers associated with each area, and the breakers that opened and the DG(s) that were disconnected for a fault in that area.

Table 5-14 Distance Protection Area Attributes for Multi-Feeder Test System

Area	From Node	To Node	Length of Protected Area (miles)	Distance Relay Controlled Breakers Associated	Breaker(s) Open During Fault	DG Disconnected during Fault
I	800	814	19.6534	Substation Relay 1, BRK1	BRK1	None
II	814	834	15.1326	BRK2, BRK3	BRK3	DG1
III	834	848	1.0985	BRK4, BRK5	BRK4, BRK5	DG1, DG2
IV	834	836	1.2159	BRK5, BRK6	BRK6	DG1, DG2
V	800	828	21.8068	Substation Relay 2, BRK7	BRK7	None
VI	828	832	10.9470	BRK8, BRK9	BRK9	DG3
VII	832	890	2	BRK10, BRK11	BRK10, BRK11	DG3, DG4
VIII	832	836	2.9223	BRK11, BRK12	BRK12	DG3, DG4

Distance relays were set based on the directional mho characteristic circle. When plotted on an R-X diagram, a mho characteristic circle was one whose circumference passed through the origin. For each phase of a distance relay on the distribution system, the center and the radius of the mho characteristic circle was defined. As mentioned in Section 3.1.2, the distance relays were set based on zone 2 overreaching distance elements, and were 120% of the impedance of the protected line segment(s) in the coordination area. The use of distance relays for the protection of distribution lines is sometimes affected due to the high prevalence of long laterals or tapped lines in distribution systems [47]. The distance protection settings for all areas are shown in shown Table 5-15 below. The table illustrates the number and the length of the longest outfeeds in each area, the protected area boundary distance relay controlled breakers, and the attributes of each mho circle for their respective distance relays. The distance relays at the boundaries of protection coordination areas II, V, and VI were set based on the methodology for setting distance relays for tapped lines presented in [47].

Table 5-15 Distance Protection Settings for All Areas

Phase	Area	Number of Outfeeds	Length of Longest Outfeed (miles)	From BRK	Radius of Mho Circle	Center of Mho Circle		To BRK	Radius of Mho Circle	Circle of Mho Circle	
						x	y			x	y
A	I	1	1.0992	Substation Relay 1	12.6795	4.0859	12.0031	BRK1	12.6795	4.0859	12.0031
B					12.9808	3.9798	12.3557		12.9808	3.9798	12.3557
C					12.8494	4.0258	12.2024		12.8494	4.0258	12.2024
A	II	5	12.0454	BRK2	22.0285	15.4576	15.6946	BRK3	31.0372	18.5784	24.8627
B					9.9949	3.0643	9.5135		9.9949	3.0643	9.5135
C					9.8936	3.0998	9.3955		9.8936	3.0998	9.3955
A	III	0	N/A	BRK4	0.7087	0.2284	0.6709	BRK5	0.7087	0.2284	0.6709
B					0.7255	0.2224	0.6868		0.7255	0.2224	0.6868
C					0.7182	0.2250	0.6820		0.7182	0.2250	0.6820
A	IV	1	0.9735	BRK5	1.2537	0.4040	1.1868	BRK6	1.2537	0.4040	1.1868
B					2.7080	1.716	2.095		2.7080	1.6507	2.1468
C					1.2704	0.3980	1.2065		1.2704	0.3980	1.2065
A	V	3	12.0454	Substation Relay 2	31.8957	18.1166	26.2511	BRK7	21.1851	14.4531	15.4892
B					14.4031	4.4159	13.7095		14.4031	4.4159	13.7095
C					14.2572	3.0998	13.5394		14.2572	3.0998	13.5394
A	VI	1	4.4186	BRK8	8.3528	2.6917	7.9072	BRK9	7.0625	2.2759	6.6858
B					8.5205	2.6326	8.1036		11.5423	6.5927	9.4742
C					8.4474	2.6582	8.0182		7.1571	2.2424	6.7968
A	VII	0	N/A	BRK10	1.2903	0.4158	1.2215	BRK11	1.2903	0.4158	1.2215
B					1.3210	0.4050	1.2574		1.3210	0.4050	1.2574
C					1.3076	0.4097	1.2418		1.3076	0.4097	1.2418
A	VIII	2	0.3068	BRK11	1.8854	0.6076	1.7848	BRK12	1.8854	0.6076	1.7848
B					1.9302	0.5918	1.8372		1.9302	0.5918	1.8372
C					1.9106	0.5986	1.8144		1.9106	0.5986	1.8144
A	IX	0	N/A	BRK12	0.6280	0.2024	0.5945	BRK6	0.6280	0.2024	0.5945
B					1.7044	0.9735	1.3991		1.7044	0.9735	1.3991
C					0.6365	0.1994	1.9453		0.6365	0.1994	1.9453

5.2.3 Secondary Distribution System for Multi-Feeder Test System

The IEEE 34 Node Radial Test Feeder is an actual distribution system in Phoenix, Arizona. Metered readings of the maximum kW and kVAR for spot loads and customer billing records of an unspecified month for distributed loads were presented in [44], and are shown in Table 5-2 and Table 5-16 respectively. The balanced three-phase ratings of the spot loads coupled with the fact that only their maximum demands were reported suggested that they could be either commercial or industrial type loads. The distributed loads reported monthly energy consumption of several customers, and they were all connected to one of the three phases of the distribution system. Therefore, the distributed loads were classified as residential customers.

Table 5-16 IEEE 34 Node Radial Test Feeder Customer Total Energy Consumption for Specific Month

Node A	Node B	Phase A		Phase B		Phase C	
		# of Customers	Energy Consumption (kWh)	# of Customers	Energy Consumption (kWh)	# of Customers	Energy Consumption (kWh)
802	806	0	0	68	10375	67	8465
808	810	0	0	7	3415	0	0
818	820	6	7706	0	0	0	0
820	822	101	53860	0	0	0	0
816	824	0	0	1	39	0	0
824	826	0	0	36	14325	0	0
824	828	0	0	0	0	3	390
828	830	5	1073	0	0	0	0
854	856	0	0	1	500	0	0
832	858	10	1420	2	127	4	864
858	864	2	69	0	0	0	0
858	834	11	813	15	3205	14	3233
834	860	13	3980	14	5602	104	42985

Table 5-16 Continued

Node A	Node B	Phase A		Phase B		Phase C	
		# of Customers	Energy Consumption (kWh)	# of Customers	Energy Consumption (kWh)	# of Customers	Energy Consumption (kWh)
860	836	16	7844	8	2235	14	12369
836	840	4	3294	8	5077	0	0
862	838	0	0	34	8840	0	0
842	844	1	1380	0	0	0	0
844	846	0	0	61	7928	35	6934
846	848	0	0	2	3953	0	0
Total		203	90279	223	56781	241	75240

A secondary distribution design that included estimating the secondary load rating and distribution transformer sizing, was developed to allow for the determination of the maximum loading downstream of the substation on the multi-feeder test system. In distribution systems, the maximum loading is used to set the pickup setting of the substation overcurrent relay. The representation of individual residential customer loads on the secondary distribution system is divided into four (4) steps, which are characterized as follows:

Step 1: Calculate the per interval average demand per customer - For loads that report the customer energy consumption (kWh) for a month, the per interval average demand of the customer over the same monthly period is found using (22).

$$\text{per interval Average Demand}_k = \frac{\text{Energy Consumption for a Month}_k}{\text{Number of Hours in a Month}} \tag{22}$$

where the per interval average demand is the average of customer k's demands over a specified interval in a month. For example, the 15-minute average demand of a

customer represents the amount of power (demand) the customer would be using every 15-minutes if the customer were to be closely monitored over a period of a month.

Step 2: Estimate the per interval maximum demand per customer - To calculate the per interval maximum demand of a customer, it is necessary to estimate their 'load factor'. The load factor is a term used to compare the customer's per interval average demand to the customer's per interval maximum demand over the same time period. The optimal load factor is 1.00. The load factor of a customer, k, is the ratio of customer k's per interval average demand to customer k's per interval maximum demand of the customer over the same month. The per interval maximum demand of customer, k, can be obtained from (23).

$$\text{per interval Maximum Demand}_k = \frac{\text{per interval Average Demand}_k}{\text{Load Factor}_k} \quad (23)$$

where typical load factors for residential customers is 10-15%, commercial is 25-30%, and industrial is 70-80% [48].

Step 3: Distribution transformer allocation - A distribution transformer provides power to one or more customers. Based on [49], the secondary of the distribution transformer can serve up to 12 customers if the customers are within a radius of up to 250 feet of the transformer. Therefore, to determine the amount of distribution transformers on the distribution system, the length of the line segments and the layout of the customers around the line segments must be known.

Step 4: Distribution transformer sizing - Every customer has a unique loading characteristic; therefore each customer served by the same distribution transformer may not experience a maximum loading at the same time. The difference in the timing of

individual maximum demands is referred to as diversity. The diversity factor is the ratio of the distribution transformer's maximum per interval non-coincidental demand and the distribution transformer's maximum per interval diversified demand for a month, and it is defined in (24).

$$\text{Diversity Factor}_g = \frac{\text{Maximum per interval Non-Coincidental Demand}_g}{\text{Maximum Diversified per interval Demand}_g} \quad (24)$$

where distribution transformer, g's, maximum per interval non-coincidental demand for a month is the sum of the maximum per interval demands of each customer, k, served by distribution transformer, g, without the constraint that they occur at the same time. The maximum per interval diversified demand of distribution transformer, g, is the greatest value of the sum of the per interval demands of the group of customers served from, g, over the same month. The diversity factor of distribution transformer, g, is used to size the distribution transformer. This is shown in (25).

$$\text{Maximum kVA Demand}_g = \frac{\text{Maximum per interval Non-Coincidental Demand}_k}{\text{Diversity Factor}_g \times \text{Power Factor}_g} \quad (25)$$

where the power factor is the ratio of the real power supplied by distribution transformer, g, and the rated apparent power of distribution transformer, g; maximum kVA demand represents the maximum apparent power the distribution transformer, g, will sense due to the customers it serves. Equation (25) does not yield a standard transformer size, so the closest size below the calculated value is chosen from Table 5-17 (which shows the

standard kVA ratings of overhead type distribution transformers), to be the size of the transformer allocated to serve the loads.

Table 5-17 Standard kVA Ratings of Overhead Distribution Transformers

Overhead Type	
Single-Phase	Three-Phase
5	15
10	30
15	45
25	75
37½	112½
50	150
75	225
100	300
167	500
250	
333	

The above methodology presented how the secondary distribution system was developed for the multi-feeder test system. Due to the large number of customers, the derivation of load is illustrated for the six (6) customers that are located on line segment 818-820 (row 3 of Table 5-16). The length of this line segment is 48150ft or 9.1193182 miles. A 15-minute demand interval was assumed for the purposes of this work. See APPENDIX II for the complete tables of customer data for the secondary distribution system of the multi-feeder test system.

Table 5-16 presented the energy consumption per a group of customers in an unspecified month. With this information the average monthly consumption for a customer was determined using (26).

$$\text{Average Energy Consumption per Customer} = \frac{\text{Total Energy Consumption}}{\text{Number of Customers}} \quad (26)$$

where the total energy consumption is the total energy (kWh) consumed by the group of customers in a month. For the customers, a random number signifying their total energy consumption was assigned, such that the number was in the range of 25% of the average energy consumption per customer, and the sum of the numbers was equal to the total energy consumption. The results of this are illustrated in Table 5-18 below. The average energy consumption per customer in the month was 1284.33 kWh (found using (26)). To determine the energy consumption per customer, random values were assigned to each customer to within 25% of this value. The sum of these assigned values was equal to the total energy consumed by the six customers on this line segment.

Table 5-18 Estimated Energy Consumption per Customer between Nodes 818 and 820

Node A	**Node B**	**Number of Customers**	**Total Energy Consumption in Unspecified Month (kWh)**	**Average Energy Consumption per Customer (kWh)**	**Energy Consumption per Customer in a Month (kWh)**
818	820	6	7706	1284.33	966
					1494
					1363
					1257
					1450
					1176
Total					7706

Using (22) and the energy consumption per customer in a month from Table 5-18, the 15-minute average demand per customer was determined, and is illustrated in Table 5-19. The total number of hours assuming a 30-day month was 720 hours.

Table 5-19 Average 15-Minute Demand per Customer for the Customers between Nodes 818 and 820

Node A	Node B	# Of Customers	Energy per Customer in an Unspecified Month (kWh)	15-minute Average Demand per Customer (kW)
818	820	6	966	1.34
			1494	2.08
			1363	1.89
			1257	1.75
			1450	2.01
			1176	1.63

The maximum 15-minute demand per customer was determined using (23) where the load factor was assumed to be within the range for residential customers. The load factor was randomized between 10-15% (Residential). Table 5-20 shows the 15-minute maximum demand for each residential customer.

Table 5-20 15-Minute Maximum Demand per Customer for the Customers between Nodes 818 and 820

Node A	Node B	# Of Customers	15-minute Average Demand per Customer (kW)	Load Factor	15-minute Maximum Demand per Customer (kW)
818	820	6	1.34	0.140	9.58
			2.08	0.140	14.82
			1.89	0.140	13.52
			1.75	0.120	14.55
			2.01	0.110	18.31
			1.63	0.140	11.67

Table 5-21 shows the lengths of the line segments on the IEEE 34 Node Radial Test Feeder. Based on the information given in [49], the secondary of the distribution transformer can serve up to 12 customers if the customers are within a radius of up to 250 feet from the distribution transformer.

Table 5-21 Length of Line Segments in IEEE 34 Node Test Feeder

Node A	Node B	Length (feet)
800	802	2580
802	806	1730
806	808	32230
808	810	5804
808	812	37500
812	814	29730
814	850	10
816	818	1710
816	824	10210
818	820	48150
820	822	13740
824	826	3030
824	828	840
828	830	20440
830	854	520
832	858	4900
832	888	0
834	860	2020
834	842	280
836	840	860
836	862	280
842	844	1350
844	846	3640
846	848	530
850	816	310
852	832	10
854	856	23330
854	852	36830
858	864	1620
858	834	5830
860	836	2680
862	838	4860
888	890	10560

Without knowledge of the exact arrangement of customers along a certain line segment, it was assumed that if the mean length of a line segment was less than 250ft, one common secondary transformer was assigned to a group of 12 customers. Otherwise, a single distribution transformer was assigned to each individual customer with the thought that the customers were located far away from one another. Table 5-22

shows the number of distribution transformers that were allocated to the customers along the line segment 818-820. The mean length of the line segment between the customers was 8025ft and so each customer was allocated their own transformer. Since each customer was assigned a single-service distribution transformer, the maximum 15-minute non-coincidental demand of each transformer is the same as the 15-minute maximum demand of the corresponding customer.

Table 5-22 Number of Distribution Transformers Allocated based on Mean Length of Line Segment between Nodes 818 and 820

Node A	Node B	Length of Line Segment (feet)	# of Customers	Mean Length of Line Segment between Customers	# Of Transformers	Transformer, g	Maximum 15-minute Demand per Customer (kW)	Maximum 15-minute Non-coincidental Demand
818	820	48150	6	8025	6	1	9.58	9.58
						2	14.82	14.82
						3	13.52	13.52
						4	14.55	14.55
						5	18.31	18.31
						6	11.67	11.67

Table 5-23 shows the diversity factors for the number of customers ranging from one to 70. In the table, N represents the number of customers, while DF represents the diversity factor corresponding to the group. The maximum 15-minute diversified demand of each customer's distribution transformer was obtained using (24); the maximum 15-minute non-coincidental demand was obtained from Table 5-22 and the diversity factors in Table 5-23.

Table 5-23 Diversity Factors [50]

N	DF	N	DF	N	DF	N	DF	N	DF	N	DF	N	DF
1	1	11	2.67	21	2.9	31	3.05	41	3.13	51	3.15	61	3.18
2	1.6	12	2.7	22	2.92	32	3.06	42	3.13	52	3.15	62	3.18
3	1.8	13	2.74	23	2.94	33	3.08	43	3.14	53	3.16	63	3.18
4	2.1	14	2.78	24	2.96	34	3.09	44	3.14	54	3.16	64	3.19
5	2.2	15	2.8	25	2.98	35	3.1	45	3.14	55	3.16	65	3.19
6	2.3	16	2.82	26	3	36	3.1	46	3.14	56	3.17	66	3.19
7	2.4	17	2.84	27	3.01	37	3.11	47	3.15	57	3.17	67	3.19
8	2.55	18	2.86	28	3.02	38	3.12	48	3.15	58	3.17	68	3.19
9	2.6	19	2.88	29	3.04	39	3.12	49	3.15	59	3.18	69	3.2
10	2.65	20	2.9	30	3.05	40	3.13	50	3.15	60	3.18	70	3.2

Assuming a power factor of 0.9 for residential loads, the max kVA rating of the transformer was found using (25). Table 5-24 shows the transformer ratings for the residential loads located between nodes 818 and 820. The diversity factor for all the customers was 1.0 because a single distribution transformer served each customer.

Table 5-24 Distribution Transformer kVA Ratings for Distributed Loads between Nodes 818 and 820

Node A	Node B	# Of Transformers	Maximum 15-minute Non-coincidental Demand	Diversity Factor	Max kVA Demand	Transformer Rating (kVA)
818	820	6	9.58	1.0	10.65	10
			14.82	1.0	18.30	15
			13.52	1.0	15.02	15
			14.55	1.0	16.17	15
			18.31	1.0	20.34	15
			11.67	1.0	12.96	10

5.2.4 Summary

The IEEE 34 Node Radial Test feeder was revised on the primary distribution level to represent an open loop multi-feeder test system as shown in Fig. 5-3. To

implement the protection scheme presented in [26], a closed switch was added to the end of both feeders such that the multi-feeder test system operated in a closed loop. The normally open switch at the beginning of both feeders (node 800) was kept open. DGs were added to the multi-feeder test system following the guidelines presented in Section 3.1.1. Each substation relay's pickup settings were set to protect the length of its respective feeder, due to the adopted dual bus substation configuration. The multi-feeder test system was also represented on the secondary distribution level such that the 15-minute maximum demand per customer, the 15-minute average demand per customer, and the number of distribution transformers on the distribution system were determined.

5.3 Illustrative Studies

5.3.1 Obtaining the Seasonal Settings for the Substation Relays

There were nine (9) protection coordination areas on the multi-feeder test system and therefore there were nine possible radial segments that could be created. In Section 5.2.3, the method to allocate distribution transformers to a single customer or group of customers was presented. There were 672 customers (667 residential customers, 5 industrial and commercial customers) on each feeder of the multifeeder test system. The 15-minute maximum and 15-minue average demands per customer (obtained from Table II-1, Table II-2, and Table II-3 in Appendix II) that were derived for the multi-feeder test system in Section 5.2.3 were used to generate 35040 (96 15-minute intervals per day, 365 days per year) 15-minute demands for each customer on the multi-feeder test

system. The 15-minute demands were varied during each season of the year. The number of 15-minute demands per customer that was generated for an entire year, based on Table 4-1, is shown in Table 5-25. The 15-minute maximum and 15-minute average demands obtained from Table II-1, Table II-2, and Table II-3 were assumed to be the base demands for each customer in the Fall season. These values were then varied within the range of the 15-minute average demand being the lowest value and the 15-minute maximum demand being the highest value. This was done until each customer had 8640 values, which represented the 90 days of fall and the 96 15-minute demands in each day. The 15-minute maximum demand for each customer in the spring season was assumed to be equal to that of the fall. The 15-minute maximum demand for the winter season was assumed to be 125% of the demands for the fall season. For the summer season, the 15-minute maximum demand per customer was assumed to be 90% of the 15-minute maximum demand in the winter season [51].

Table 5-25 Number of 15-minute Demands that were Generated per Customer

Season	Number of Days in Season	Number of 15-minute Demands Generated
Winter	90	8640
Spring	92	8832
Summer	92	8832
Fall	91	8736

After this was completed for all customers on the multi-feeder test system, the values were arranged in a (365x96) matrix for each customer as illustrated in (2). Table II-1, Table II-2, and Table II-3 were used to determine the distribution transformers that

served the various customers on the multi-feeder test system and (4) was used to determine each distribution transformer's 15-minute diversified demand for each day of the year. Table 5-26 shows the location and the number of distribution transformers in each radial segment. The substation source column in the table represents the only source of fault current for a fault in the radial segment. The (II) next to the node number, signifies the node was located on feeder 2 of the multi-feeder test system. There were a total of 152 distribution transformers (147 single-phase transformers – residential loads, 5 three-phase transformers – commercial/industrial loads) on each feeder of the multi-feeder test system.

Table 5-26 Number of Distribution Transformers in Each Radial Segment on the Multi-Feeder Test System

Radial Segment	**Substation Source**	**From Node**	**To Node**	**# of Distribution Transformers**		
				Phase A	**Phase B**	**Phase C**
I	Substation I	800	814	0	13	6
II	Substation I	800	834	44	36	28
III	Substation I	800	848	47	46	33
IV	Substation I	800	836(II)	58	61	46
V	Substation II	800(II)	828(II)	15	17	9
VI	Substation II	800(II)	832(II)	20	18	9
VII	Substation II	800(II)	890(II)	21	19	10
VIII	Substation II	800(II)	836(II)	54	59	46
IX	Substation II	800(II)	838(II)	57	59	46

The 15-minute diversified demand of each phase in each radial segment for each day of the year, was determined using (7), and Table 5-26 to determine the phasing of the distribution transformers in the multi-feeder test system. The maximum 15-minute diversified demands for each day, of each season of the year, for each phase, in each radial segment was determined using (9)-(12). The greatest seasonal maximum

diversified demand value for each phase, in each radial segment, was found using (13)-(16) and is shown in Table 5-27.

Table 5-27 Seasonal Maximum Diversified Demand per Radial Segment of the Multi-Feeder Test System

Radial Segment	Spring/Fall (kW)			Winter (kW)			Summer (kW)		
	Phase A	Phase B	Phase C	Phase A	Phase B	Phase C	Phase A	Phase B	Phase C
I	0	107.5	57.4	0	139.9	71.8	0	119.5	65.6
II	620.8	364.3	237.35	740.4	460	292.5	700.8	414.5	273.15
III	776.02	600.81	424.57	926.22	754.721	528.52	877.19	682.29	492.64
IV	1022.84	777.34	840.49	1218.11	972.708	1066.61	1148.75	885.65	972.90
V	459.7	200.8	61.2	549.6	263.1	78	521.1	228.2	71
VI	480.6	215.2	79.95	574.2	280.8	100.5	544.4	244.5	92.25
VII	593.1	327.7	327.7	709.2	415.8	235.5	671.9	372	219.75
VIII	885.25	688.55	824.1	1061.33	857.234	1046.73	1007.07	780.67	954.32
IX	944.85	688.55	824.1	1134.03	857.234	1046.73	1073.17	780.67	954.32

The phase currents through the substation relays were found for the corresponding seasonal maximum diversified demands per radial segment using (17)-(20). These values are illustrated in Table 5-28.

Table 5-28 Phase Currents Measured by Substation Relay for each Radial Segment for Seasonal Maximum Diversified Demand

Radial Segment	Spring/Fall			Winter			Summer		
	Phase Currents (A)								
	Phase A	Phase B	Phase C	Phase A	Phase B	Phase C	Phase A	Phase B	Phase C
I	2.429	7.642	3.5989	2.431	9.9156	4.525	2.426	8.491	4.203
II	48.927	27.441	16.271	57.966	34.856	20.291	54.0789	31.283	18.738
III	57.0185	42.866	31.41	67.976	54.38	36.012	63.918	48.744	34.796
IV	71.283	60.377	60.351	85.0937	76.875	75.286	79.988	69.102	69.019
V	35.233	15.141	3.906	43.124	20.061	5.378	40.539	17.27	4.901
VI	35.887	16.173	5.253	44.241	21.297	7.161	41.417	18.409	6.581
VII	45.108	24.989	14.162	55.017	32.377	17.281	51.578	28.382	16.103
VIII	63.916	49.538	58.287	77.507	62.174	73.954	73.085	56.437	67.469
IX	62.376	57.208	57.598	76.682	71.324	72.586	71.815	64.64	66.47

The radial segment pickup settings for the substation relay were determined by multiplying the largest phase current in each radial segment, for each season, by a factor of 1.5. These settings were configured into each substation relay, along with the distance relay signal that was sent when the modified POTT scheme of the protection scheme opened a breaker(s). This is shown in Fig. 5-4 below.

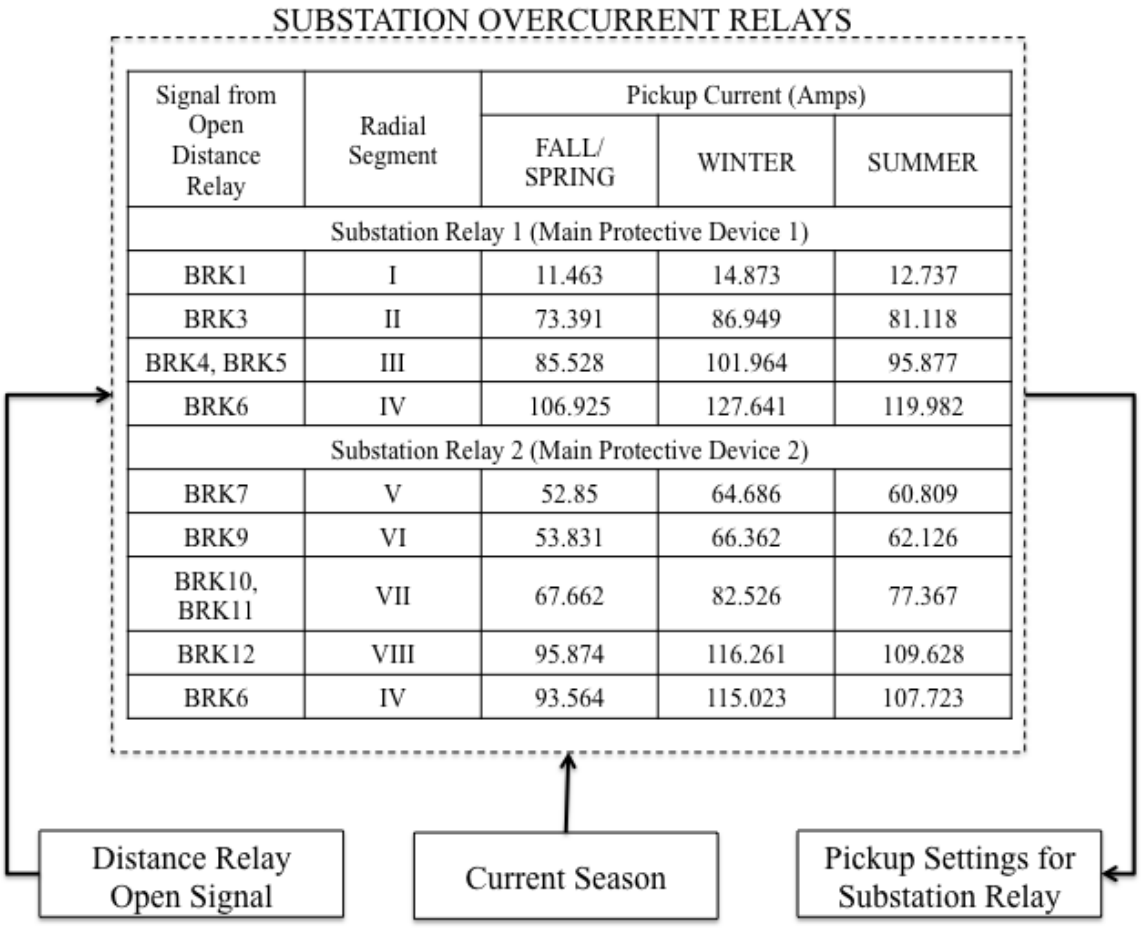

Signal from Open Distance Relay	Radial Segment	Pickup Current (Amps)		
		FALL/ SPRING	WINTER	SUMMER
Substation Relay 1 (Main Protective Device 1)				
BRK1	I	11.463	14.873	12.737
BRK3	II	73.391	86.949	81.118
BRK4, BRK5	III	85.528	101.964	95.877
BRK6	IV	106.925	127.641	119.982
Substation Relay 2 (Main Protective Device 2)				
BRK7	V	52.85	64.686	60.809
BRK9	VI	53.831	66.362	62.126
BRK10, BRK11	VII	67.662	82.526	77.367
BRK12	VIII	95.874	116.261	109.628
BRK6	IV	93.564	115.023	107.723

Fig. 5-4. Pickup settings for substation overcurrent relays for the multi-feeder test system.

The first transient simulation studies involved staging faults within the nine (9) protection coordination areas of the multi-feeder system and drawing a comparison of the tripping times of the substation relays with a pickup setting based on maximum loading and a seasonal pickup setting. Faults were placed both on the main feeder and laterals to simulate the operation of the substation relay as the primary and backup protective device. The second transient simulation studies involved staging faults in one protection coordination area of the multi-feeder test system and drawing a comparison of the tripping times of the substation relays with their seasonal settings. At the start of the transient simulations, the DGs were operated as simple 3-phase sources and were switched to machine modes at 0.8s. The connected DGs reached the 60Hz system frequency at about 3s. The frequency response of the DGs on both feeders is depicted in Fig. 5-5.

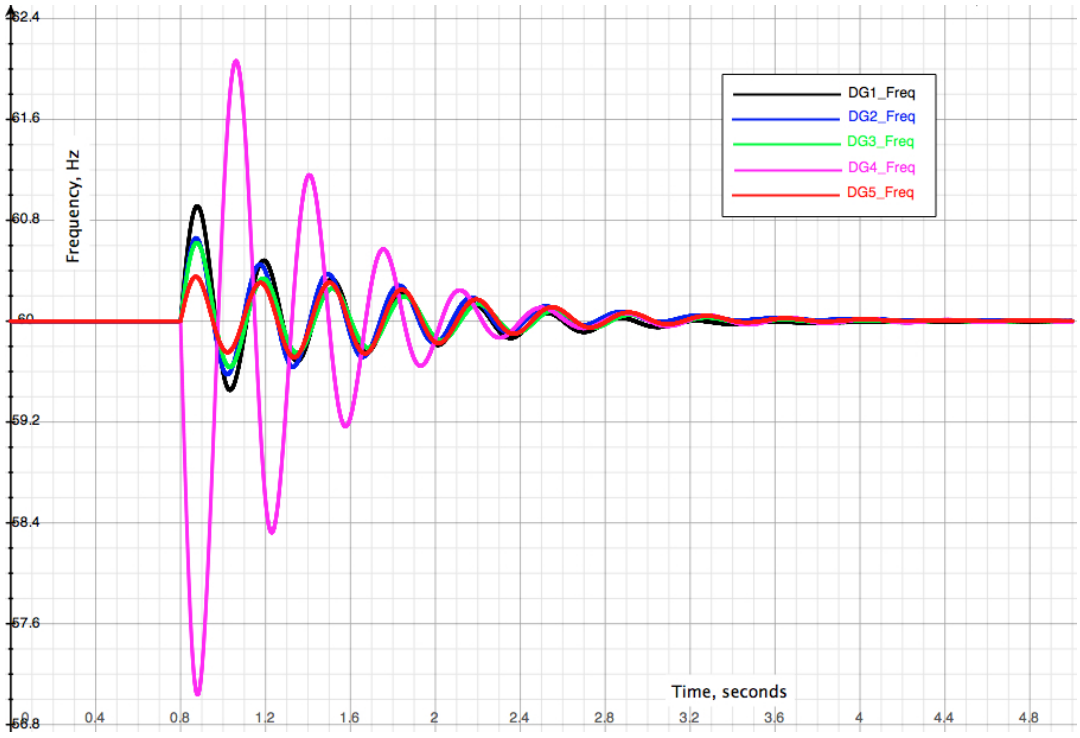

Fig. 5-5. Frequency of synchronous-based distributed generators.

5.3.2 Case Study 1 - Comparison between Setting based on Maximum Load and Seasonal Setting of Substation Relays for Faults in All Coordination Areas in One Season

Referring to Fig. 5-3, an A-G fault with negligible fault resistance was simulated at 5s on the end of lateral 2, at node 822 on feeder one. Lateral 2 was a single-phase (A-phase) lateral from node 816 to 822 located in protection coordination area II. The distance relays controlling the breakers, BRK2 and BRK3, were coordinated using the modified POTT scheme. BRK2 and BRK3 were located at nodes 814 and 834, respectively, and the distance from the terminals of their distance relays was 15.132576 miles. The length of lateral 2 was 12.045455 miles; *Lat2*, which was an inverse-time

overcurrent relay with a moderately inverse characteristic and a time-dial setting (TDS) of 0.5, denoted its primary protection. In radial operation, *Substation Relay 1*, located at bus 800, operated as the backup protection for a fault on lateral 2. Substation relay 1 was an inverse-time overcurrent relay with a moderately inverse characteristic and a time-dial setting of 1.0.

When the fault occurred, both distance relays detected the fault and saw impedances that were within the circumference of their respective mho circles. As dictated by the modified POTT scheme (Section 3.1.2), for a fault in a protected area on the main feeder, only one distance-relay breaker opens. Consequently, BRK3 opened at 5.0165s and DG1 disconnected. This is illustrated in Fig. 5-6. Table 5-29 shows the fault current measured by the lateral 2 relay during the fault and after BRK3 was opened by the modified POTT scheme. From the table, it can be seen that after the modified POTT scheme broke up the loop by opening BRK3 for a fault in protection coordination area II, the only source of fault current was *Substation Transformer 1* (measured by *Substation Relay 1*).

Table 5-29 Current Measured by Lateral 2 Relay after BRK3 Opened

Element	**Current After BRK3 Opened (Amps)**
Lateral 2 Relay, Lat2	317.56
Substation 1, Substation Relay 1	356.63
DG1	0

Referring to Table 5-8, the pickup setting for Lat2 was based on the maximum load downstream of its location and was set at 82.97A. The pickup setting of the

substation relay, Substation Relay 1, was based on the maximum load of feeder 1, and was set at 168.74A. The tripping time for *Lat2*, the primary protection and *Substation Relay 1*, the backup protection is shown in Table 5-30. The current used to calculate the multiples of pickup was the current through the relay after BRK3 opened. From the table, it can be seen that radial coordination between Substation Relay 1 and Lat2 was maintained in the protection scheme. If Lat2 failed to operate to isolate the fault, Substation Relay 1 would operate as the backup protection, approximately 2.525 seconds later.

Table 5-30 Tripping Times of Lateral 2 and Substation 1 Overcurrent Relays for an A-G Fault on Lateral 2 of Feeder 1 of the Multi-Feeder Test System

Relay	**Pickup Setting (Amps)**	**Multiples of Pickup**	**Tripping Time (seconds)**
Lat2 Relay	82.97	3.8273	1.004
Substation Relay 1	168.74	1.0559	3.529

The same A-G fault with negligible fault resistance was simulated again at 5s on the end of lateral 2 on feeder one, with Substation Relay 1 having a Fall/Spring seasonal pickup setting. As mentioned, when a fault occurred in Area II, BRK3 opened and DG1 was disconnected, thus forming radial segment II as illustrated in Fig. 5-6. Radial segment II contained 108 distribution transformers, 44 on phase A, 36 on phase B, and 28 on phase C. (Refer to Table 5-26).

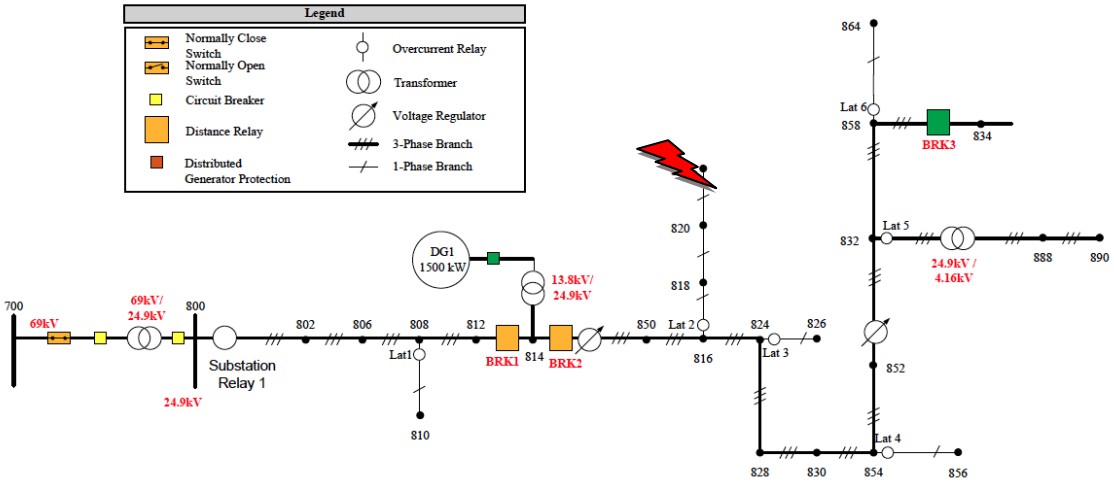

Fig. 5-6. Radial segment II of multi-feeder test system created by the modified POTT scheme.

For the fault shown, the distance relay that controls BRK3 operated, and simultaneously sent a signal to *Substation Relay 1*. The pickup setting of Substation Relay I based on the Fall/Spring seasonal maximum diversified demand was 73.391A, which was 57% lower than the original pickup setting based on maximum load. Fig. 5-7 shows the new pickup setting chosen for *Substation Relay 1* based on the operation described in Fig. 5-4.

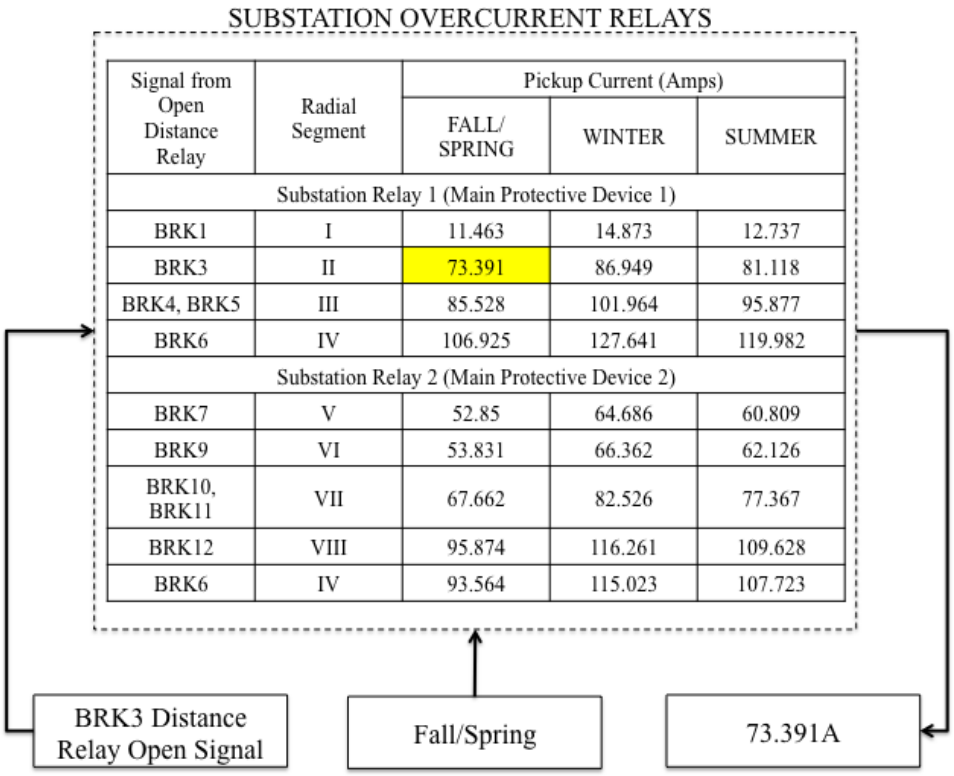

Signal from Open Distance Relay	Radial Segment	Pickup Current (Amps)		
		FALL/ SPRING	WINTER	SUMMER
Substation Relay 1 (Main Protective Device 1)				
BRK1	I	11.463	14.873	12.737
BRK3	II	73.391	86.949	81.118
BRK4, BRK5	III	85.528	101.964	95.877
BRK6	IV	106.925	127.641	119.982
Substation Relay 2 (Main Protective Device 2)				
BRK7	V	52.85	64.686	60.809
BRK9	VI	53.831	66.362	62.126
BRK10, BRK11	VII	67.662	82.526	77.367
BRK12	VIII	95.874	116.261	109.628
BRK6	IV	93.564	115.023	107.723

Fig. 5-7. New pickup setting of substation relay 1 for radial segment II.

The fault current measured by Substation Relay 1 was 356.630A, and 317.564A measured by Lat2. Table 5-31 compares the tripping times of *Substation Relay 1* between the Fall/Spring seasonal pickup setting and the pickup setting based on the maximum loading of feeder 1. The table also shows the tripping times of the Lat2 relay. The Lat2 relay was set based on the maximum load downstream of its location, and its setting was not changed. The table shows that Lat2 operated first for the A-G fault at node 822 in both instances and so radial protection selectivity was maintained. The seasonal pickup setting showed that there was approximately a 1.8 second improvement

in the tripping time of *Substation Relay 1* when compared to the pickup setting based on maximum load.

Table 5-31 Comparison of Substation Relay I Tripping Times with a Pickup Setting based on Maximum Loading and a Fall/Spring Seasonal Pickup Setting for Fault on Lateral 2 in Radial Segment II

	Lat2 Relay – Maximum Loading	**Substation Relay 1 – Maximum Loading**	**Substation Relay 1 – Fall/Spring Seasonal**
Pickup Setting (Amps)	82.974	168.74	73.391
Fault Current through Relay (Amps)	317.564	356.630	356.630
Multiples of Pickup	3.8273	2.113	4.8593
Tripping Time (seconds)	1.0035	3.529	1.7172

In the second scenario, sequential faults in two (2) different areas on Feeder 2 of the multi-feeder test system were simulated. First, an A-G fault with negligible fault resistance was simulated at 5s on lateral 2 between nodes 818(II) and 820(II) on feeder 2. Secondly, an AB-phase fault was initiated at 5.05s between nodes 830(II) and 854(II) on feeder 2. Lateral 2 was a single-phase (A-phase) lateral from node 816(II) to 822(II) located in protection coordination area V. The distance function of *Substation Relay 2* and the distance relay controlling BRK7 were coordinated using a modified POTT scheme for protection coordination area V.

Coordination area V had three outfeeds as illustrated in Fig. 5-8. Substation Relay 2 and BRK7 were located at nodes 800(II) and 828(II), respectively, and the distance from the terminals of their distance relays was 21.806818 miles. The length of lateral 2 was 12.045455 miles and Lat2b, which served as its primary protection, was an inverse-time overcurrent relay with a moderately inverse characteristic and a time-dial setting (TDS) of 0.5. In radial operation, *Substation Relay 2*, located at bus 800(II),

operated as the backup protection for a fault on lateral 2 on feeder 2. *Substation Relay 2* was an inverse-time overcurrent relay with a moderately inverse characteristic and a time-dial setting of 1.0.

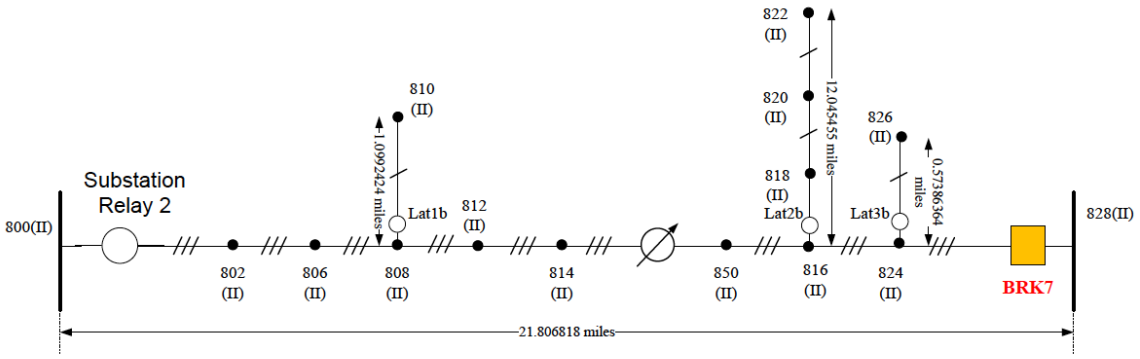

Fig. 5-8. Distance protection coordination area V.

Coordination area VI, had one outfeed and is shown in Fig. 5-9. BRK8 and BRK9 form the boundary of this protection area, which is from nodes 828(II) to 832(II). The distance between the terminals of the distance relays for the aforementioned breakers was 10.94697 miles. The length of lateral 4 was 4.4185606 miles and Lat4b served as its primary protection, which was an inverse-time overcurrent relay with a moderately inverse characteristic and a time-dial setting (TDS) of 0.5.

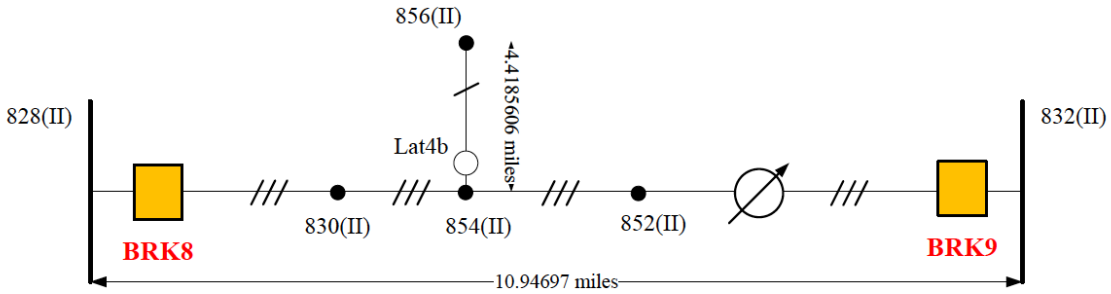

Fig. 5-9. Distance protection coordination area VI

For an A-G fault between nodes 818(II) and 820(II), the distance function of *Substation Relay 2* and the distance relay at BRK7 both detected the fault using the modified POTT scheme, and BRK7 opened. For the AB-phase fault that occurred at 5.05s in Area VI, the distance relay at BRK8 and BRK9 detected the fault. BRK9 opened and DG3 was disconnected, thus Area VI was left de-energized. Meanwhile, the A-G fault in Area V was still energized, only being sourced by substation transformer 2. Lat2b acted as the primary protection for this fault, while the overcurrent relay, Substation Relay 2 was the backup protection. The tripping time for Lat2b operating as primary protection and Substation Relay 2 operating as backup protection is shown in Table 5-32.

Table 5-32 Tripping Times of Lateral 2 and Substation 2 Overcurrent Relays

Relay	Fault Current Through Relay	Pickup Setting (Amps)	Multiples of Pickup	Tripping Time (seconds)
Lat2 Relay	550.889	82.974	6.6393	0.724
Substation Relay 1	554.332	168.74	3.2851	2.253

The same sequential faults were simulated again with Substation Relay 2 having a Fall/Spring seasonal pickup setting. When there was a fault in Area V, BRK7 opened and radial segment V was formed. This is illustrated in Fig. 5-10. Radial segment V contains three (3) laterals and is from node 800 to the terminals of node 828. Lat2b overcurrent relay, which is the primary protection for the fault shown, has a moderately inverse characteristic and a TDS of 0.5. Substation Relay 2, which is the backup protection for the fault shown, also has a moderately inverse characteristic, but with a TDS of 1.0.

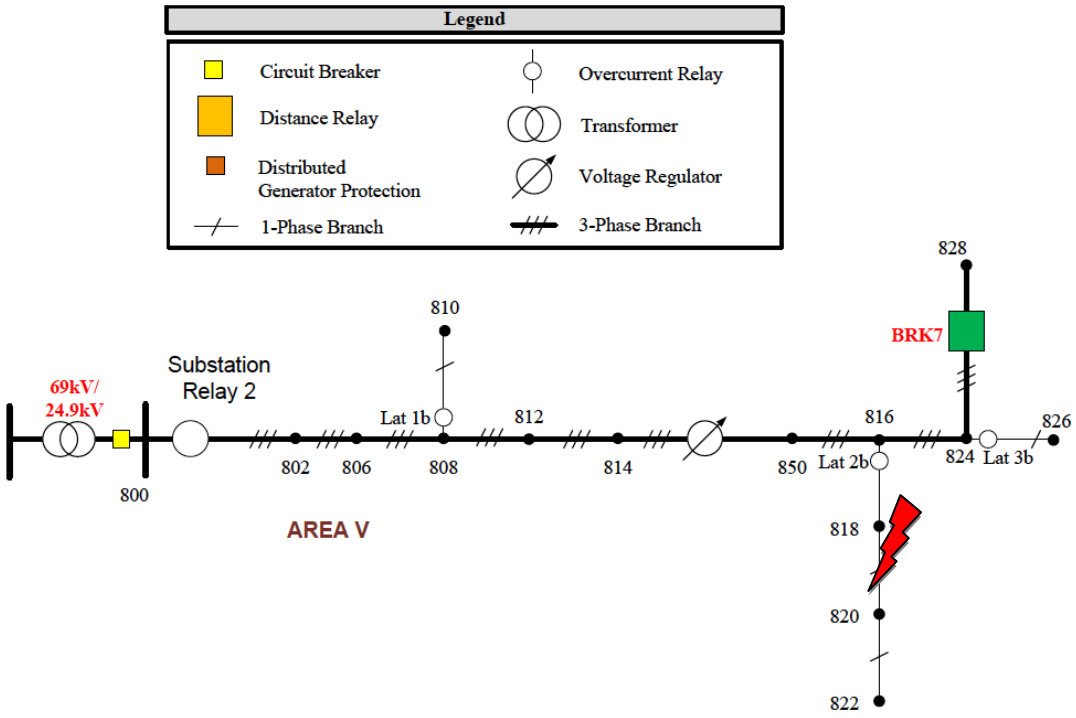

Fig. 5-10. Radial segment V of multi-feeder test system created by modified POTT scheme.

When the fault occurred in Area VI at 5.05s, BRK7 was already opened by the modified POTT scheme during the occurrence of the first fault in Area V. The modified POTT scheme then opened BRK9 and disconnected DG3 when the distance relays at BRK8 and BRK9 detected the second fault. This caused Area VI to be de-energized. For the fault shown in Fig. 5-10, the distance relay that controlled BRK7 operated and simultaneously sent a signal to Substation Relay 2. In the Fall/Spring season, for radial segment V, the pickup setting that was based on seasonal maximum diversified demand was 52.85A. Fig. 5-11 shows the new pickup setting for *Substation Relay 2*.

SUBSTATION OVERCURRENT RELAYS

Signal from Open Distance Relay	Radial Segment	Pickup Current (Amps)		
		FALL/ SPRING	WINTER	SUMMER
Substation Relay 1 (Main Protective Device 1)				
BRK1	I	11.463	14.873	12.737
BRK3	II	73.391	86.949	81.118
BRK4, BRK5	III	85.528	101.964	95.877
BRK6	IV	106.925	127.641	119.982
Substation Relay 2 (Main Protective Device 2)				
BRK7	V	52.85	64.686	60.809
BRK9	VI	53.831	66.362	62.126
BRK10, BRK11	VII	67.662	82.526	77.367
BRK12	VIII	95.874	116.261	109.628
BRK6	IV	93.564	115.023	107.723

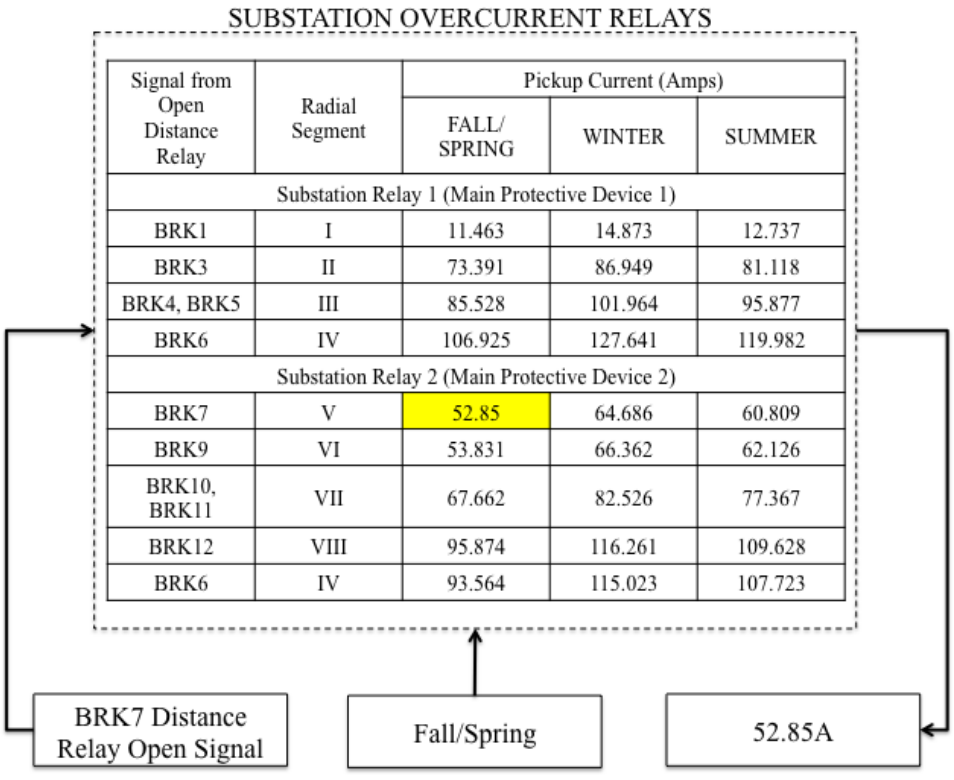

Fig. 5-11. New pickup setting for substation relay 2 for radial segment V.

Substation transformer 2 was the only source that energized A-G fault in Area V. The tripping time for Lat2b operating as primary protection and Substation Relay 2 operating as backup protection is shown in Table 5-33. The table shows that Lat2b operates first for the A-G fault between 818(II) and 820(II) on feeder, thus radial protection selectivity was maintained. The seasonal pickup setting resulted in approximately a 1.06 second improvement in tripping time of the substation relay.

Table 5-33 Comparison of Substation Relay 2 Tripping Times with a Pickup Setting based on Maximum Loading and a Fall/Spring Seasonal Pickup Setting for Fault on Lateral 2 in Radial Segment V

	Lat2b Relay – Maximum Loading	**Substation Relay 2 – Maximum Loading**	**Substation Relay 2 – Fall/Spring Seasonal**
Pickup Setting (Amps)	82.974	168.74	52.85
Fault Current through Relay (Amps)	550.889	554.332	554.332
Multiples of Pickup	6.6393	3.2851	10.4889
Tripping Time (seconds)	0.724	2.253	1.184

In the following scenarios, different faults were placed on the main feeder and the laterals in all coordination areas on the multi-feeder test system. The Fall/Spring seasonal setting was used for the two substation relays and the settings for the maximum loading was used for the lateral relays. For the pickup settings based on maximum load and the seasonal pickup setting, Table 5-34 compares the tripping times of the substation relay for faults on the main feeder. The fault type, fault location, and the fault current measured by the substation relay are shown in the table. The last column of the table compares how much faster the tripping times are for the substation relay using the seasonal pickup setting over the maximum load pickup setting. For example, an ABC three-phase fault was simulated at node 840 on Feeder 2 of the multi-feeder test system.

This node was located in radial segment VI. The fault current measured by *Substation Relay 2,* was 599.416A. The Fall/Spring seasonal pickup setting for radial segment VI was 106.9245A and the static pickup setting based on maximum load of the entire feeder was 168.74A. The tripping times, in seconds, of *Substation Relay 2* for the Fall/Spring seasonal setting, and the maximum load pickup setting, were 1.582 and 2.210, respectively. This represented a 33.98% faster trip time of *Substation Relay* 2 with the seasonal pickup setting than the maximum load pickup setting. The multiples of pickup current for the Fall/Spring seasonal pickup setting and the static pickup setting based on maximum load were 5.606 and 3.552, respectively. Table 5-35 compares the tripping times of the substation relay for faults on the lateral, between the maximum load pickup setting and the seasonal pickup setting. The lateral relay pickup setting was included to determine if selectivity was maintained when the pickup setting for the substation relay was changed. For example, an A-G ground fault was simulated between nodes 846-848 on Feeder 1 of the multi-feeder test system. The fault current as measured by *Substation Relay 1* was used to calculate the multiple of pickup current through the lateral relay. For the aforementioned fault, the lateral pickup current was 34.8825A and the multiple of pickup current, for a fault current of 382.994A measured by *Substation Relay 1,* was 10.980. This represented a tripping time of 0.582 seconds for the lateral relay.

Table 5-34 Faults on Main Feeder in All Areas – Comparison between Spring/Fall Seasonal Setting and Maximum Load Static Setting

Radial Segment	Pickup Settings (Amps)		Fault Type	Fault Location	Fault Current at Substation (A)	Multiples of Pickup		Tripping Time (seconds)		%Faster with Seasonal Setting
	Seasonal	Static				Seasonal	Static	Seasonal	Static	
I	11.4630	168.74	A-G	800-802	4154.308	362.410	24.619	0.526	0.892	69.73%
			C-G	802-806	3477.895	303.402	20.610	0.539	0.940	74.21%
			AB	808	1961.6178	171.126	11.625	0.589	1.138	93.09%
			AC	812	1281.488	111.793	7.594	0.635	1.359	114.08%
			BC	800-802	3831.169	334.224	22.704	0.532	0.913	71.71%
			ABC	812-814	1284.759	112.073	7.614	0.634	1.357	113.93%
II	73.3905	168.74	C-G	832	408.997	5.573	2.424	1.587	2.997	88.80%
			AC	832-858	592.631	8.075	3.512	1.321	2.138	61.84%
			BC	824	736.428	10.034	4.364	1.205	1.836	52.35%
			ABC	858-834	663.928	9.047	3.935	1.258	1.968	56.50%
IV	106.9245	168.74	A-G	860-836	388.42	3.633	2.302	2.085	3.177	52.41%
			C-G	840(II)	369.939	3.46	2.192	2.1636	3.369	55.75%
			ABC	840(II)	599.416	5.606	3.552	1.582	2.120	33.98%
			BC	860-836	508.088	4.752	3.011	1.741	2.424	39.29%
V	52.8495	168.74	C-G	812	916.352	17.339	5.430	0.991	1.610	62.48%
			AB	824-828	947.568	17.930	5.615	0.981	1.581	61.20%
			AC	816-824	971.666	18.386	5.758	0.973	1.559	60.27%
			ABC	816-824	1103.786	20.885	6.541	0.936	1.459	55.96%

Table 5-34 Continued

Radial Segment	Pickup Settings (Amps)		Fault Type	Fault Location	Fault Current at Substation (A)	Multiple of Pickup		Tripping Time (seconds)		%Faster with Seasonal Setting
	Seasonal	Static				Seasonal	Static	Seasonal	Static	
VI	53.8305	168.74	AB	828-830	837.31	15.555	4.962	1.027	1.696	65.17%
			BC	830-854	633.746	11.773	3.756	1.133	2.034	79.59%
			ABC	854-852	685.096	12.727	4.060	1.101	1.926	74.98%
VIII	95.8740	168.74	B-G	834-860	381.863	3.983	2.263	1.952	3.241	66.09%
			C-G	834-860	370.495	3.864	2.196	1.993	3.362	68.70%
			AB	858-834	597.993	6.237	3.544	1.495	2.124	42.04%
			AC	860-836	526.97	5.496	3.123	1.599	2.350	46.90%

Table 5-35 Fault on Laterals in All Areas – Comparison between Fall/Spring Seasonal Setting and Maximum Load Static Setting

Radial Segment	Pickup Settings (Amps)			Fault Type	Fault Location	Fault Current at Substation (A)	Multiple of Pickup			Tripping Time			%Faster with Seasonal Setting
	Lateral Relay	Substation Relay					Lateral Relay	Substation Relay		Lateral Relay	Substation Relay		
		Seasonal	Static					Seasonal	Static		Seasonal	Static	
I	3.648	11.4630	168.74	B-G	810	1063.54	291.541	92.780	6.303	0.271	0.657	1.487	126.34%
II	82.974	73.3905	168.74	A-G	822	356.630	4.082	4.615	2.113	0.96	1.772	3.529	105.53%
	17.736			B-G	824-826	565.399	31.879	7.704	3.351	0.416	1.35	2.218	64.34%
	17.955			AB	888	672.029	37.429	9.157	3.983	0.4	1.251	1.952	55.98%

Table 5-35 Continued

Radial Segment	Pickup Settings (Amps)			Fault Type	Fault Location	Fault Current at Substation (A)	Multiple of Pickup			Tripping Time			%Faster with Seasonal Setting
	Lateral Relay	Substation Relay					Lateral Relay	Substation Relay		Lateral Relay	Substation Relay		
		Seasonal	Static					Seasonal	Static		Seasonal	Static	
III	34.8825	85.5278	168.74	ABC	844-846	620.809	17.797	7.259	3.679	0.491	1.387	2.065	48.84%
				A-G	846-848	382.994	10.980	4.478	2.270	0.582	1.806	3.230	78.85%
				BC	844	507.396	14.546	5.933	3.007	0.525	1.535	2.427	58.17%
				C-G	842-844	368.470	10.563	4.308	2.184	0.590	1.851	3.385	82.86%
IV	9.1785	106.9245	168.74	B-G	862-838	372.905	40.628	3.488	2.210	0.392	2.150	3.336	55.17%
V	82.974	52.8495	168.74	A-G	816	766.756	9.241	14.508	4.544	0.623	1.051	1.789	70.23%
	3.648			B-G	808	1219.512	334.296	23.075	7.227	0.266	0.909	1.390	52.97%
	17.736			B-G	824-826	567.576	32.001	10.739	3.364	0.416	1.173	2.211	88.48%
VI	0.564	53.8305	168.74	B-G	856	417.018	739.394	7.747	2.471	0.239	1.346	2.934	117.98%
				B-G	854	477.744	847.064	8.875	2.831	0.235	1.268	2.563	102.12%
VII	17.955	67.6620	168.74	C-G	888	485.775	27.055	7.179	2.879	0.435	1.395	2.524	80.94%
VIII	0.087	95.8740	168.74	A-G	858	417.702	4801.172	4.357	2.475	0.196	1.838	2.929	59.37%
				A-G	864	397.136	4564.782	4.142	2.353	0.197	1.900	3.097	62.98%
	34.8825			BC	848	496.106	14.222	5.175	2.940	0.529	1.655	2.476	49.62%
				ABC	844-846	619.009	17.746	6.456	3.668	0.492	1.469	2.070	40.88%
IX	9.1785	93.5640	168.74	B-G	862-838	474.178	51.662	5.068	2.810	0.371	1.675	2.581	54.06%

5.3.3 Case Study 2 - Faults in Protection Coordination Area VIII for All Seasons Using Adaptive Overcurrent Protection Scheme

In this section, the results for faults in Area VIII for the three different seasons will be discussed. In this scenario, an AB phase-to-phase fault was simulated at 5s on the line segment 858(II)-834(II) on Main Feeder 2. The fault was on the main feeder and was in protection coordination Area VIII. For a fault in this area, the distance relay at BRK11 and the distance relay at BRK12 were coordinated via the modified POTT scheme and BRK12 opened, thereby creating radial segment VIII. DG4 was also disconnected for the fault. This is illustrated in Fig. 5-12.

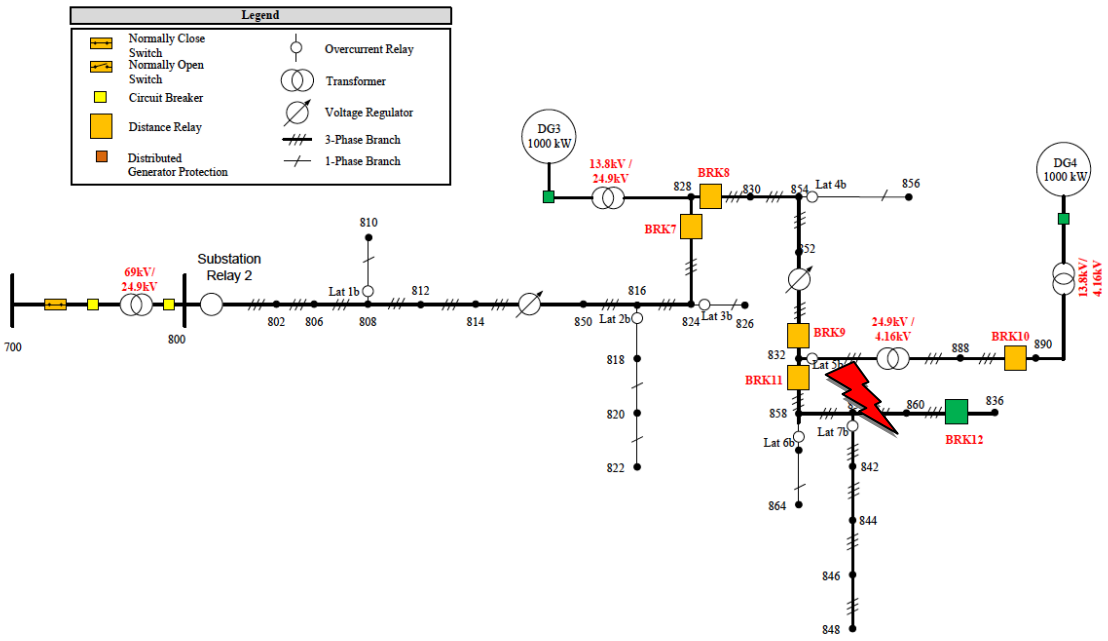

Fig. 5-12. Radial segment VIII of multi-feeder test system.

For the fault shown, the distance relay that controlled BRK12 operated and simultaneously sent a signal to Substation Relay 2. In the Fall/Spring season, for radial segment VIII, the pickup setting for Substation Relay 2 that was based on seasonal maximum diversified demand was 95.874A. This is illustrated in Fig. 5-13. The corresponding pickup setting for the winter and summer seasons were 116.261A and 109.628A, respectively.

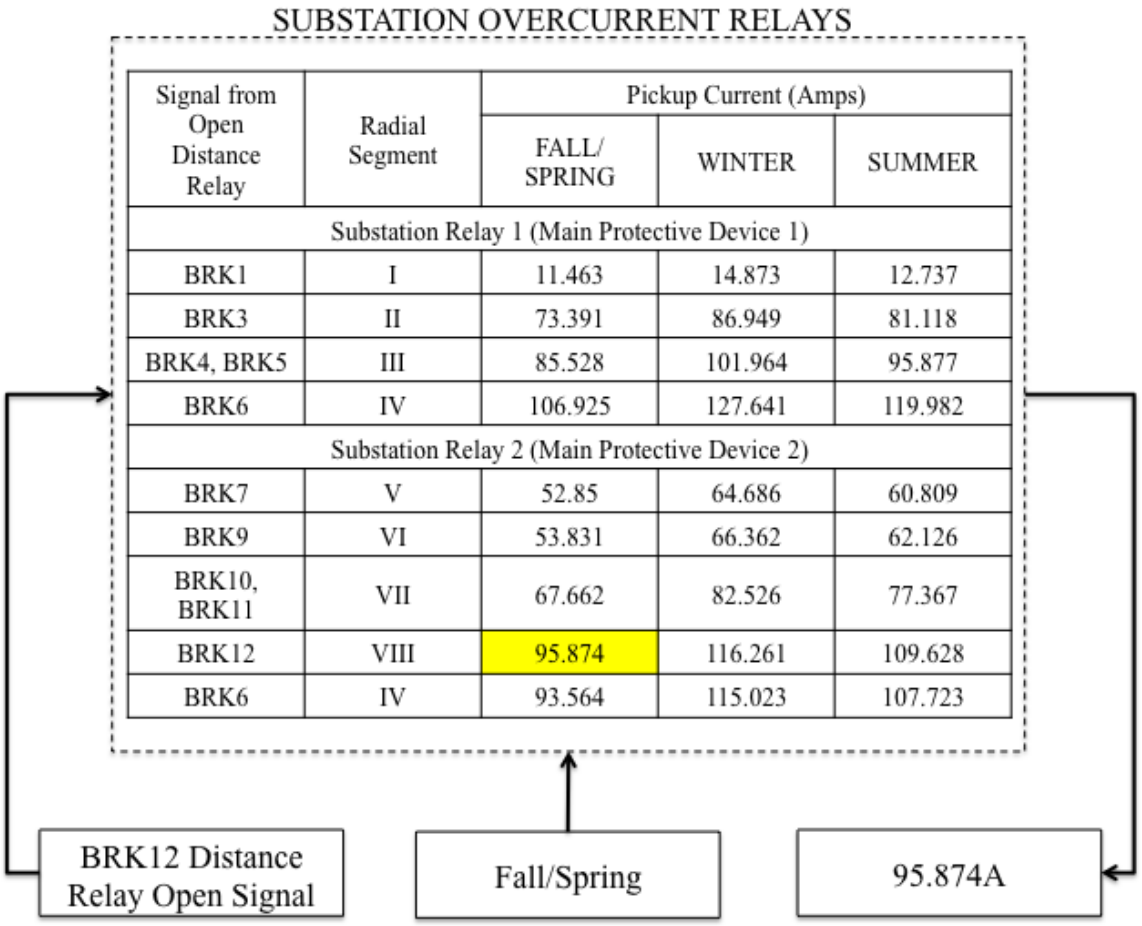

Signal from Open Distance Relay	Radial Segment	Pickup Current (Amps)		
		FALL/ SPRING	WINTER	SUMMER
Substation Relay 1 (Main Protective Device 1)				
BRK1	I	11.463	14.873	12.737
BRK3	II	73.391	86.949	81.118
BRK4, BRK5	III	85.528	101.964	95.877
BRK6	IV	106.925	127.641	119.982
Substation Relay 2 (Main Protective Device 2)				
BRK7	V	52.85	64.686	60.809
BRK9	VI	53.831	66.362	62.126
BRK10, BRK11	VII	67.662	82.526	77.367
BRK12	VIII	95.874	116.261	109.628
BRK6	IV	93.564	115.023	107.723

Fig. 5-13. Fall/Spring seasonal pickup setting for substation relay 2 for radial segment VIII.

The fault current measured by *Substation Relay 2* was 597.993A. Table 5-36 compares the tripping times of Substation Relay 2 with different pickup settings based on the three seasons and same radial segment VIII. The difference in tripping time between the Fall/Spring and the winter seasonal setting is approximately 0.15s, whereas when the former is compared to the summer seasonal setting, the difference is approximately 0.11s. When compared to the maximum load pickup setting, the difference in tripping times of all three adaptive seasonal pickup settings is 0.63s, 0.46s, and 0.51s (Spring/Fall, Winter, and Summer).

Table 5-36 Comparison of Substation Relay 2 Tripping Times with a Pickup Setting based on Maximum Loading and a Fall/Spring, Winter, and Summer Seasonal Pickup Setting for Fault on Main Feeder in Radial Segment VIII

	Substation Relay 2 – Fall/Spring Seasonal	**Substation Relay 2 – Winter Seasonal**	**Substation Relay 2 – Summer Seasonal**	**Substation Relay 2 – Maximum Loading**
Pickup Setting (Amps)	95.874	116.261	109.628	168.74
Fault Current through Relay (Amps)	597.993			
Multiples of Pickup	6.237	5.144	5.455	3.544
Tripping Time (seconds)	1.495	1.661	1.606	2.124

Table 5-37 provides a comparison between the tripping times of Substation Relay 2 with a pickup setting based on the seasonal maximum diversified demand for Radial Segment VIII and a pickup setting based on the maximum load of feeder 2. In these cases, Substation Relay 2 was the primary protection for all faults on the main feeder and the backup protection for faults on the laterals in this radial segment.

Table 5-37 Fault on Main Feeder in Radial Segment VIII – Comparison between Fall/Spring, Winter, and Summer Seasonal Settings and Maximum Load Non-Adaptive Setting

Radial Segment	Pickup Setting (Amps)				Fault Type	Fault Location	Fault Current at Substation (A)	Multiples of Pickup				Tripping Time (seconds)			
	Fall/Spring	Winter	Summer	Static				Fall/Spring	Winter	Summer	Static	Fall/Spring	Winter	Summer	Static
VIII	95.87	116.26	109.63	168.74	A-G	858	417.70	4.357	3.593	3.810	1.237	1.838	2.102	2.013	12.204
					A-G	864	397.14	4.142	3.416	3.623	1.176	1.900	2.185	2.089	15.980
					B-G	834-860	381.86	3.983	3.285	3.483	1.131	1.952	2.254	2.152	21.054
					C-G	834-860	370.5	3.864	3.187	3.380	1.097	1.993	2.310	2.203	27.896
					AB	858-834	598	6.237	5.144	5.455	1.771	1.495	1.661	1.606	4.595
					AC	860-836	526.97	5.496	4.533	4.807	1.560	1.599	1.792	1.728	5.876
					BC	848	496.11	5.175	4.267	4.525	1.469	1.655	1.863	1.794	6.784
					ABC	844-846	619.01	6.456	5.324	5.646	1.833	1.469	1.628	1.576	4.338

5.4 Summary of Results

The smart meter load information was used to generate seasonal maximum 15-minute diversified demands for each radial segment of the multi-feeder test system. The values were then used to obtain the seasonal pickup settings for every radial segment for the corresponding substation overcurrent relay. In the first case study, the trip times of the substation relays for phase and ground faults in each radial segment were monitored using a pickup setting that was obtained based upon the maximum loading of each feeder (using the conventional approach for determining pickup settings), and a Spring/Fall pickup setting that was obtained from the proposed methodology of the seasonal pickup settings. In the second case study, the trip times of substation relay 2 for phase and ground faults in radial segment VIII were monitored using pickup settings obtained based on the Spring/Fall, Summer, and Winter seasonal pickup settings from the proposed methodology.

The case studies revealed that using pickup settings based on the knowledge of seasonal maximum 15-minute diversified demands in each phase of each radial segment can reduce primary and backup tripping times of the corresponding substation relay. The Fall/Spring seasonal settings for Substation Relay 1 and Substation Relay 2 were simulated for faults in all radial segments that were created by the modified POTT scheme, which was described in Section 3.1.1. The percentage improvement in the sensitivity of the substation OC relays was at least 42% faster when a Fall/Spring seasonal setting was used compared to a static pickup setting based on maximum loading (Case 1). The Fall/Spring, Winter, and Summer seasonal settings for Substation Relay 2

was simulated for faults in radial segment VIII. Comparison between seasonal settings, however, showed at most a 0.317 second difference in the tripping time of substation overcurrent relay 2, when faults were simulated in protection coordination area 8 – (Radial Segment VIII). Comparing the tripping times for each seasonal pickup setting to the static pickup setting based on maximum load of the entire feeder, each seasonal pickup setting caused the substation relays to have faster tripping times. For the C-G fault on the line segment 834-860, the difference in tripping time of Substation Relay 2 between the Fall/Spring seasonal pickup setting and static pickup setting based on maximum load was 25.586 seconds. The studies carried out on this test system showed that OCPD selectivity was maintained between the substation overcurrent relays and the lateral relays, even though the pickup settings of the lateral relays were not modified.

6 CONCLUSIONS AND FUTURE WORK

6.1 Conclusions

This thesis discussed an approach for utilizing smart meter load information in order to improve the sensitivity of substation relays in a non-adaptive protection scheme [26] that addresses the impacts of distributed generators on overcurrent protection of radially operated meshed distribution systems. The IEEE 34 Node Radial Distribution Test Feeder was modified into a multi-feeder test system and a secondary distribution system was designed for the multi-feeder system. The multi-feeder test system and its various components were modeled in EMTP™/PSCAD®. System model verification through transient simulations studies was performed. Five DGs were connected at selected nodes on the multi-feeder test system (two on Feeder 1, three on Feeder 2). The tripping times of the substation overcurrent (OC) relays for all radial segments that were created by the modified POTT scheme of the non-adaptive protection scheme [26], were compared using seasonal pickup settings from smart meter load information and a pickup setting based on the maximum loading of a feeder.

The non-adaptive protection scheme [26] involved operating two radial feeders as a closed loop system. A closed switch was added to the multi-feeder test system so that the both feeders were connected to each other at their ends (node 840). The normally open switch at the substation of the multi-feeder test system (node 800) remained opened, thereby creating a closed loop operation. Distance relay-controlled breakers were added depending on the connection point of the DGs. For DGs on the

main feeder, two breakers were added and for DGs on the end of a lateral, three breakers were added. The breakers formed the boundaries of protection coordination areas, and their distance relays were coordinated using a modified POTT scheme. The modified POTT scheme tripped one breaker, and disconnected all DGs upstream (in the direction of the substation) of the opened breaker for faults in protection coordination areas located on the main feeder. For faults in protection coordination areas located on a lateral two breakers are opened, and all DGs upstream of the opened breaker on the main feeder and downstream the opened breaker on the end of the lateral, were disconnected. The modified POTT scheme caused the faulted section to assume a radial configuration – referred to as a radial segment, with its only source of fault current being supplied by the substation. Overcurrent relays were then used to isolate the fault.

The overcurrent protection for the laterals were set based on the maximum load downstream of the relay terminals, and the overcurrent protection for each substation relay was set based on the maximum loading of their entire feeder. The overcurrent protection included inverse-time overcurrent relays, where the lateral devices operated on a moderately inverse characteristic with a TDS of 0.5, and the substation devices, with a TDS of 1.0. On the multi-feeder test system designed in this thesis there were a total of nine protection coordination areas. The tripping times of substation relays with a pickup setting based on maximum loading were compared to the tripping times of the substation relays with pickup settings based on seasonal maximum diversified demand obtained from an approach for using smart meter demand data.

The approach for using smart meter demand data involved obtaining 15-minute demand information for each day of the year for all distributed and spot loads on the multi-feeder test system. This daily demand information was then summed to represent the daily 15-minute diversified demand per distribution transformer for a year for each phase in each radial segment that was created by the modified POTT scheme. It was assumed that the utility would have knowledge of the number of distribution transformers in the distribution system and the amount of customers being served by each distribution transformer. There were nine radial segments created by the protection scheme on the multi-feeder test system. In each possible radial segment, the number of distribution transformers was determined through the secondary distribution system design that was developed for the multi-feeder test system. A year was divided into seasons, and the daily 15-minute diversified demands for each distribution transformer for each phase in each radial segment for a year was summed to yield the per phase radial segment daily 15-minute diversified demand for a year.

The seasonal settings of the substation relays on the multi-feeder test system showed an improvement in tripping times of the substation relay, whether it operated as the primary protection or backup protection, when compared to the pickup setting based on the maximum load of the feeder. The percentage improvement in the tripping of the substation OC relays was at least 42% faster when a Fall/Spring seasonal pickup setting was used compared to a static pickup setting based on maximum loading. Comparing the seasonal pickup settings for faults in the same radial segment, there was little change in the tripping times of the substation relays. Comparison between seasonal settings,

showed at most a 0.317 second difference in the tripping time of substation overcurrent relay 2, when faults were simulated in protection coordination area VIII (Radial segment VIII).

The modified protection scheme also maintained the selectivity of the radial segment overcurrent protection due to the choice of the characteristic curves and the TDS chosen for the lateral and substation relays. In distribution systems where the characteristic curve between the substation relays and lateral relays are different, the lateral relays may also need to be adaptive as well.

6.2 Future Work

Future research will focus on investigating the adaptive protection scheme on a multifeeder system that is more heavily loaded so that there can a distinction in the seasonal maximum diversified demands as viewed from the substation. Also, studies will be investigated for long radial distribution feeders that have several tie points with other feeders several overcurrent protective devices on the main feeder.

REFERENCES

[1] J. Casazza and F. Delea, "Benefits of Electric Power and a History of the Electric Power Industry," in *Understanding Electric Power Systems*. New Jersey: John Wiley & Sons, Inc., 2010, pp. 1-14.

[2] J. Casazza and F. Delea, "The Electric Power System," in *Understanding Electric Power Systems*. New Jersey: John Wiley & Sons, Inc., 2010, pp. 15-25.

[3] The Smart Grid: An Introduction, U.S. Department of Energy, October 2011. [Online]. Available: http://energy.gov/oe/downloads/smart-grid-introduction-0.

[4] R. E. Brown, "Impact of Smart Grid on Distribution System Design," in *Power and Energy Society General Meeting - Conversion and Delivery of Electrical Energy in the 21st Century, 2008 IEEE*, pp. 1-4, July 2008.

[5] J. Casazza and F. Delea, "Distribution," in *Understanding Electric Power Systems*. New Jersey: John Wiley & Sons, Inc., 2010, pp. 115-127.

[6] *IEEE Application Guide for IEEE Std 1547, IEEE Standard for Interconnecting Distributed Resources with Electric Power Systems*, IEEE Std 1547.2-2008*,* pp. 1-207, 2009.

[7] H. Willis, "Power Delivery Systems," in *Power Distribution Planning Reference Book,* Second Edition. New York: Marcel Dekker, 2004.

[8] A. Girgis and S. Brahma, "Effect of Distributed Generation on Protective Device Coordination in Distribution System," in *Proc. Large Eng. Syst. Conf.*, Halifax, NS, Canada, 2001, pp. 115–119.

[9] J. A. Martinez and J. Martin-Arnedo, "Impact of Distributed Generation on Distribution Protection and Power Quality," presented at the IEEE Power Energy Soc. General Meet., Calgary, AB, Canada, Jul. 2009.

[10] B. Hussain, S. M. Sharkh, and S. Hussain, "Impact Studies of Distributed Generation on Power Quality and Protection Setup of an Existing Distribution Network," in *Power Electronics Electrical Drives Automation and Motion (SPEEDAM), 2010 International Symposium on*, 2010, pp. 1243-1246.

[11] D. T. K. Abdel-Galil, D. E. F. El-Saadany, D. A. Girgis, D. M. M. A. Salama, and D. H. H. M. Zeineldin, "Protection Coordination Planning with Distributed Generation," Qualsys Engco. Inc. CETC Number 2007-49 /2007-09-14.

[12] H. Zayandehroodi, A. Mohamed, H. Shareef, and M. Jafari, "An Overview of Protection Coordination Methods in Distribution Network with DGs," presented at Internation Conference: Electrical Enery and Industrial Electronic Systems, Penang, Malaysia, Dec. 2009.

[13] T. Short, "Fundamentals of Distribution Systems," in *Electric Power Distribution Handbook*. New York: CRC Press, 2003.

[14] H. Willis, "Load Curve and End-Use Modeling," in *Spatial Electric Load Forecasting* New York: Marcel Dekker, 2002.

[15] H. Willis, "Consumer Demand and Electric Load," in *Power Distribution Planning Reference Book,* Second Edition. New York: Marcel Dekker, 2004.

[16] ITERES SMART GRID: Filling the Gap for New Technology, (2011). [Online]. Available: http://www.iteresgroup.com/services/smart-grid/.

[17] S. Horowitz, A. Phadke, and B. Renz, "The Future of Power Transmission," *Power and Energy Magazine, IEEE,* vol. 8, pp. 34-40, 2010.

[18] D. Reilch. (May 2008). Smart meters on a Roll in Canada. [Online]. Available: http://mthink.com/utilities/knowledge/smart-meters-roll-canada.

[19] K. Jan and B. Anne-Marie, "Distributed Generation," in *Distributed Generation The Power Paradigm for the New Millenium*. New York: CRC Press, 2001.

[20] J. M. Gers and E. J. Holmes, "Fuses, Reclosers and Sectionalisers," in *Protection of Electricity Distribution Networks* (2nd Edition): Institution of Engineering and Technology, 2004, pp. 109-136.

[21] J. M. Gers and E. J. Holmes, "Distance Protection," in *Protection of Electricity Distribution Networks* (2nd Edition): Institution of Engineering and Technology, 2004, pp. 186-188.

[22] M. Geidl, "Protection of Power Systems with Distributed Generation: State of the Art," Swiss Federal Institute of Technology (ETH) Zurich, July 2005.

[23] G. D. Rockefeller, C. L. Wagner, J. R. Linders, K. L. Hicks, and D. T. Rizy, "Adaptive Transmission Relaying Concepts for Improved Performance," *Power Delivery, IEEE Transactions on,* vol. 3, pp. 1446-1458, 1988.

[24] G. Tang and M. R. Iravani, "Application of a Fault Current Limiter To Minimize Distributed Generation Impact on Coordinated Relay Protection", International Conference on Power Systems Transients (IPST'05) in Montreal, Canada on June 19-23, 2005 Paper No. IPST05 – 158.

[25] A. Agheli, H. A. Abyaneh, R. M. Chabanloo, and H. H. Dezaki, "Reducing the Impact of DG in Distribution Networks Protection Using Fault Current Limiters," in *2010 4th International Power Engineering and Optimization Conference (PEOCO),* June 2010, pp. 298-303.

[26] F. A. Viawan, D. Karlsson, A. Sannino, and J. Daalde, "Protection Scheme for Meshed Distribution Systems with High Penetration of Distributed Generation," in *PS '06 Power Systems Conference: Advanced Metering, Protection, Control, Communication, and Distributed Resources*, March 2006, pp. 99-104.

[27] S. M. Brahma and A. A. Girgis, "Microprocessor-Based Reclosing to Coordinate Fuse and Recloser in a System with High Penetration of Distributed Generation," in *Proceedings IEEE Power Engineering Society Winter Meeting,* vol. 1, 2002, pp. 453-458.

[28] A. Zamani, T. Sidhu, and A. Yazdani, "A Strategy for Protection Coordination in Radial Distribution Networks with Distributed Generators," in *2010 IEEE Power and Energy Society General Meeting,* 2010, pp. 1-8.

[29] H. B. Funmilayo and K. L. Butler-Purry, "An Approach To Mitigate The Impact Of Distributed Generation On The Overcurrent Protection Scheme For Radial Feeders," in 2009 *IEEE/PES Power Systems Conference and Exposition,* , pp. 1-11.

[30] L. Zhongwei, T. Weiming, L. Fengge, and F. Shenghu, "Study on Adaptive Protection System of Power Supply and Distribution Line," in *International Conference on Power System Technology, PowerCon 2006.*, October 2006, pp. 1-6.

[31] A. Conde and E. Vazquez, "Application of a Proposed Overcurrent Relay in Radial Distribution Networks," *Electric Power Systems Research,* vol. 81, pp. 570-579, 2011.

[32] A. C. EnrÌquez and E. Vazquez-MartÌnez, "Enhanced Time Overcurrent Coordination," *Electric Power Systems Research,* vol. 76, pp. 457-465, 2006.

[33] A. C. EnrÌquez, E. Vazquez-MartÌnez, and J. C. Escobar MartÌnez, "Time Coordination by Time Adaptive Function," Computacion y Sistemas*,* Mexico, vol. 13, pp. 247-256,. March 2010.

[34] A. C. EnrÌquez, E. Vazquez-MartÌnez, and H. J. Altuve-Ferrer, "Time Overcurrent Adaptive Relay," *International Journal of Electrical Power & Energy Systems,* vol. 25, pp. 841-847, 2003.

[35] S. A. M. Javadian and M. R. Haghifam, "Designing a New Protection System for Distribution Networks Including DG," in *IET 9th International Conference on Developments in Power System Protection,* March 2008, pp. 675-680.

[36] S. M. Brahma and A. A. Girgis, "Development of Adaptive Protection Scheme for Distribution Systems with High Penetration of Distributed Generation," *IEEE Transactions on Power Delivery,* vol. 19, pp. 56-63, January 2004.

[37] P. Mahat, Z. Chen, B. Bak-Jensen, and C. L. Bak, "A Simple Adaptive Over-Current Protection of Distribution Systems with Distributed Generation," *IEEE Transactions on Smart Grid,* pp. 1-10, September 2010.

[38] M. Baran and I. El-Markabi, "Adaptive Overcurrent Protection for Distribution Feeders with Distributed Generators," in *2004 IEEE PES Power Systems Conference and Exposition*, October 2004, pp. 715-719 vol.2.

[39] Y. L. L. J. L. Sun, S. W. Li, and Q. Jin, "A New Protection Scheme for Distribution System with Distributed Generations," *The International Conference on Electrical Engineering,* 2009.

[40] M. Jing, L. Jinlong, and W. Zengping, "An Adaptive Distance Protection Scheme for Distribution System with Distributed Generation," in *2010 5th International Conference on Critical Infrastructure (CRIS)*, September 2010, pp. 1-4.

[41] J. Blackburn and T. Domin, "Protection Fundamentals and Basic Design Principles," in *Protective Relaying Principles and Applications,* 3rd Edition. New York: CRC Press, 2006.

[42] M. Shahidehpour, Yamin, Hatim., "Short-Term Load Forecasting," in *Market Operations in Electric Power Systems: Forecasting, Scheduling, and Risk Management*. New York: Institute of Electrical and Electronics Engineers, Wiley-Interscience, pp 21-55 .

[43] W. H. Kersting, "Radial Distribution Test Feeders," in *Proc. 2001 IEEE Power Engineering Soc. Winter Meeting*, Columbus, OH , USA, Jan. 2001, vol. 2, pp. 908-912.

[44] W. H. Kersting and W. H. Phillips, "Modeling and Analysis of Rural Electric Distribution Feeders," *IEEE Transactions on Industry Applications,* vol. 28, pp. 767-773, July/August 1992.

[45] *IEEE Standard Inverse-Time Characteristic Equations for Overcurrent Relays*, *IEEE Standard C37.112-1996*, 1997.

[46] G. Benmouyal, M. Meisinger, J. Burnworth, W. A. Elmore, K. Freirich, P. A. Kotos, P. R. Leblanc, P. J. Lerley, J. E. McConnell, J. Mizener, J. Pinto de Sa, R. Ramaswami, M. S. Sachdev, W. M. Strang, J. E. Waldron, S. Watansiriroch, and S. E. Zocholl, "IEEE Standard Inverse-Time Characteristic Equations for overcurrent relays," *IEEE Transactions on Power Delivery,* vol. 14, pp. 868-872, July 1999.

[47] AIEE Committee Report, "Protection of Multiterminal and Tapped Lines," *Transactions of the American Institute of Electrical Engineers Power Apparatus and Systems, Part III.,* vol. 80, pp. 55-65, April 1961.

[48] A. Pabla, "Electricity Forecasting" in *Electric Power Distribution*. New Dehli: Tata McGraw-Hill, 2004, pp 26-74.

[49] H. Willis, "Basic Line Segment and Transformer Sizing Economics," in *Power Distribution Planning Reference Book,* Second Edition. New York: Marcel Dekker, 2004, pp 389-418.

[50] W. H. Kersting, "The Nature of Loads," in *Distribution System Modeling and Analysis*. New York: CRC Press, 2002, pp. 11-38.

[51] P. M. Subcommittee, "IEEE Reliability Test System," *IEEE Transactions on Power Apparatus and Systems,* vol. PAS-98, pp. 2047-2054, 1979.

APPENDIX I

IMPEDANCE MATRICES OF THE LINE CONFIGURATIONS USED IN THE MULTI-FEEDER TEST SYSTEM

The type of cables that were used in the multifeeder test system was shown in Table 5-4. The line segment impedance matrices for each configuration are shown in (27), (28) and (29). Configuration 300 represents the impedances for a three-phase line. Configuration 302 and 303 represents the impedances for single-phase lines.

Configuration 300 = R + jX

$$= \begin{bmatrix} 0.3465+j1.0179 & 0.1560+j0.5017 & 0.1580+j0.4326 \\ 0.1560+j0.5017 & 0.3375+j1.0478 & 0.1535+j0.3849 \\ 0.1580+j0.4326 & 0.1535+j0.3849 & 0.3414+j1.0348 \end{bmatrix} \Omega/\text{mile} \quad (27)$$

Configuration 302 = R + jX =

$$\begin{bmatrix} 1.3292+j1.3475 & 0 & 0 \\ 0 & 0 & 0 \\ 0 & 0 & 0 \end{bmatrix} \Omega/\text{mile} \quad (28)$$

Configuration 303 = R + jX =

$$\begin{bmatrix} 0 & 0 & 0 \\ 0 & 1.3292+j1.3475 & 0 \\ 0 & 0 & 0 \end{bmatrix} \Omega/\text{mile} \quad (29)$$

APPENDIX II

SECONDARY DISTRIBUTED LOADS AND TRANSFORMER RATINGS FOR THE MULTI-FEEDER TEST SYSTEM

Table II-1, Table II-2, and Table II-3 shows the number and the per interval demands of the customers on Phase-A #, Phase-B #, and Phase-C #, respectively, and the number and ratings of the transformers between each line segment.

Table II-1 Phase A Secondary Distribution Load Ratings

Node A	Node B	Phase-A #	# of Xfmers	Energy Consumption per Customer per Month (kWh)	Average 15-Minute Demand (kW) Per Customer	Maximum 15-Minute Demand Per Customer	Xfmer kVA Rating
802	806	0	N/A	0	0.00	0.00	N/A
808	810	0	N/A	0	0.00	0.00	N/A
818	820	6	6	966	1.34	9.58	10.00
				1494	2.08	14.82	15.00
				1363	1.89	13.52	15.00
				1257	1.75	14.55	15.00
				1450	2.01	18.31	15.00
				1176	1.63	11.67	10.00
820	822	101	9	557	0.77	5.95	25.00
				551	0.77	6.96	
				484	0.67	5.17	
				493	0.68	6.22	
				480	0.67	5.56	
				559	0.78	5.97	
				501	0.70	6.33	
				567	0.79	5.63	
				532	0.74	6.72	
				557	0.77	5.95	

Table II-1 Continued

Node A	Node B	Phase-A #	# of Xfmers	Energy Consumption per Customer per Month (kWh)	Average 15-Minute Demand (kW) Per Customer	Maximum 15-Minute Demand Per Customer	Xfmer kVA Rating
				509	0.71	5.44	
				482	0.67	4.78	
				506	0.70	7.03	
				505	0.70	4.68	
				498	0.69	4.61	
				553	0.77	5.12	
				583	0.81	5.40	
				475	0.66	6.00	25.00
				563	0.78	6.52	
				553	0.77	6.98	
				540	0.75	7.50	
				528	0.73	5.24	
				573	0.80	7.96	
				543	0.75	5.80	
				520	0.72	7.22	
				521	0.72	4.82	
				561	0.78	6.49	
				513	0.71	5.48	
				553	0.77	5.49	
				515	0.72	6.50	25.00
				504	0.70	5.38	
				581	0.81	6.72	
				593	0.82	5.88	
				564	0.78	6.03	
				500	0.69	4.96	
				542	0.75	6.27	
				466	0.65	4.62	
				568	0.79	7.17	
				518	0.72	6.54	25.00
				565	0.78	7.13	
				580	0.81	5.37	
				504	0.70	5.38	

Table II-1 Continued

Node A	Node B	Phase-A #	# of Xfmers	Energy Consumption per Customer per Month (kWh)	Average 15-Minute Demand (kW) Per Customer	Maximum 15-Minute Demand Per Customer	Xfmer kVA Rating
				556	0.77	6.44	
				549	0.76	7.63	
				563	0.78	7.82	
				584	0.81	5.79	
				517	0.72	5.98	
				553	0.77	6.98	
				527	0.73	5.63	
				556	0.77	5.15	
				513	0.71	4.75	
				561	0.78	5.57	
				560	0.78	7.78	
				534	0.74	5.71	
				562	0.78	7.10	25.00
				561	0.78	5.19	
				550	0.76	5.88	
				509	0.71	4.71	
				488	0.68	6.16	
				574	0.80	5.31	
				552	0.77	7.67	
				491	0.68	6.82	
				576	0.80	6.67	
				586	0.81	6.26	
				481	0.67	4.45	
				510	0.71	6.44	
				529	0.73	4.90	25.00
				576	0.80	5.71	
				526	0.73	7.31	
				494	0.69	6.86	
				484	0.67	6.72	
				533	0.74	7.40	
				552	0.77	7.67	

Table II-1 Continued

Node A	Node B	Phase-A #	# of Xfmers	Energy Consumption per Customer per Month (kWh)	Average 15-Minute Demand (kW) Per Customer	Maximum 15-Minute Demand Per Customer	Xfmer kVA Rating
				450	0.63	4.46	25.00
				503	0.70	6.99	
				527	0.73	7.32	
				517	0.72	5.13	
				586	0.81	8.14	
				488	0.68	5.65	
				525	0.73	7.29	
				554	0.77	6.41	
				513	0.71	7.13	
				542	0.75	7.53	
				564	0.78	7.83	
				508	0.71	6.41	
				482	0.67	6.69	25.00
				561	0.78	5.57	
				507	0.70	5.87	
				501	0.70	5.35	
				494	0.69	5.72	
				584	0.81	7.37	
				577	0.80	6.16	
				504	0.70	5.83	
				558	0.78	5.54	
				551	0.77	5.89	
				522	0.73	7.25	
				516	0.72	4.78	
				568	0.79	7.17	10.00
				554	0.77	6.41	
				529	0.73	5.65	
				508	0.71	5.04	
				572	0.79	5.30	

Table II-1 Continued

Node A	Node B	Phase-A #	# of Xfmers	Energy Consumption per Customer per Month (kWh)	Average 15-Minute Demand (kW) Per Customer	Maximum 15-Minute Demand Per Customer	Xfmer kVA Rating
816	824	0	N/A	0	0.000	0.000	N/A
824	826	0	N/A	0	0.000	0.000	N/A
824	828	0	N/A	0	0.000	0.000	N/A
828	830	5	5	217	0.30	2.51	5.00
				209	0.29	2.07	5.00
				214	0.30	2.97	5.00
				221	0.31	2.05	5.00
				212	0.29	2.94	5.00
854	856	0	N/A	0	0.000	0.000	N/A
832	858	10	10	149	0.21	1.59	5.00
				140	0.19	1.39	5.00
				125	0.17	1.45	5.00
				154	0.21	1.65	5.00
				144	0.20	1.67	5.00
				142	0.20	1.31	5.00
				142	0.20	1.31	5.00
				147	0.20	1.86	5.00
				127	0.18	1.76	5.00
				150	0.21	2.08	5.00
858	864	2	2	35	0.05	0.44	5.00
				34	0.05	0.36	5.00
858	834	11	11	77	0.11	0.76	5.00
				68	0.09	0.79	5.00
				78	0.11	0.72	5.00
				72	0.10	1.00	5.00
				72	0.10	0.67	5.00
				73	0.10	0.72	5.00
				72	0.10	0.83	5.00
				79	0.11	0.73	5.00
				73	0.10	0.84	5.00
				71	0.10	0.66	5.00
				78	0.11	0.83	5.00

Table II-1 Continued

Node A	Node B	Phase-A #	# of Xfmers	Energy Consumption per Customer per Month (kWh)	Average 15-Minute Demand (kW) Per Customer	Maximum 15-Minute Demand Per Customer	Xfmer kVA Rating
834	860	13	2	308	0.43	3.29	15.00
				302	0.42	3.00	
				305	0.42	3.03	
				316	0.44	2.93	
				305	0.42	3.26	
				294	0.41	3.14	
				313	0.43	4.35	
				275	0.38	3.82	
				320	0.44	2.96	
				319	0.44	2.95	
				297	0.41	4.13	
				305	0.42	3.53	
				321	0.45	3.18	5.00
860	836	16	2	536	0.74	5.73	25.00
				500	0.69	6.31	
				457	0.64	5.77	
				458	0.64	6.36	
				498	0.69	6.92	
				459	0.64	5.31	
				500	0.69	6.94	
				488	0.68	6.16	
				506	0.70	5.02	
				453	0.63	5.24	
				461	0.64	4.27	
				459	0.64	5.80	
				523	0.73	5.59	10.00
				518	0.72	6.54	
				513	0.71	5.09	
				515	0.72	5.96	

Table II-1 Continued

Node A	Node B	Phase-A #	# of Xfmers	Energy Consumption per Customer per Month (kWh)	Average 15-Minute Demand (kW) Per Customer	Maximum 15-Minute Demand Per Customer	Xfmer kVA Rating
836	840	4	1	839	1.165	9.711	15.00
				799	1.110	7.927	
				812	1.128	11.278	
				844	1.172	8.373	
862	838	0	N/A	0	0.00	0.00	N/A
842	844	1	1	1380	1.92	17.42	15.00
844	846	0	N/A	0	0.00	0.00	N/A
846	848	0	N/A	0	0.00	0.00	N/A

Table II-2 Phase B Secondary Distribution Load Ratings

Node A	Node B	Phase-B #	# of Xfmers	Energy Consumption per Customer per Month (kWh)	Average 15-Minute Demand (kW) Per Customer	Maximum 15-Minute Demand Per Customer	Xfmer kVA Rating
802	806	68	6	147	0.20	1.46	5.00
				155	0.22	2.15	
				158	0.22	1.46	
				156	0.22	1.67	
				156	0.22	1.55	
				147	0.20	2.04	
				151	0.21	2.10	
				145	0.20	1.34	
				146	0.20	1.35	
				152	0.21	1.62	
				159	0.22	1.47	
				158	0.22	1.83	
				146	0.20	1.56	5.00
				149	0.21	2.07	
				155	0.22	1.96	
				146	0.20	1.84	
				154	0.21	1.78	
				154	0.21	1.78	
				158	0.22	1.99	
				158	0.22	2.19	
				159	0.22	2.01	
				148	0.21	1.58	
				158	0.22	1.99	
				160	0.22	2.22	
				149	0.21	1.48	5.00
				153	0.21	1.77	
				154	0.21	1.78	
				154	0.21	1.78	
				157	0.22	2.18	
				152	0.21	1.92	
				141	0.20	1.78	
				157	0.22	2.18	

Table II-2 Continued

Node A	Node B	Phase-B #	# of Xfmers	Energy Consumption per Customer per Month (kWh)	Average 15-Minute Demand (kW) Per Customer	Maximum 15-Minute Demand Per Customer	Xfmer kVA Rating
				146	0.20	1.69	
				160	0.22	2.22	
				159	0.22	1.47	
				155	0.22	1.44	
				152	0.21	1.92	5.00
				146	0.20	1.35	
				147	0.20	1.46	
				154	0.21	1.53	
				152	0.21	2.11	
				155	0.22	1.79	
				155	0.22	2.15	
				160	0.22	1.48	
				156	0.22	1.97	
				155	0.22	1.79	
				147	0.20	1.86	
				156	0.22	1.55	
				145	0.20	1.68	5.00
				146	0.20	2.03	
				154	0.21	1.65	
				159	0.22	2.21	
				155	0.22	2.15	
				153	0.21	1.93	
				158	0.22	1.83	
				145	0.20	1.55	
				154	0.21	1.78	
				147	0.20	2.04	
				150	0.21	1.39	
				149	0.21	1.59	
				155	0.22	2.15	5.00
				146	0.20	2.03	
				151	0.21	1.91	
				152	0.21	1.76	
				153	0.21	2.13	

Table II-2 Continued

Node A	Node B	Phase-B #	# of Xfmers	Energy Consumption per Customer per Month (kWh)	Average 15-Minute Demand (kW) Per Customer	Maximum 15-Minute Demand Per Customer	Xfmer kVA Rating
				158	0.22	1.57	
				151	0.21	1.61	
				147	0.20	1.36	
808	810	7	7	479	0.67	5.54	5.00
				535	0.74	7.43	5.00
				496	0.69	4.92	5.00
				494	0.69	5.28	5.00
				451	0.63	5.69	5.00
				477	0.66	6.02	5.00
				483	0.67	5.16	5.00
818	820	0	N/A	0	0.000	0.000	N/A
820	822	0	N/A	0	0.000	0.000	N/A
816	824	1	1	39	0.05	0.54	5.00
824	826	36	3	391	0.54	5.43	15.00
				403	0.56	3.73	
				419	0.58	4.85	
				394	0.55	3.65	
				406	0.56	3.76	
				397	0.55	4.59	
				372	0.52	3.97	
				378	0.53	3.75	
				383	0.53	4.09	
				428	0.59	4.25	
				399	0.55	3.96	
				384	0.53	3.56	
				365	0.51	5.07	15.00
				392	0.54	4.54	
				368	0.51	3.93	
				386	0.54	4.47	
				390	0.54	4.17	
				430	0.60	5.43	
				410	0.57	4.07	

Table II-2 Continued

Node A	Node B	Phase-B #	# of Xfmers	Energy Consumption per Customer per Month (kWh)	Average 15-Minute Demand (kW) Per Customer	Maximum 15-Minute Demand Per Customer	Xfmer kVA Rating
				378	0.53	3.75	
				398	0.55	4.61	
				401	0.56	5.57	
				391	0.54	4.94	
				429	0.60	4.97	
				428	0.59	4.57	15.00
				425	0.59	4.22	
				407	0.57	4.71	
				425	0.59	4.22	
				416	0.58	4.44	
				380	0.53	3.77	
				364	0.51	3.61	
				366	0.51	3.91	
				408	0.57	5.15	
				380	0.53	3.77	
				424	0.59	5.35	
				410	0.57	4.75	
824	828	0	N/A	0	0.000	0.000	N/A
828	830	0	N/A	0	0.000	0.000	N/A
854	856	1	1	500	0.69	4.96	5.00
832	858	2	2	64	0.09	0.63	5.00
				63	0.09	0.88	5.00
858	864	0	N/A	0	0.000	0.000	N/A
858	834	15	15	203	0.28	1.88	5.00
				216	0.30	2.00	5.00
				217	0.30	2.32	5.00
				209	0.29	2.07	5.00
				229	0.32	2.65	5.00
				225	0.31	3.13	5.00
				207	0.29	1.92	5.00
				216	0.30	2.31	5.00
				220	0.31	2.55	5.00

Table II-2 Continued

Node A	Node B	Phase-B #	# of Xfmers	Energy Consumption per Customer per Month (kWh)	Average 15-Minute Demand (kW) Per Customer	Maximum 15-Minute Demand Per Customer	Xfmer kVA Rating
				207	0.29	2.21	5.00
				201	0.28	1.86	5.00
				204	0.28	1.89	5.00
				210	0.29	2.43	5.00
				217	0.30	2.15	5.00
				224	0.31	2.59	5.00
834	860	14	2	384	0.53	4.10	15.00
				429	0.60	4.26	
				382	0.53	3.79	
				365	0.51	3.90	
				440	0.61	4.37	
				392	0.54	4.95	
				405	0.56	4.33	
				406	0.56	4.70	
				397	0.55	4.59	
				436	0.61	5.51	
				379	0.53	3.51	
				384	0.53	4.10	
				369	0.51	4.66	5.00
				434	0.60	4.02	
860	836	8	8	258	0.36	3.26	5.00
				271	0.38	2.90	5.00
				299	0.42	3.46	5.00
				255	0.35	3.54	5.00
				278	0.39	3.51	5.00
				300	0.42	4.17	5.00
				273	0.38	2.92	5.00
				301	0.42	2.99	5.00
836	840	8	1	671	0.93	7.77	25.00
				669	0.93	7.74	
				695	0.97	9.65	
				632	0.88	6.75	

Table II-2 Continued

Node A	Node B	Phase-B #	# of Xfmers	Energy Consumption per Customer per Month (kWh)	Average 15-Minute Demand (kW) Per Customer	Maximum 15-Minute Demand Per Customer	Xfmer kVA Rating
				609	0.85	7.05	
				622	0.86	6.17	
				578	0.80	5.35	
				601	0.83	7.59	
862	838	34	3	224	0.31	2.22	15.00
				242	0.34	2.40	
				288	0.40	3.08	
				222	0.31	2.20	
				210	0.29	2.08	
				266	0.37	2.64	
				263	0.37	3.65	
				251	0.35	3.49	
				292	0.41	2.70	
				245	0.34	2.27	
				293	0.41	2.71	
				296	0.41	2.94	
				226	0.31	3.14	10.00
				247	0.34	3.12	
				233	0.32	2.70	
				294	0.41	4.08	
				293	0.41	3.70	
				274	0.38	2.54	
				267	0.37	2.47	
				270	0.38	2.68	
				278	0.39	2.57	
				225	0.31	2.08	
				296	0.41	3.74	
				255	0.35	2.36	
				234	0.33	2.71	10.00
				252	0.35	3.50	
				276	0.38	3.48	
				223	0.31	2.21	

Table II-2 Continued

Node A	Node B	Phase-B #	# of Xfmers	Energy Consumption per Customer per Month (kWh)	Average 15-Minute Demand (kW) Per Customer	Maximum 15-Minute Demand Per Customer	Xfmer kVA Rating
				256	0.36	2.74	
				276	0.38	3.83	
				284	0.39	3.94	
				230	0.32	2.90	
				263	0.37	3.32	
				296	0.41	3.43	
842	844	0	N/A	0	0.00	0.00	N/A
844	846	61	6	125	0.17	1.16	5.00
				130	0.18	1.20	
				129	0.18	1.38	
				136	0.19	1.45	
				126	0.18	1.35	
				136	0.19	1.35	
				136	0.19	1.45	
				129	0.18	1.19	
				136	0.19	1.26	
				126	0.18	1.59	
				136	0.19	1.45	
				127	0.18	1.76	
				130	0.18	1.64	5.00
				135	0.19	1.88	
				127	0.18	1.47	
				132	0.18	1.83	
				133	0.18	1.85	
				132	0.18	1.31	
				126	0.18	1.75	
				135	0.19	1.25	
				125	0.17	1.16	
				129	0.18	1.28	
				135	0.19	1.44	
				133	0.18	1.85	
				132	0.18	1.53	5.00
				127	0.18	1.76	

Table II-2 Continued

Node A	Node B	Phase-B #	# of Xfmers	Energy Consumption per Customer per Month (kWh)	Average 15-Minute Demand (kW) Per Customer	Maximum 15-Minute Demand Per Customer	Xfmer kVA Rating
				124	0.17	1.57	
				126	0.18	1.59	
				134	0.19	1.33	
				135	0.19	1.34	
				134	0.19	1.69	
				136	0.19	1.45	
				131	0.18	1.52	
				127	0.18	1.26	
				136	0.19	1.45	
				126	0.18	1.75	
				131	0.18	1.30	
				105	0.15	0.97	
				135	0.19	1.88	
				129	0.18	1.38	
				133	0.18	1.42	
				130	0.18	1.29	
				131	0.18	1.21	5.00
				125	0.17	1.45	
				128	0.18	1.27	
				132	0.18	1.22	
				124	0.17	1.72	
				132	0.18	1.41	
				125	0.17	1.16	
				134	0.19	1.55	
				125	0.17	1.45	
				126	0.18	1.17	
				132	0.18	1.53	
				126	0.18	1.75	5.00
				132	0.18	1.83	
				129	0.18	1.38	
				133	0.18	1.32	
				134	0.19	1.33	
				126	0.18	1.35	

Table II-2 Continued

Node A	Node B	Phase-B #	# of Xfmers	Energy Consumption per Customer per Month (kWh)	Average 15-Minute Demand (kW) Per Customer	Maximum 15-Minute Demand Per Customer	Xfmer kVA Rating
				128	0.18	1.27	
844	846	1	1	131	0.18	1.30	5.00
846	848	2	2	1977	2.75	22.88	15.00
				1978	2.75	19.62	25.00

Table II-3 Phase C Secondary Distribution Load Ratings

Node A	Node B	Phase-C #	# of Xfmers	Energy Consumption per Customer per Month (kWh)	Average 15-Minute Demand (kW) Per Customer	Maximum 15-Minute Demand Per Customer	Xfmer kVA Rating
802	806	67	6	123	0.17	1.31	5.00
				118	0.16	1.37	
				127	0.18	1.18	
				128	0.18	1.27	
				133	0.18	1.23	
				125	0.17	1.34	
				126	0.18	1.59	
				134	0.19	1.55	
				122	0.17	1.13	
				132	0.18	1.53	
				129	0.18	1.49	
				124	0.17	1.32	
				127	0.18	1.36	5.00
				116	0.16	1.07	
				122	0.17	1.69	
				123	0.17	1.22	
				127	0.18	1.60	
				128	0.18	1.62	
				114	0.16	1.13	
				120	0.17	1.39	
				128	0.18	1.48	
				115	0.16	1.23	
				133	0.18	1.68	
				139	0.19	1.76	
				135	0.19	1.34	5.00
				124	0.17	1.23	
				125	0.17	1.58	
				130	0.18	1.64	
				127	0.18	1.26	

Table II-3 Continued

Node A	Node B	Phase-C #	# of Xfmers	Energy Consumption per Customer per Month (kWh)	Average 15-Minute Demand (kW) Per Customer	Maximum 15-Minute Demand Per Customer	Xfmer kVA Rating
				121	0.17	1.20	
				136	0.19	1.26	
				137	0.19	1.73	
				114	0.16	1.44	
				131	0.18	1.40	
				128	0.18	1.27	
				116	0.16	1.24	
				123	0.17	1.31	5.00
				120	0.17	1.19	
				138	0.19	1.60	
				134	0.19	1.24	
				120	0.17	1.52	
				130	0.18	1.39	
				134	0.19	1.24	
				114	0.16	1.13	
				127	0.18	1.18	
				126	0.18	1.35	
				118	0.16	1.17	
				121	0.17	1.29	
				124	0.17	1.44	5.00
				116	0.16	1.61	
				137	0.19	1.27	
				121	0.17	1.53	
				135	0.19	1.88	
				130	0.18	1.39	
				120	0.17	1.28	
				119	0.17	1.38	
				132	0.18	1.53	
				125	0.17	1.16	
				129	0.18	1.63	
				124	0.17	1.44	
				129	0.18	1.49	5.00
				134	0.19	1.86	

Table II-3 Continued

Node A	Node B	Phase-C #	# of Xfmers	Energy Consumption per Customer per Month (kWh)	Average 15-Minute Demand (kW) Per Customer	Maximum 15-Minute Demand Per Customer	Xfmer kVA Rating
				130	0.18	1.39	
				135	0.19	1.25	
				134	0.19	1.43	
				116	0.16	1.07	
				133	0.18	1.54	
808	810	0	N/A	0	0.000	0.000	N/A
818	820	0	N/A	0	0.000	0.000	N/A
820	822	0	N/A	0	0.000	0.000	N/A
816	824	0	N/A	0	0.000	0.000	N/A
824	826	0	N/A	0	0.000	0.000	N/A
824	828	3	3	130	0.18	1.81	5.00
				140	0.19	1.62	5.00
				120	0.17	1.11	5.00
828	830	0	N/A	0	0.000	0.000	N/A
854	856	0	N/A	0	0.000	0.000	N/A
832	858	4	4	216	0.30	3.00	5.00
				210	0.29	2.08	5.00
				205	0.28	2.59	5.00
				233	0.32	3.24	5.00
858	864	0	N/A	0	0.000	0.000	N/A
858	834	14	14	229	0.32	2.12	5.00
				227	0.32	2.25	5.00
				230	0.32	2.90	5.00
				217	0.30	2.32	5.00
				237	0.33	2.35	5.00
				216	0.30	2.14	5.00
				233	0.32	3.24	5.00
				246	0.34	2.63	5.00
				253	0.35	3.19	5.00
				234	0.33	2.95	5.00
				242	0.34	2.59	5.00
				227	0.32	2.10	5.00

Table II-3 Continued

Node A	Node B	Phase-C #	# of Xfmers	Energy Consumption per Customer per Month (kWh)	Average 15-Minute Demand (kW) Per Customer	Maximum 15-Minute Demand Per Customer	Xfmer kVA Rating
				218	0.30	2.02	5.00
				224	0.31	2.83	5.00
834	860	104	9	388	0.54	4.49	15.00
				401	0.56	3.71	
				410	0.57	4.38	
				389	0.54	4.16	
				373	0.52	3.70	
				433	0.60	6.01	
				439	0.61	5.08	
				403	0.56	3.73	
				385	0.53	4.11	
				411	0.57	3.81	
				438	0.61	5.07	
				424	0.59	5.89	
				393	0.55	4.20	15.00
				416	0.58	3.85	
				377	0.52	3.49	
				388	0.54	4.15	
				444	0.62	4.11	
				392	0.54	3.63	
				393	0.55	4.20	
				430	0.60	3.98	
				373	0.52	4.71	
				391	0.54	4.94	
				404	0.56	4.68	
				414	0.58	4.11	
				422	0.59	4.19	15.00
				431	0.60	5.99	
				412	0.57	3.81	
				433	0.60	6.01	
				416	0.58	5.78	
				431	0.60	5.99	

Table II-3 Continued

Node A	Node B	Phase-C #	# of Xfmers	Energy Consumption per Customer per Month (kWh)	Average 15-Minute Demand (kW) Per Customer	Maximum 15-Minute Demand Per Customer	Xfmer kVA Rating
				407	0.57	4.35	
				396	0.55	3.93	
				376	0.52	4.35	
				444	0.62	6.17	
				441	0.61	4.71	
				395	0.55	4.22	
				409	0.57	3.79	
				442	0.61	5.12	
				397	0.55	3.94	
				441	0.61	5.57	
				419	0.58	5.82	
				412	0.57	5.72	
				455	0.63	5.74	15.00
				463	0.64	5.85	
				407	0.57	3.77	
				441	0.61	5.57	
				403	0.56	4.31	
				428	0.59	4.25	
				460	0.64	4.26	
				394	0.55	4.97	
				400	0.56	3.97	
				439	0.61	4.06	
				459	0.64	5.80	
				443	0.62	5.59	
				372	0.52	5.17	15.00
				426	0.59	4.55	
				446	0.62	6.19	
				373	0.52	5.18	
				397	0.55	5.51	
				412	0.57	4.77	
				382	0.53	4.08	15.00
				383	0.53	4.43	

Table II-3 Continued

Node A	Node B	Phase-C #	# of Xfmers	Energy Consumption per Customer per Month (kWh)	Average 15-Minute Demand (kW) Per Customer	Maximum 15-Minute Demand Per Customer	Xfmer kVA Rating
				381	0.53	3.78	
				385	0.53	4.86	
				424	0.59	5.89	
				373	0.52	5.18	
				399	0.55	4.62	
				383	0.53	3.80	
				395	0.55	3.92	
				426	0.59	4.23	
				412	0.57	4.77	
				442	0.61	4.09	
				419	0.58	3.88	
				433	0.60	4.30	
				430	0.60	3.98	
				450	0.63	5.68	
				439	0.61	4.69	
				420	0.58	5.30	15.00
				384	0.53	3.81	
				405	0.56	4.69	
				398	0.55	5.03	
				392	0.54	3.89	
				460	0.64	4.56	
				406	0.56	4.34	
				419	0.58	4.48	
				391	0.54	3.62	
				460	0.64	6.39	
				411	0.57	4.39	
				431	0.60	4.60	15.00
				378	0.53	3.50	
				420	0.58	5.30	
				377	0.52	3.74	
				406	0.56	5.64	
				415	0.58	5.24	

Table II-3 Continued

Node A	Node B	Phase-C #	# of Xfmers	Energy Consumption per Customer per Month (kWh)	Average 15-Minute Demand (kW) Per Customer	Maximum 15-Minute Demand Per Customer	Xfmer kVA Rating
				452	0.63	4.19	
				397	0.55	5.51	
				388	0.54	4.90	
				450	0.63	6.25	
				384	0.53	4.85	
				450	0.63	4.81	15.00
				414	0.58	5.75	
				450	0.63	4.17	
				383	0.53	3.80	
				437	0.61	4.34	
860	836	14	2	939	1.30	11.86	50.00
				888	1.23	9.49	
				802	1.11	9.28	
				842	1.17	9.00	
				860	1.19	8.53	
				962	1.34	13.36	
				902	1.25	8.95	
				824	1.14	11.44	
				863	1.20	9.22	
				828	1.15	9.58	
				940	1.31	10.88	
				875	1.22	11.05	
				947	1.32	8.77	10.00
				897	1.25	8.90	
836	840	0	N/A	0	0.000	0.000	N/A
862	838	0	N/A	0	0.000	0.000	N/A
842	844	0	N/A	0	0.000	0.000	N/A
844	846	35	3	191	0.27	2.41	10.00
				206	0.29	2.04	
				202	0.28	2.00	
				202	0.28	2.00	
				199	0.28	2.13	

Table II-3 Continued

Node A	Node B	Phase-C #	# of Xfmers	Energy Consumption per Customer per Month (kWh)	Average 15-Minute Demand (kW) Per Customer	Maximum 15-Minute Demand Per Customer	Xfmer kVA Rating
				197	0.27	1.82	
				208	0.29	2.22	
				208	0.29	1.93	
				193	0.27	2.68	
				191	0.27	1.89	
				195	0.27	1.93	
				197	0.27	2.49	
				202	0.28	2.81	
				180	0.25	1.92	
				191	0.27	2.21	
				217	0.30	2.74	
				207	0.29	1.92	
				185	0.26	1.98	10.00
				198	0.28	2.29	
				184	0.26	1.83	
				179	0.25	2.26	
				192	0.27	2.67	
				179	0.25	2.26	
				209	0.29	2.42	
				192	0.27	2.67	
				200	0.28	2.31	
				205	0.28	2.37	
				217	0.30	2.74	
				204	0.28	2.36	
				179	0.25	2.07	5.00
				216	0.30	2.50	
				195	0.27	2.71	
				205	0.28	2.37	
				201	0.28	2.15	
				208	0.29	2.89	
846	848	0	N/A	0	0.000	0.000	N/A

VITA

Richard Henry Douglin received his Bachelor of Science degree in electrical engineering from Prairie View A&M University at Prairie View in 2007. He entered the electrical engineering program at Texas A&M University in September 2009 and received his Master of Science degree in May 2012.

Mr. Douglin may be reached at Department of Electrical and Computer Engineering, 214 Zachry Engineering Center, Texas A&M University, College Station, TX 77843-3128. His email is richard.douglin@gmail.com.